UNCLASSIFIED

AD NUMBER
AD035275
CLASSIFICATION CHANGES
TO: unclassified
FROM: confidential
LIMITATION CHANGES
TO: Approved for public release; distribution is unlimited.
FROM: Distribution authorized to U.S. Gov't. agencies and their contractors; Administrative/Operational Use; 28 FEB 1954. Other requests shall be referred to Air Force Cambridge Research Labs., Hanscom AFB, MA. NOFORN.
AUTHORITY
28 Feb 1966, DoDD 5200.10; AFCRL ltr dtd 20 Apr 1969

THIS PAGE IS UNCLASSIFIED

UNCLASSIFIED

AD NUMBER
AD035275
CLASSIFICATION CHANGES
TO: **confidential**
FROM: **secret**
AUTHORITY
28 Feb 1957, DoDD 5200.10

THIS PAGE IS UNCLASSIFIED

SECRET

SPECIAL HANDLING REQUIRED

THE INFORMATION CONTAINED IN THIS DOCUMENT WILL NOT BE DISCLOSED TO FOREIGN NATIONALS OR THEIR REPRESENTATIVES.

NORTHEASTERN UNIVERSITY

54W P 14555

SECRET

U3408-5-5

SECRET

Copy No. 55

FINAL REPORT

Contract No. AF 19(122)-7, Items II & III

February 28, 1954

Item II: Reliability Research
Item III: Coding Circuitry

SPECIAL HANDLING REQUIRED

THE INFORMATION CONTAINED IN THIS DOCUMENT WILL NOT BE DISCLOSED TO FOREIGN NATIONALS OR THEIR REPRESENTATIVES.

Prepared by

S. H. Chang
M. W. Essigmann
E. J. Craig
W. H. Lob
J. S. Rochefort
H. L. Stubbs
L. J. Nardone
J. Wiren
A. M. Briana
J. J. Kelly
A. G. Marcotte
T. J. White

Submitted for the staff by

Martin W. Essigmann

Martin W. Essigmann
Coordinator of Electronics Research

SECRET

INTRODUCTION

This final report summarizes the procedures followed and results obtained in performing research directed toward: (1) the specification and design of the communications part of an IFF system of high reliability, and (2) the evaluation and design of certain transistorized coding circuits for use in this system. The reliability research under (1) was begun on November 2_, 1951, as Item II of Contract No. AF 19(122)-7, and the work on coding circuitry was begun on December 1, 1952, as Item III. Research under Item I, entitled Visual Message Presentation and unclassified, was begun on May 1, 1949; and the final report for this item is being issued separately.

For practical reasons it has not appeared expedient to include all of the details of the research in this final report. Instead, emphasis is placed herein on the presentation of results and on recommendations for future work pertaining to the subject topics. This final report, then, is intended to summarize the results of the research reported in the seven quarterly (and one letter) progress reports prepared to date, and not necessarily to serve as a replacement for the progress reports.

Listed below are the names of the research personnel who have been assigned at some time to the work under Items II and III. Many of those listed have served only in part-time capacities, and in some instances for only short periods of time. Work under Item II began with a staff equivalent to 3.6 full-time persons, and the number of persons has steadily increased until at the present time there are 7.5 full-time equivalents (including secretaries and technicians). The staff under Item III has remained fairly constant at 3.6 full-time equivalents. The reader requiring the details of service of the personnel listed is referred to the quarterly progress reports for this information.

Professors

S. H. Chang — M. W. Essigmann

Associate Professor

G. E. Pihl

Assistant Professors

E. J. Craig — J. S. Rochefort*
W. H. Lob* — H. L. Stubbs

Research Associates

M. L. Bovarnick — L. J. Nardone**
T. P. Cheatham, Jr. — J. Wiren

* Essentially full time Item II for the entire period.
** Full time Item III for its entire period.

Research Assistants

A. M. Briana
J. J. Kelly
J. J. Klein
A. G. Marcotte
T. J. White

Technician

W. F. Goddard

Secretaries

M. C. Cahall
P. J. Puccio
M. D. Reynolds

Cooperative-Student Assistants

C. U. Knowles
R. H. Lawson
G. A. Macomber
L. J. O'Connor

TABLE OF CONTENTS

CHAPTER V

CHAPTER VI

CHAPTER VII

CHAPTER VIII

Pg.

APPENDICES

RELIABILITY RESEARCH

and

CODING CIRCUITRY

FINAL REPORT

ABSTRACT

This final report summarizes the results of theoretical and experimental studies performed during the period from November 20, 1951, through February 28, 1954, on the general communication and circuitry problems involved in the design of a highly reliable pulse-type IFF system of specified form. Factors considered which lead to low reliability, and therefore need to be overcome, include enemy jam, noise, and equipment failure.

It is shown that game theory, matched filters, pulse-train correlation, redundancy codes, repeated challenges, multi-round operation, and marginal checking all provide techniques applicable to the problem, and the extent to which each has been applied is described. A mock-up of the system has been constructed to demonstrate the feasibility and effectiveness of pulse-train correlation and matched filtering.

Treatment is also given to certain approaches to the overall problem that deviate from the specified system. Such topics include the use of stored signals at the transpondor, rotating antennas at the transpondor, noise-like signals, and enemy jam to perform the challenge function.

CHAPTER I

GENERAL ANALYSIS OF THE IFF PROBLEM

A. Statement of the Problem

Experience has shown that past and present IFF systems have an insufficient degree of security and reliability. Security can be improved by the introduction of cryptographic techniques; and more reliable operation will result if effort is devoted to system planning and equipment design. This problem of reliability has been studied under Item II of this contract.

Stated in general form, this item of the contract has been concerned with the study of the communication aspects of the IFF problem, with the specific aim of determining methods for improving the performance reliability of a particular IFF system. This system operates in accordance with the scheme shown in Fig. 1; and is one in which the challenge as generated by the interrogator is an n-digit binary number, and an encoder at the airborne transpondor provides an r-digit reply. The reply, on reception at the responsor on the ground, is compared with a locally encoded version to determine whether or not it is correct.

The two transmission links in the specified system differ in that the correct signal is available at the terminal of the air-to-ground link, thus providing the possibility of using cross-correlation techniques in the reception of the coded reply. Less powerful means must be employed at the airplane, since the system precludes any a priori knowledge of the challenge at the transpondor.

When dealing with the problems of security and reliability, the enemy's behavior must be taken into account. His resourcefulness and technical competence should never be underestimated. It is assumed that as a result of espionage or capture of equipment, the enemy has a knowledge of the IFF system that is complete except for the cryptographic key in use during a particular sortie period. Consequently security can only be maintained if the cryptographic level of the system is such that the system is secure against an enemy who can only listen. The two encoders are assumed to meet this requirement and hence cryptographic security is not included in the problem. Furthermore, it is assumed that if an IFF system is vulnerable to some form of jamming, the enemy will not be deterred by expense or equipment complexity from exerting every possible effort to render the system useless.

The foregoing has applied to research under Item II. For this writing, the work under Item III can be considered as supporting research with the main object that of developing techniques for the design and analysis of reliable circuits for eventual use in the IFF system.

B. Reliability-reducing Factors

The first step in designing or evaluating a reliable IFF system is an analysis of all reliability-reducing factors. The problem of system reliability may be divided into two parts which may be termed transmission and equipment reliability. Transmission reliability refers to the performance of the system if all

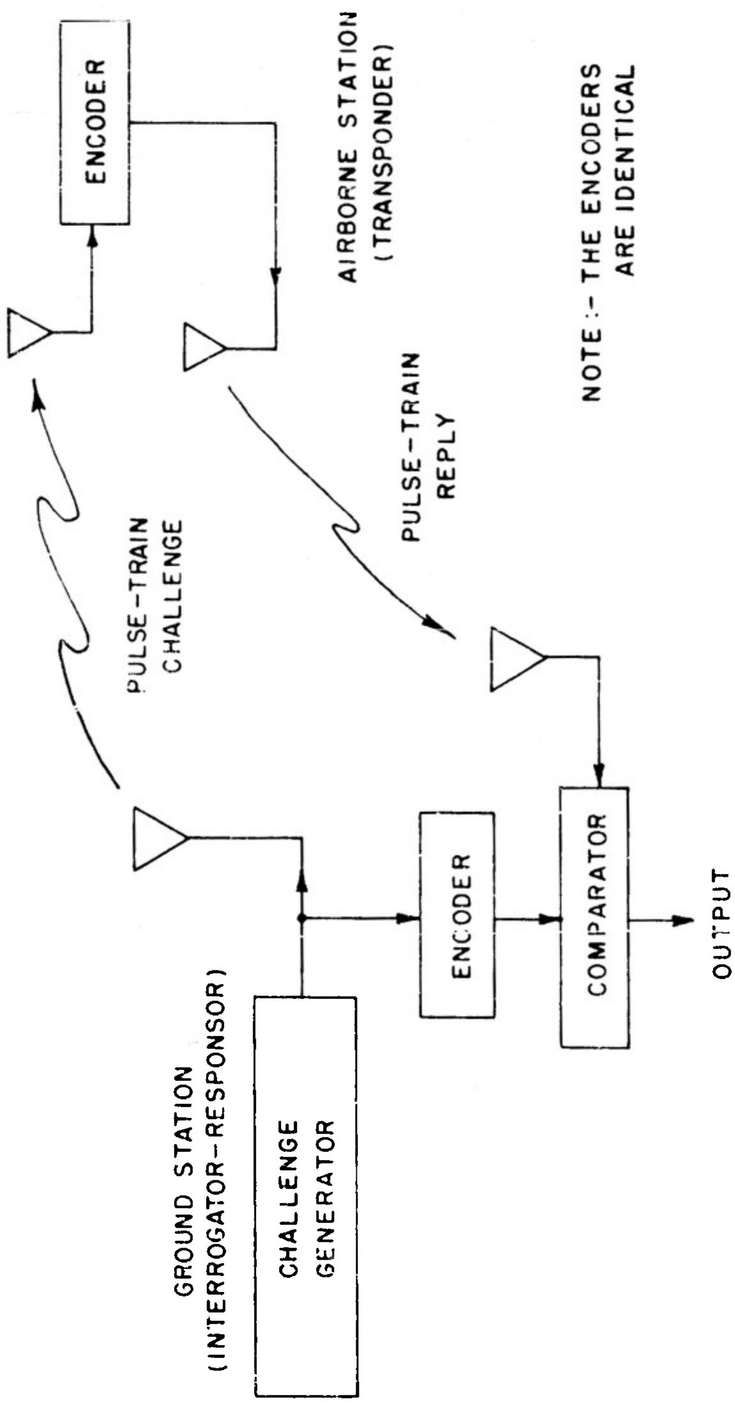

FIG. 1. BLOCK DIAGRAM OF BASIC IFF SYSTEM UNDER STUDY.

equipment operates perfectly, and equipment reliability refers to the performance of the equipment alone. Of these two sub-divisions, it has been felt that transmission reliability should be considered first. Consequently it has received the entire effort of Item II of the contract, and, except for some specialized studies performed under Item III, equipment reliability has been deferred until the problem of reliability-in-transmission is brought to a satisfactory solution.

A detailed breakdown of reliability-reducing factors is shown in Fig. 2. As is indicated, failure in transmission can be divided into that which results from the system design, and that due to enemy action. (It should be noted that the possible presence of an enemy is the main factor which distinguishes a radio communication system destined for military use from that intended for civilian use. An optimum peacetime system could be far from the best for wartime usage.) These two divisions are further sub-divided, and the following defines some of the terms appearing on the diagram.

Garbling results from harmful overlap of the responses of various transpondors to one challenge.

Fruit is caused by replies to challenges from different interrogators.

Destructive jamming is the transmission by the enemy of signals or noise in an attempt to prevent identification of friendly planes. It can be aimed at either the ground-to-air or the air-to-ground communication link, or both.

Deception in challenge is the transmission by the enemy of signals designed to cause friendly transpondors to reply, and could be used for the following purposes: (1) To obtain information about the presence, number, and location of friendly planes; (2) To obtain information about the cryptographic relation between challenge and reply; (3) To exhaust the transpondor's channel capacity and thereby prevent replies to friendly challenges. This is a combination of jamming and deception.

Deception in reply is the attempt of an enemy plane to appear as a friend by giving the correct reply.

The reliability reducing factors included under the heading "inherent in system design" have been given considerable attention by others[1-6*], whereas those included under "due to enemy action" have often been treated lightly. Destructive jamming is considered to be of first-order importance and consequently has received considerable attention under Item II. Deception is considered to be of second-order importance since: (1) transpondors can be turned off when planes are over enemy territory, thus greatly reducing the opportunity for the enemy to obtain information with respect to presence, number, and location of friendly planes; (2) proper design of the ground-to-air link can probably minimize its vulnerability to overloaded channel capacity; and (3) a high level of cryptographic security can prevent the enemy from either obtaining the cryptographic key, or deducing the correct reply during a particular sortie period.

* Number superscripts refer to references given in the Bibliography.

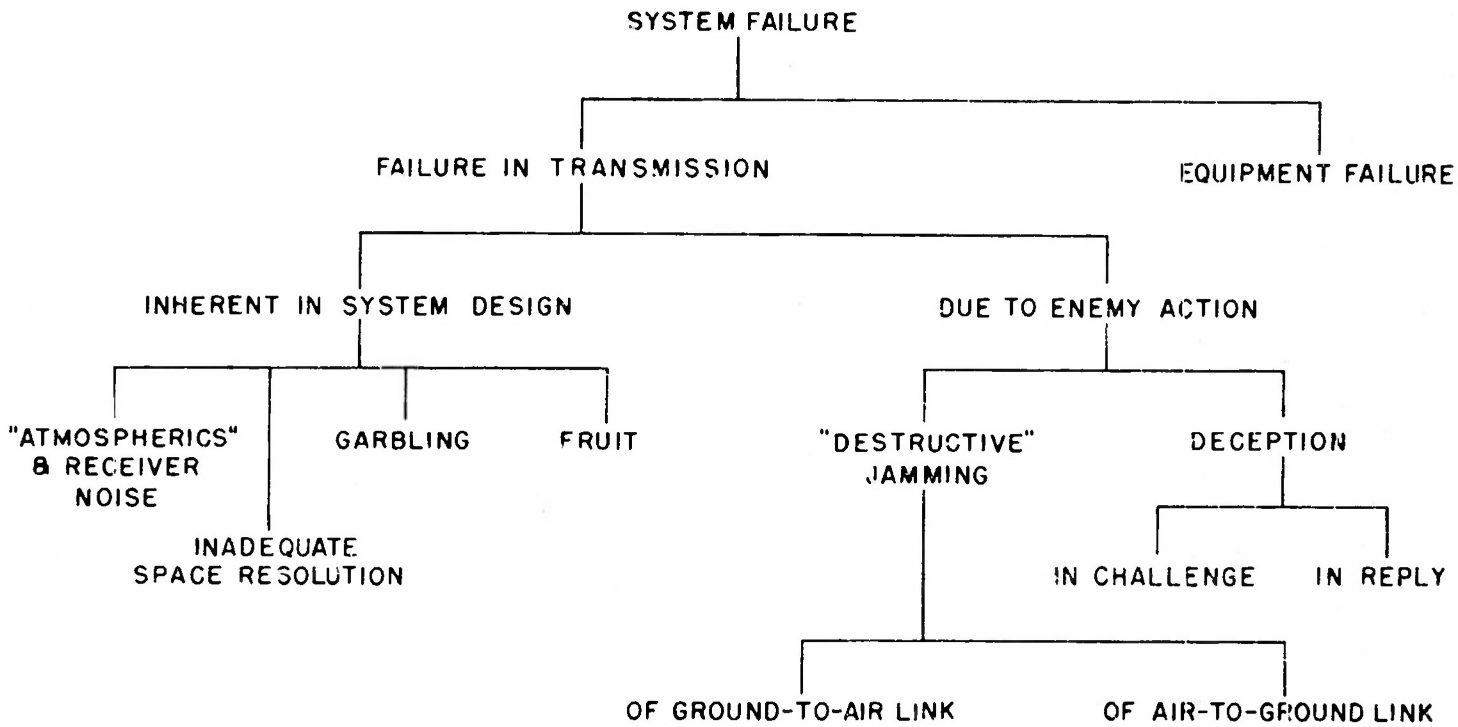

FIG. 2. BREAKDOWN OF RELIABILITY — REDUCING FACTORS.

C. Theory of Games

One method of analyzing the IFF problem, and of answering at least some restricted questions about it, is the theory of games developed by John von Neumann and others[7,8]. This theory concerns any situation which can be characterized by sets of alternative "strategies" for each of several "players" and by a matrix of "pay-offs" for each player which specifies how much he can expect to win (or lose) under every possible combination of strategies. The simplest case, which has wide application to military situations, is the "zero-sum" two-person game, where the term "zero-sum" implies that there is essentially only one pay-off matrix because one player wins exactly the same amount that the other loses. Although attempts to apply this formulation to the entire problem of designing an IFF system cannot be expected to have much success, for reasons to be explained below, there are certain restricted situations where the theory can be useful.

It is possible, in theory, to enumerate all IFF systems under consideration as strategies for the air-defense program, and to enumerate all systems of jamming and deception as enemy strategies. In order to construct a pay-off matrix, it is necessary to assign relative values a, b and c, d to correct and incorrect identifications for both friendly and enemy airplanes respectively and to assume a value for the a priori probability, p, that an unidentified airplane is friendly. It is also necessary to assume a value for the reliability r of each system in the presence of each system of counter-measures.* It seems at this point that if all the necessary information for game-theory analysis were available, the decision could be made by simple reasoning without requiring any mathematical theory. This is, in fact, the case, because game theory amounts to more than simple reasoning only when "mixed strategies" are permitted, as in poker, for example, where one sometimes, but not always, bluffs with a weak hand. Since it is not feasible to confuse the enemy by using one IFF system one day and a completely different one the next day, the best principle that can be obtained from game theory is the "minimax" principle of choosing the system which maximizes the minimum gain. That is, different systems should be compared on the basis of the performance of each one in the presence of the worst corresponding system of jamming and deception.

Several subordinate IFF problems which are of some interest, although not primarily concerned with reliability, have been treated by game theory in the literature, and will be briefly summarized here.

(1) The Rand Corporation[9] has investigated the advantages of "code complexity", measured only by the number n of possible replies, assuming that the enemy knows the list of possible replies and may guess one at random. The conclusions depend on the assumed values of the various quantities mentioned above, but under the most realistic assumptions there was very little advantage found in having a large n (1000 compared with 10 or 100). Another conclusion from the same study was that, when the differences in value between correct and incorrect identification are of the same order of magnitude for friend and enemy, the reliability r must be greater than p, the a priori probability of a friend. Otherwise the best strategy is to ignore the IFF system and call every unidentified airplane a friend.

* A more detailed formulation of these assumptions is given in Quarterly Progress Report No. 11, Appendix B.

(2) Another study by the Rand Corporation[10] concludes that if n code signals are available, they should be used with equal probability, as would be expected, and that the enemy in trying to guess the correct reply should also use the n signals with equal probability. In this study, which assumes perfect reliability, it is also shown that the indication of the system should be believed only if

$$p > \frac{c - d}{c - d + n(a - b)}.$$ Otherwise, the best strategy is to call everyone an enemy.

(3) Game theory has also been used* to investigate the desirability of operating an air-to-air IFF system during a bombing mission, for example, when the airborne interrogator may be used by the enemy as a beacon. Here it was assumed that the probability p of an unidentified airplane being friendly is a function of distance from target, and hence the best strategy is also a function of this distance.

These examples indicate what type of limited problem can be handled by game-theory analysis. A similar problem which may be considered is that of combatting pulse jamming by a choice of the number of ones and zeros in a pulse train, where the enemy's strategy is his choice of the probability of sending a jamming pulse. In most cases, however, it appears that the unrealistic assumptions required to perform this type of analysis make the conclusions of only academic interest.

D. General System Considerations

The primary purpose of an IFF system is to operate in coordination with a radar system and supply information concerning which planes are friendly. A particular target can be selected for interrogation if the ground station is equipped with a directional antenna. The beam angle of the antenna is determined by the required azimuth resolution. Adequate range resolution results in freedom from garbling and is primarily determined by the length of the reply. Range resolution can be further improved if one plane replies for a group of planes flying in tight formation, or if the responsor is capable of separating interlaced replies. (This latter feature is further discussed in a later section.) Whenever garbling occurs, the effect on the responsor is the same as jamming and consequently should be considered as such.

In general, the airborne antenna should be omnidirectional since friendly aircraft are expected to reply to challenges originating at all points of the compass. Fruit will result if replies to challenges from different interrogators are received on the same responsor. Freedom from fruit will result if interrogators in a given IFF net are synchronized so that no two challenge the same sector simultaneously, or if aircraft are equipped with directional antennae. (This latter feature is further discussed in a later section.) Fruit, whenever it occurs, can be considered as jamming and can be dealt with accordingly.

Communication systems operating in the microwave band are seldom bothered by the atmospheric disturbances which affect transmission at radio frequencies. However attenuation due to rainfall increases as higher frequencies are used. On the other hand, the physical size of the antenna required to produce a given

* by Haller, Raymond, and Brown, State College, Pa., as explained in a conference with Northeastern personnel.

beam width increases as lower frequencies are used. Although physical size is not a serious problem for ground installations, it can become an important factor if directional antennas are installed on aircraft. With this thought in mind a brief survey was made in the past and results indicated that over a 200-mile distance an average rainfall rate of 12.5 mm/hr would rarely be exceeded in temperate latitudes, and an average rate of 50 mm/hr would rarely be exceeded anywhere in the world. These results are sufficiently promising that a more complete survey has been initiated by the Propagation Laboratory of AFCRC. It is hoped that the survey will result in a recommendation of the highest operating frequency which can be tolerated in an all-weather IFF system which must operate over a given range.

The following five chapters summarize the findings of Item II insofar as means of improving reliability in presence of enemy jamming are concerned. It is felt that the most pernicious forms of jamming are of the noise and pulse variety since other types can be overcome by appropriate design. Matched filters are discussed as a means of improving the detection of pulses immersed in noise. Pulse-train correlation and redundancy are discussed as techniques for improving reliability in the presence of both noise and pulse jamming. The material discussed in chaps II through V is directly related to the system diagrammed in Fig. 1. Chapter VI discusses other schemes for improving reliability all of which constitute a departure, in some manner or other, from the IFF system which is considered to be the main problem of this item of the contract. Chapter VII summarizes the results obtained under Item III.

CHAPTER II

MATCHED FILTERS

Introduction

Noise is one factor which reduces the reliability of an IFF system. Noise jamming may produce a low signal-to-noise ratio at the input to the receiver; and the noise generated in the input stages of the receiver will reduce the sensitivity to weak signals. Proper choice of the frequency characteristic of the receiver will prevent much of the noise power introduced by these two sources from appearing at the output, and thus improve the ratio of peak-signal amplitude to rms noise voltage. The maximum signal-to-noise ratio can only be obtained when the frequency characteristic of the receiver is developed from the theory of optimum-filter design.

For the purposes of this discussion, optimum filters can be divided into two classes: (1) those which minimize the mean-square error between the output and the actual signal - and thus attempt to preserve waveshape, and (2) those which maximize the peak-signal amplitude to rms-noise ratio - and thus only indicate when the signal occurs. The first class of filters is best suited for those applications where maximum information is only obtained when the filter output is an exact replica of the actual signal. The mean-square-error criterion serves this purpose well since it minimizes the error (i.e. the noise) and therefore produces an output which closely resembles the actual signal. The second class of filters are often referred to as "matched filters" and are optimum for those applications where the signal is known, and the time of occurrence of the signal is the only information which is required. As such, matched filtering techniques can be readily applied to the IFF system.

The correct reply to a given challenge is available at the terminal of the air-to-ground link. Consequently the "signal" for the purposes of matched filtering can be considered to be the "correct" pulse-train reply. The expected challenge, on the other hand, is not available at the terminal of the ground-to-air link, and consequently the correct signal is unknown. However, the "signal" may be redefined as "the pulse used to represent a one in the pulse-train challenge". Under these circumstances matched filtering techniques can be applied to the ground-to-air link and each challenge can be evaluated on a digit-by-digit basis. The improvement in signal-to-noise ratio will be less than that obtained if the challenge were known, but greater than that obtainable with conventional filtering.

The problem of detecting the time of occurrence of a given pulse or pulse train immersed in noise has been extensively treated in the literature.[11-17] In those applications where the noise can be considered white noise, or where the noise is extremely broad-band and the observation time is comparable to the signal duration, the optimum filter is the so-called North, or matched, filter. The impulse response of this filter should be an image of the expected signal, taken about its mid-point in time. The output signal-to-noise ratio is then maximized at the trailing edge of the signal. If the signal is symmetrical about its midpoint in time, the matched filter should have an inpulse response identical with the signal.

B. Video Filter

If a rectangular pulse of duration δ is considered as the signal, the required impulse response may be closely approximated as is shown below. If a voltage impulse is

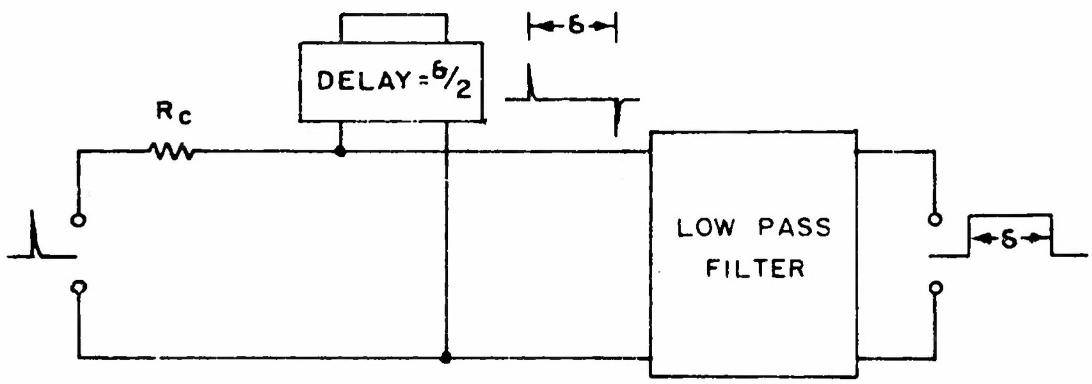

applied to the input, it will appear at half strength across the inputs of the delay line and low-pass filter. Since the delay line is driven from its characteristic impedance R_o, and short-circuited at the far end, a single reflection consisting of a negative impulse will occur. Consequently a positive and a negative half-strength impulse, separated by δ seconds, will appear across the input of the low-pass filter. The output of the filter, and consequently the impulse response of the device, will then be of the form

$$h(t) = \frac{1}{2RC}\left[\varepsilon^{-\frac{t}{RC}} - \varepsilon^{-\frac{(t-\delta)}{RC}} u(t-\delta)\right].$$

If the time constant (RC) of the low-pass filter is long in comparison with δ, the output will be essentially a rectangle described by the expression

$$h(t) \approx \begin{cases} \frac{1}{2RC} & \text{for } 0 < t < \delta \\ 0 & \text{for all other time.} \end{cases}$$

Consequently the magnitude of the gain characteristic of the filter can be expressed as

$$|H(\omega)| = \left|\frac{1}{2RC}\int_0^{\delta} \varepsilon^{-j\omega t}\, dt\right|$$

or

$$|H(\omega)| = \left(\frac{\delta}{2RC}\right)\left|\frac{\sin\frac{\omega\delta}{2}}{\frac{\omega\delta}{2}}\right|.$$

Let the signal applied to the input of the filter be a video pulse defined by

$$v(t) = \begin{cases} v & \text{for } t_1 < t < t_1 + \delta \\ 0 & \text{for all other time.} \end{cases}$$

It has been shown in the Quarterly Progress Reports of this contract, that under these conditions, the maximum ratio of peak-signal-power to rms-noise-power at the output is given by $P_{S/N\ max} = \frac{\delta V^2}{N_0}$, where N_0 is the power-spectral density of the input noise. The ratio of the above value of $P_{S/N}$ to that obtained with an R-C low-pass filter with its half-power point located at $f = 1/\delta$ was shown to be 3.14, thus indicating an improvement of 4.97 db. A matched filter was constructed for a rectangular pulse of 0.6 µs duration and is shown in Fig. 3. Two inputs are provided: one for signal pulses and the other for noise. The first tube and its associated circuitry comprise the adding circuit, while the second tube serves as delay-line driver. The delay is obtained with a six-inch length of Millen delay cable. The input impedance of the low-pass filter is made large in comparison with the characteristic impedance of the delay line in order to avoid loading difficulties.

The frequency response of the circuit was measured between the signal input and output terminals and is plotted in Fig. 4. The crosses indicate the experimental data while the smooth curve was plotted from the expression

$$\frac{\sin\left(\frac{\omega\delta}{2}\right)}{\left(\frac{\omega\delta}{2}\right)} \qquad \text{where} \qquad \delta = 0.645\ \mu s.$$

Although the delay line was cut to give 0.6 µs two-way delay time, there was evidently some discrepancy between the time and frequency measurements as it was found that the theoretical curve for $\delta = 0.645$ µs was the best fit to the experimental data. The close agreement between the experimental data and theoretical curve serves to illustrate the accuracy which can be achieved with the design incorporated in the matched filter.

Evaluation of the performance of the filter in the presence of noise has been undertaken. Tests have fallen under two catagories: visual observation, and measurement.

Visual testing has been undertaken with an oscilloscope. Broad-band Gaussian noise and a δ-second rectangular pulse were combined linearly in the adding circuit of the matched video filter. The output from the filter was observed on an unsynchronized oscilloscope. The pulse amplitude of the signal was adjusted until it was readily observed at the output. Then the oscilloscope was transferred to the input of the filter and the signal amplitude readjusted until the pulse could be discerned equally well above the input noise. The ratio of the two values of pulse amplitude was then converted

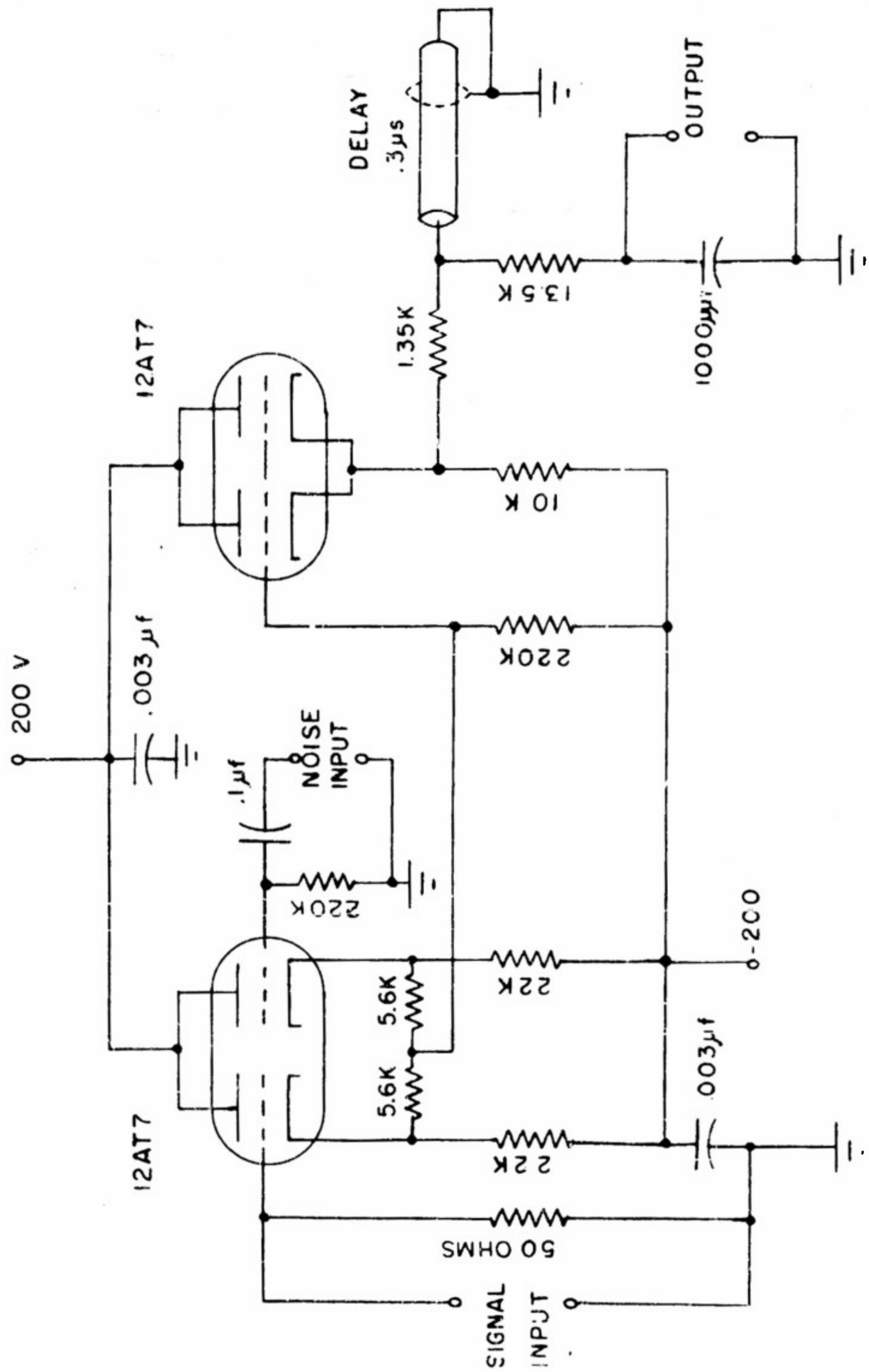

FIG. 3. MATCHED FILTER FOR 0.6 μs. PULSES.

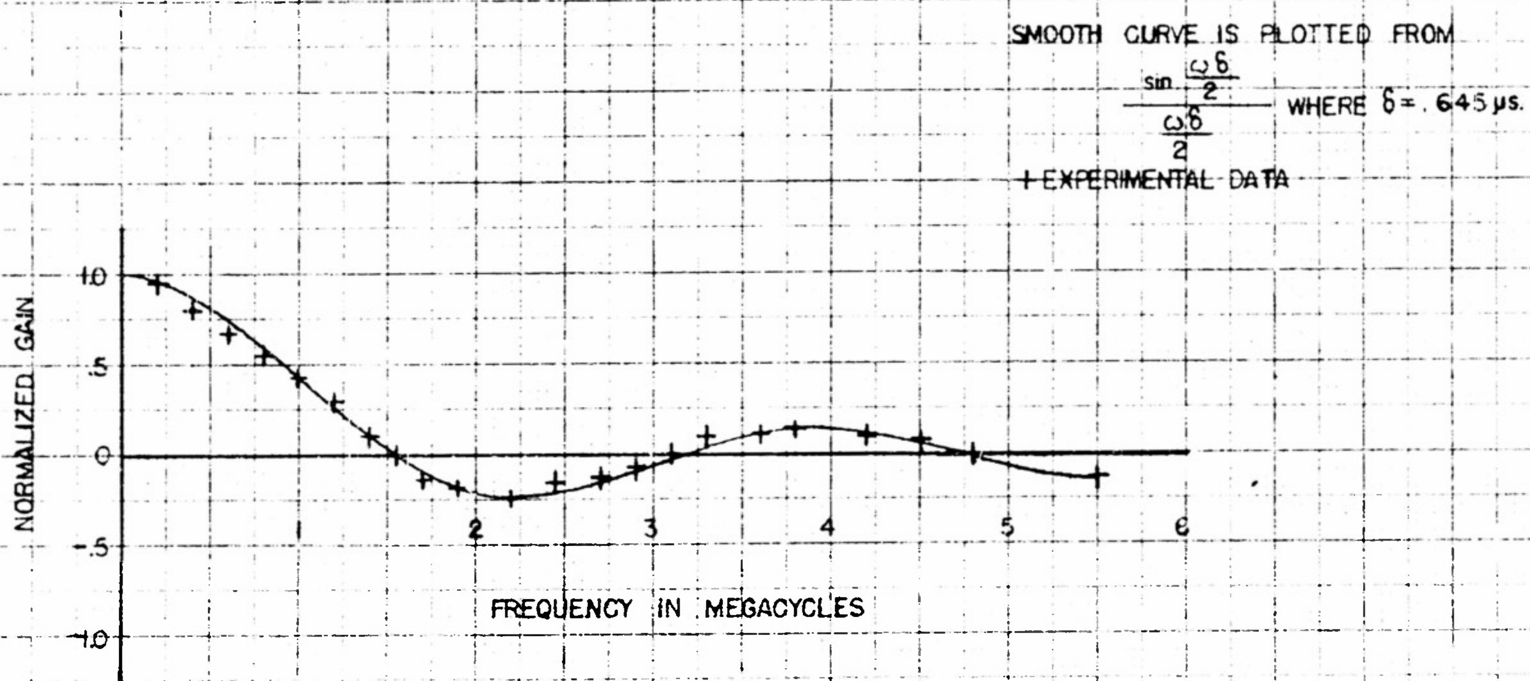

FIG. 4. THEORETICAL AND EXPERIMENTAL FREQUENCY RESPONSE OF MATCHED VIDEO FILTER.

to a power ratio and compared to the power ratio obtained when the same test was performed on a 0-to-$\frac{1}{\delta}$ cps low-pass filter. The resulting ratio indicated an improvement in peak-signal power to noise-power ratio of about 2 or 3. This result is the same order of magnitude as the value 3.14 which was calculated previously.

The second method of testing employed a similar test set-up. Once more the pulse amplitude was adjusted until the pulse was readily observed at the output. Then each input to the adding circuit was separately reduced to zero and the remaining excitation measured at both input and output of the filter. The pulse amplitude was measured with a calibrated oscilloscope, and noise voltage with a wide-band rms voltmeter. Similar measurements were then made on the 0-to-$\frac{1}{\delta}$ cps low-pass filter and an improvement of 2.56 obtained.

The discrepancy between the above results and the computed value of 3.14 is probably largely due to the fact that the rms voltmeter was primarily designed for measurement of sinusoidal voltages. A thermocouple type of voltmeter should be used for accurate measurement of noise voltage. However, the results are close enough to the predicted values and consequently indicate that matched filters of this type can be realized with simple circuitry.

C. Pulse-Train Filter

A matched filter for a pulse train can be obtained by following the above mentioned filter by a tapped delay line and adding circuit as shown below.

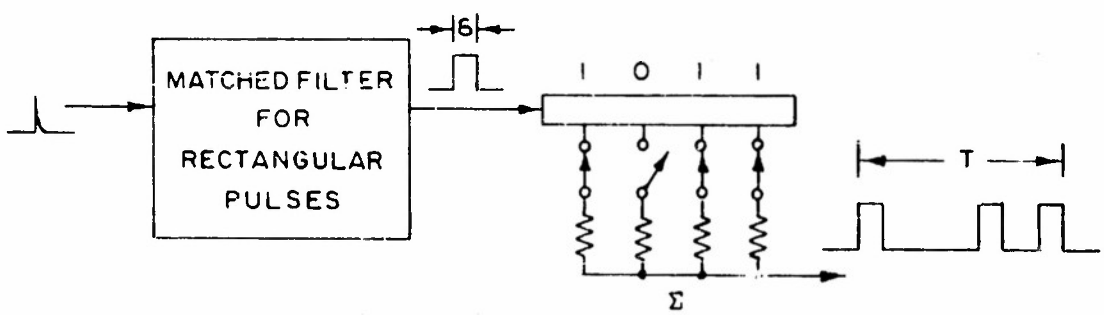

The block diagram illustrates the filter for the signal 1101. Any expected signal can be set into the filter by means of the switches. The switches are set from right to left so that the impulse response will be the image of the signal. The S/N ratio at the output is maximized at the end of the signal.

The impulse response h(t) and the correct signal s(t) are related by the expressions

$$h(t) = s(T-t) \text{ for } 0 < t < T$$
$$h(t) = s(T-t) = 0 \text{ for all other } t .$$

If the signal and additive white noise n(t) are applied to the input of the filter, then the output y(t) is given by the convolution integral as

$$y(t) = \int_{-\infty}^{\infty} s(T-t+\tau)[s(\tau)+n(\tau)]d\tau.$$

If t is replaced by $T \pm t'$, then the above expression may be rewritten as

$$y(T \pm t') = \int_{-\infty}^{\infty} s(\tau \mp t')[s(\tau)+n(\tau)]d\tau.$$

This latter expression indicates that the output of the filter, taken about $t=T$, is proportional to the crosscorrelation of the signal with the input to the filter. (The fact that t or t' can have negative values is not disturbing once it is recognized that although the signal started at $t=0$, the noise $n(t)$ had been in existence previously.)

The following chapter discusses a pulse-train correlator of the above type for application at the terminal of the air-to-ground link. This correlator is modified to include additional features for overcoming the effects of pulse-jamming. The matched filter for rectangular pulses which preceeds the delay line is omitted from that discussion since it is considered in this chapter.

Whereas video crosscorrelation, as described above, is relatively easy to carry out equipment-wise, it will not yield the improvement in reliability that could be expected if the operation were performed in the i-f section of the receiver, i.e. before the signal is passed through the non-linear second detector. (The mixer acts as a linear device as long as the local-oscillator output is large compared to the r-f signal.) The construction of an entire correlator in the i-f section, however, would be a difficult task. Consequently the tapped delay line portion of the correlator has been reserved for the video section. A prototype matched i-f filter for pulses has been constructed for use at both the ground and air terminals of the IFF system.

D. Matched I-F Filter

When the signal is a pulsed carrier, the required impulse response can be closely approximated by a delay line and narrow-band filter as shown below.

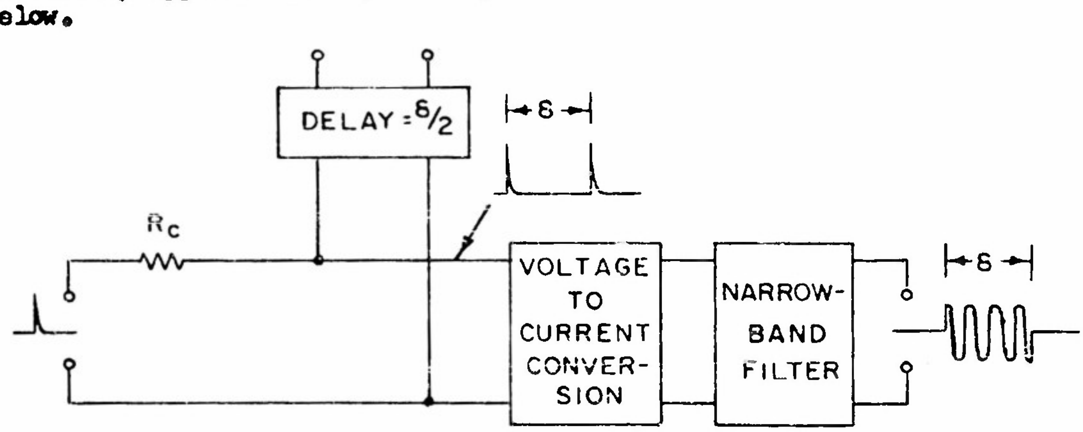

If a voltage impulse is applied to the input of the circuit, two positive current impulses separated by the two-way delay time, δ, will appear at the input to the narrow-band filter. If the filter consists of a high-Q tank circuit, the first impulse will produce a damped cosinusoid at the output. The second impulse will stop the oscillation if Q is large, and the resonant frequency of the circuit is such that $N + \frac{1}{2}$ (where N is an integer) cycles have been produced in the time δ.

A filter of this type will give a maximum output for a signal which is the image of its impulse response. However, since δ is usually large in comparison with the period of the carrier, the phase of the carrier will be relatively unimportant, as the peak output will be within a few percent of the theoretical maximum if phase coherence does not exist.

A matched filter was constructed for a pulsed-carrier and is shown in Fig. 5. The proper signal should have a duration of 0.6 µs, a 30.6 mc carrier, and a rectangular envelope. Tube V1 acts as a delay-line driver. Approximately 150 feet of RG 62/U cable is used for a delay line since time has not permitted the design of a compact delay unit. Tube V2 is used as a phase inverter to compensate for the attenuation of the delay line by subtracting the correct amount from the incident wave. Tube V3 drives the narrow-band filter, and V4 is used for an output driver. Positive feedback is employed to increase the effective Q or the narrow-band filter.

The frequency response A of the filter can be written as $A = A_1 A_2$, where A_1 is the frequency response between the input and the grid of V3, and A_2 is the frequency response between the grid of V3 and the output. The magnitude of A_1 can be expressed as

$$\left|A_1\right| = \left|\cos \frac{\omega\delta}{2}\right| .$$

At the carrier frequency, f_0, A_1 is equal to zero and consequently the above expression can be written about f_0 as

$$\left|A_1\right| = \left|\sin \frac{u\delta}{2}\right| \quad \text{where} \quad u = 2\pi(f-f_0).$$

The frequency characteristic of the remainder of the amplifier can be expressed as

$$A_2 = \frac{A_2'}{1-A_2'\beta - 4\left(\frac{u}{\omega_0}\right)^2 (Q_3Q_4) + j2\left(\frac{u}{\omega_0}\right)Q}$$

where A_2' = the open-loop gain at f_0
β = the feedback ratio
Q_3 = the quality factor of the stage containing V3
Q_4 = the quality factor of the stage containing V4
and $Q = Q_3 + Q_4$.

Over the frequency range where the imaginary term in the denominator is much greater than the real term,

$$\left|A_2\right| \approx \left|\frac{\frac{\omega_0 A_2'}{2Q}}{u}\right| = \left|\frac{\frac{\omega_0 A_2'\delta}{4Q}}{\frac{u\delta}{2}}\right| .$$

Consequently, under the above assumptions, $|A|$ may be expressed as

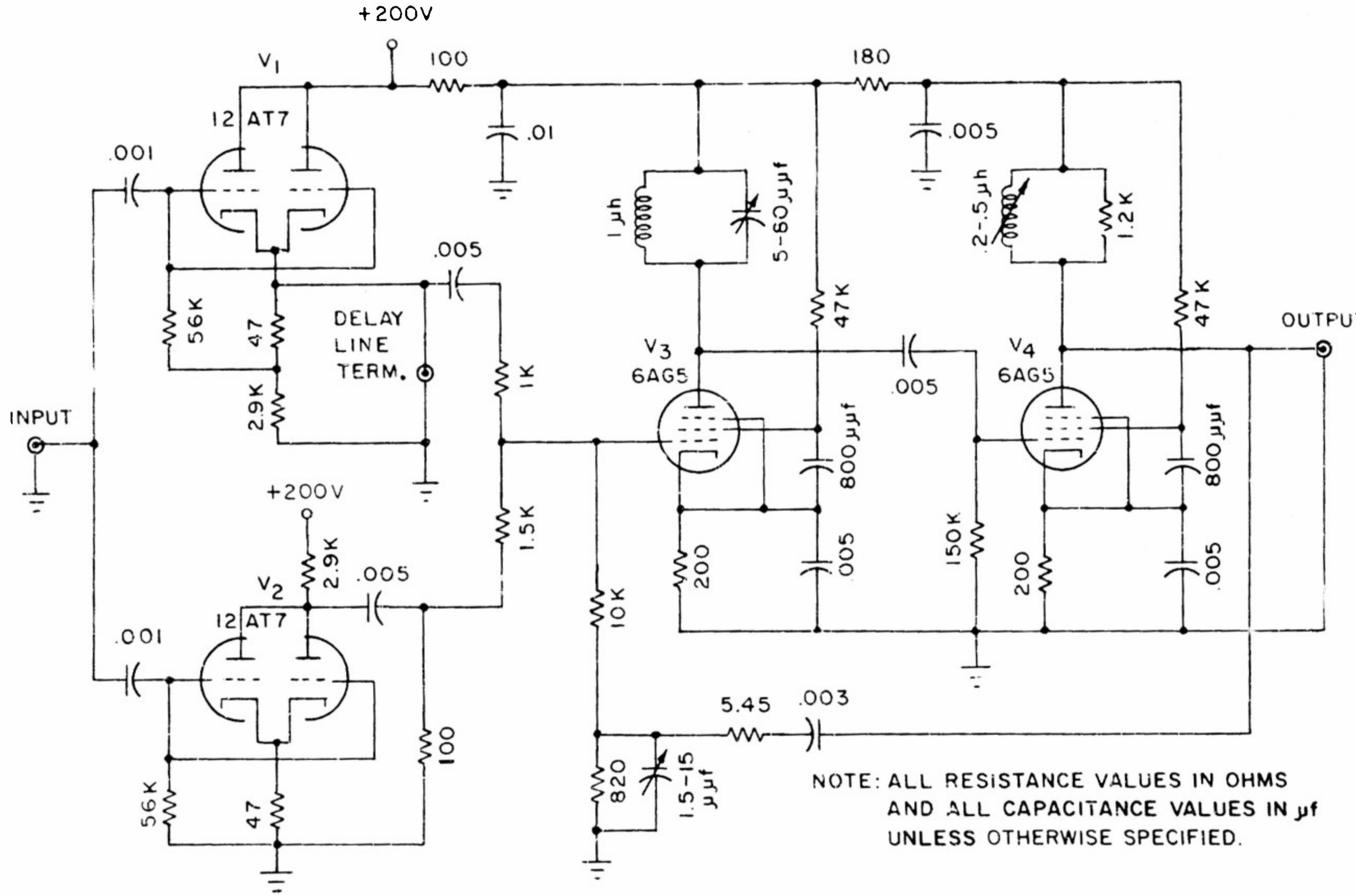

NOTE: ALL RESISTANCE VALUES IN OHMS AND ALL CAPACITANCE VALUES IN μf UNLESS OTHERWISE SPECIFIED.

FIG. 5. MATCHED FILTER FOR PULSED CARRIER.

$$|A| \approx \frac{\omega_0 A_2' \delta}{4Q} \left| \frac{\sin \frac{u\delta}{2}}{\frac{u\delta}{2}} \right| .$$

The above expression is most accurate for large values of u and least accurate in the vicinity f_0. As β is increased, the approximation becomes more accurate. In the limit, when $1-A_2'\beta = \epsilon$ and ϵ is a small positive number, the above expression holds everywhere except at f_0 where $|A|$ is equal to zero.

The measured frequency characteristic of the filter is shown in Fig. 6. The dissymmetry is apparently due to the fact that the r-f section of the filter is tuned to a slightly higher frequency than the 30.6 mc prescribed by the 0.6 μs delay. The characteristic is of the correct form for frequencies above 31.3 mc and below 29.9 mc. Further refinements are not felt necessary as the pulse response of the filter is extremely good.

The response of the matched filter to various pulse widths is shown in Fig. 7A. The pulses used as input signals had a rise time of less than .04 μs and a carrier frequency of 30.6 mc. The uppermost trace results from a .1 μs pulse, the middle trace from a 0.6 μs pulse, and the lower trace from a 1.0 μs pulse. The output waveforms are in accordance with results expected from correlation theory. Each output waveform, taken about its axis of symmetry, represents the crosscorrelation function of the input signal with the image of the impulse response of the filter.

The theoretical improvement in signal-to-noise ratio has been shown in the Quarterly Progress Reports of this contract to be 4.97 db above that obtained with a $2/\delta$ cps band-pass filter. The actual improvement in S/N ratio is demonstrated by the waveforms of Fig. 7B. The input signal consisted of a 0.6 μs pulse and additive noise resulting from modulating a 30.6 mc carrier with 0-5 mc Gaussian noise. The input signal is shown as the upper trace and the output signal is shown as the lower trace. A more rigorous determination of the improvement in S/N ratio should be undertaken. Contemplated tests are indicated in Chapter IV.

The experimental results obtained with the above filter are quite promising. However, in its present state it is not ready for direct application in a useable IFF system. A compact delay unit to replace the 150 ft. of RG 62/U cable must be constructed. The Q-multiplier section of the filter should probably be redesigned in order to achieve increased stability[18] for military useage. Some form of automatic frequency control will probably have to be introduced into the i-f section of a receiver, in order to compensate for drift in the transmitter frequency.

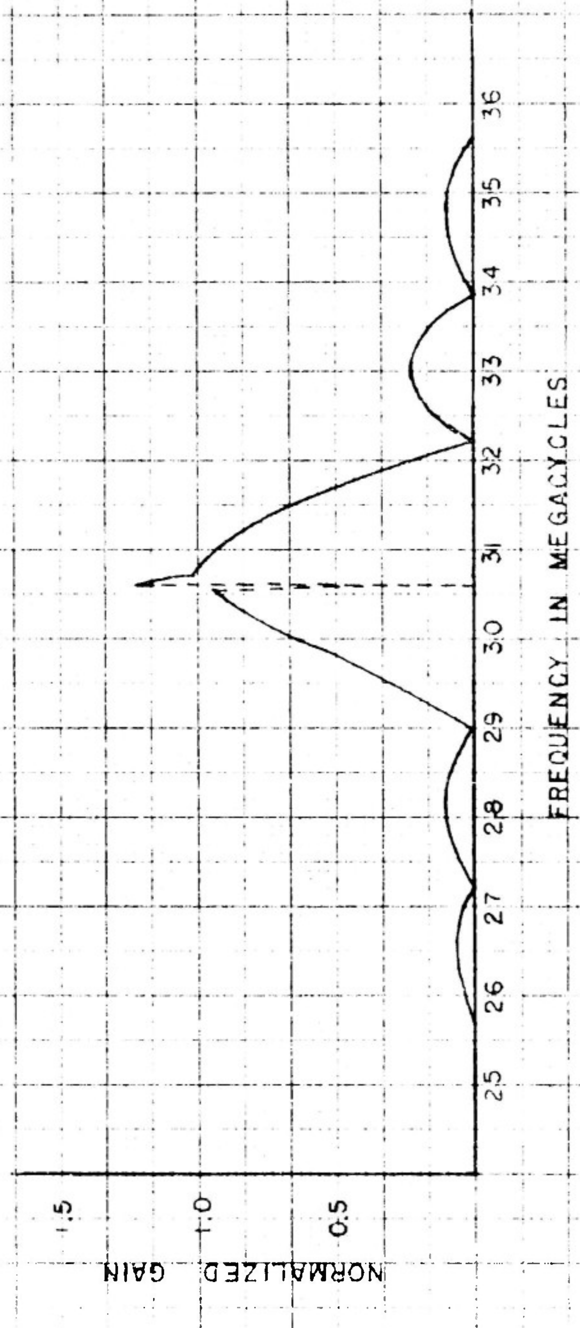

FIG. 6. GAIN CHARACTERISTIC OF MAT HED i-f FILTER.

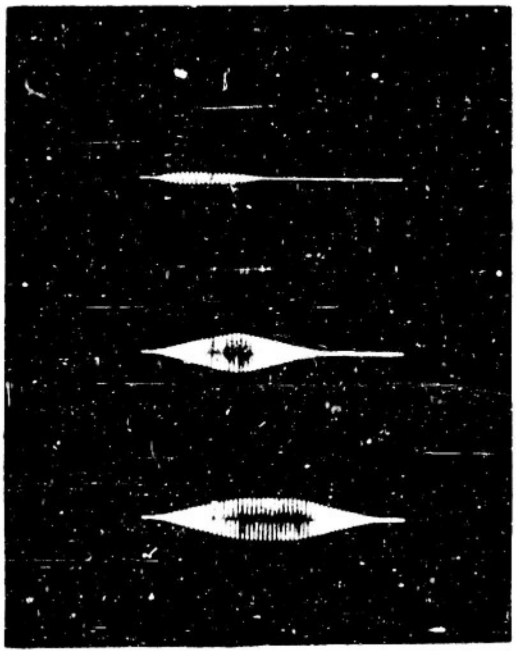

A. RESPONSE OF FILTER TO PULSES

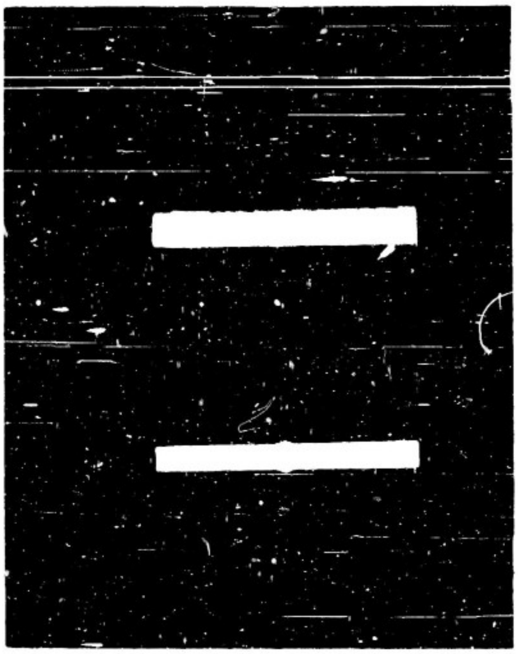

B. INPUT AND OUTPUT OF FILTER

FIG. 7. WAVEFORMS FOR MATCHED I-F FILTER.

CHAPTER III

PULSE-TRAIN CORRELATION

A. Introduction

Correlation techniques have received widespread attention in the last decade as means of improving signal-to-noise ratio. Of the two kinds of correlation, i.e. autocorrelation and crosscorrelation, autocorrelation seems to be of little value in communication systems which are subject to jamming, since for every type of bona fide signal a jamming signal can be produced which will autocorrelate just as effectively as does the friendly signal. Crosscorrelation, on the other hand, holds promise of great usefulness in comparing the received signal with a locally available version as well as for improving the signal-to-noise ratio.

Mathematically speaking the crosscorrelation function of two time functions $f_1(t)$ and $f_2(t)$ is defined as $\phi_{12}(\tau) = \lim_{T\to\infty} \frac{1}{2T}\int_{-T}^{+T} f_1(t)\, f_2(t-\tau)\, dt$. For our application, however, a more interesting function is the time function $\psi_{12}(t) \equiv \frac{1}{T}\int_{t-T}^{t} f_1(t')\, f_2(t')\, dt'$, which is obtained from the general crosscorrelation function by letting $\tau = 0$ and averaging the instantaneous product of the original time functions over the finite time interval from $(t - T)$ to t instead of over all time.

The theory of the use of crosscorrelation for communication of continuous time functions in the presence of noise has been discussed by Fano, Davenport, and others[19,20,21]. They consider the case where $f_1(t)$, representing the time function to be transmitted, is also available at the receiver and is to be correlated with $f_2(t) = f_1(t) + N(t)$, where $N(t)$ is the noise introduced in the transmission link. Their results show that the resulting signal-to-noise power ratio is $\left(\frac{S}{N}\right)_o \approx \frac{a_S + a_N}{a_F}\left(\frac{S}{N}\right)_i$, where a_S is the bandwidth of the signal $f_1(t)$, a_N is the bandwidth of the noise $N(t)$, a_F is the bandwidth of the correlation averaging filter ($a_F \approx 1/T$), and $(S/N)_i$ is the signal-to-noise power ratio of $f_2(t)$. If, on the other hand, $f_1(t)$ is not directly available at the receiver but has to be transmitted over a separate channel subject to the addition of noise, the resulting signal-to-noise power ratio becomes

$$\left(\frac{S}{N}\right)_o \approx \frac{2a_N}{a_F}\left(\frac{S}{N}\right)_i^2 \qquad \text{(Approximation for } (S/N)_i < 1).$$

If the signal $f_1(t)$ is a rectangular-pulse train, $f_1(t)$ can have only two possible values a and b, and $f_2(t)$ will be either $c + N(t)$ or $d + N(t)$, respectively. The integration can be replaced by a summation over all n corresponding

pairs of places of the two pulse trains, the pulses adding algebraically and random noise adding as the square root of the sum of the squares of its rms values.

B. Tapped-delay-line Correlator

An easy and efficient way of crosscorrelating a received pulse train with one already available (such as in the responsor of an IFF system) is to use a tapped delay line to convert the time sequence of the incoming pulse train to a space sequence*, and to use phase inverters and switches to multiply each pulse position by the stored function. This system, illustrated by the block diagram in Fig. 8, has the advantage that the stored pulse train does not have to be generated in synchronism with the received one.

It seems advantageous from the point of view of noise rejection to operate all the circuitry ahead of the adding bus class A, in other words, not to decide at each tap of the delay line individually whether a pulse exists there or not, but first to compile all the relevant information (in the adder), and then to decide (by a threshold circuit) whether a "correct" pulse train has been received. If the pulse train has n places of which m are pulses of height S, the signal in the adder will equal mS. If, on the other hand, the noise of mean value zero and of rms value N, existing at each tap, is independent of that at all other taps, the rms noise in the adder will be given by $\sqrt{N^2 + N^2 + \ldots \text{(n such terms)}} = \sqrt{nN^2} = N\sqrt{n}$. It is then evident that by the addition the signal-to-noise voltage ratio (for random noise) has been multiplied by a factor $m/\sqrt{n}$ over that in the video output of the receiver. (This corresponds to multiplying the signal-to-noise power ratio by m^2/n). The threshold device therefore can identify a correct pulse train with comparably increased reliability.

If the noise at each tap has mean value $\bar{N} \neq 0$, the rms noise in the adder becomes $\sqrt{nN^2 + ({}^mC_2 + {}^kC_2 - mk)\bar{N}^2}$** as a result of the inclusion of cross-product terms. Hence, the signal-to-noise ratio in this case has been multiplied by a factor which is greater than, equal to, or less than $\frac{m}{\sqrt{n}}$ according to whether ${}^mC_2 + {}^kC_2 - mk$ is negative, zero, or positive respectively, and it can be shown that this is equivalent to the condition that $|m-k|$ is less than, equal to, or greater than $\frac{1}{2}(1 + \sqrt{1 + 8\min\{m,k\}})$. In particular, if m=k, the improvement factor is better than $\frac{m}{\sqrt{n}}$ when the mean value of the noise is not zero.

Tap Spacing

The coincidences of some of the pulses with delay-line taps that occur prior to and subsequent to the instant of complete alignment of the incoming

* To this point, the system is identical to that discussed in references 2 and 22.

** The symbol ${}^rC_s$ is defined as $\frac{r!}{s!(r-s)!}$

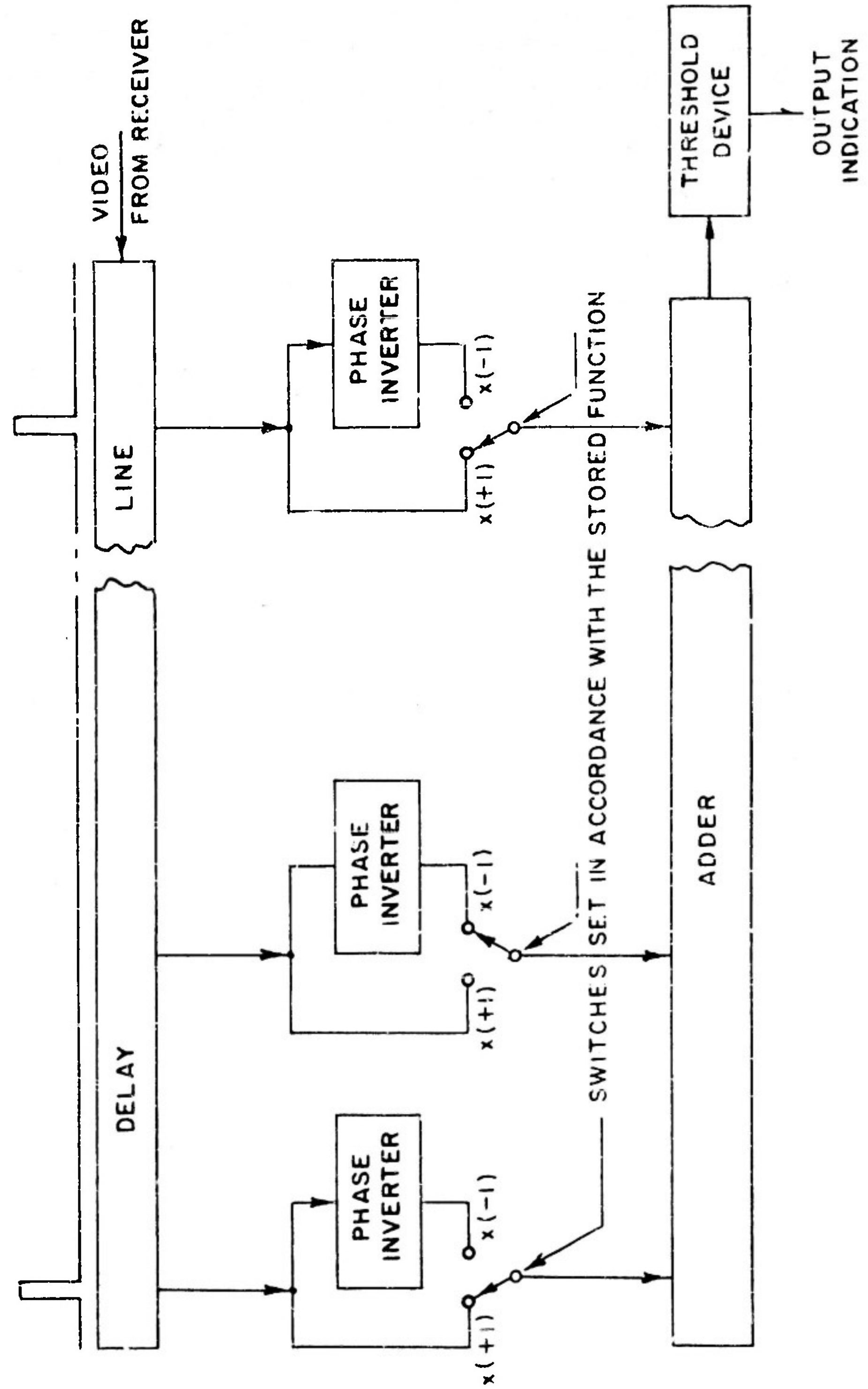

FIG. 8. SIMPLIFIED BLOCK DIAGRAM OF PULSE-TRAIN CORRELATOR.

pulse train with the taps will produce undesirable signals in the adder, similar in effect to pulse jamming. This difficulty can be minimized by spacing the digit positions of the pulse train (and hence also the taps on the delay line) at unequal intervals, in fact, assigning these intervals such values that, as the pulse train moves down the delay line, there never will be more than one digit position at a tap of the delay line at one time, except, of course, at the instant of complete alignment. In this way, the amplitude of the spurious signals in the adder is limited to that of one received pulse, whereas at the instant of complete alignment an output pulse of m pulse heights is produced.

This requirement can be satisfied by making the spacings between the n taps (or digit positions) multiples of one pulse width and, within that constraint, assigning them such values that the spacing between <u>any</u> two (not necessarily adjacent) taps be unique for that particular pair of taps. Restated in terms of the spacings between <u>adjacent</u> taps, this means that <u>these</u> spacings must form a sequence of n-1 integers (representing pulse-widths) with the property that the sum of <u>any</u> j <u>adjacent</u> integers (where j can be any numbers from one to n-1) be unique to that particular set of j numbers. A further obvious condition is that the sum of the complete sequence be the smallest possible number, since this sum determines the length of the delay line.

To date no systematic way of arriving at such a sequence has been found, and a trial-and-error method was used to obtain the sequence in use in the present eight-digit correlator. In this method it has been found expedient to check the proposed sequence by writing it in a horizontal line and constructing above it a pyramid of numbers such that each number s represents the sum of the base numbers that are included in the sub-pyramid which has s as apex. The sequence then fulfills the above conditions if no number occurs twice anywhere in the pyramid, and if the uppermost number (representing the sum of the sequence) is as small as possible. On the sequence in use at present, the further condition was imposed that its smallest number be 2 rather than 1 in order to obviate the necessity of generating a pulse train in which two pulses are contiguous, since this represents somewhat of a circuitry problem. The sequence and its pyramid are shown below.

```
                  39
               35    36
            30    32    29
         18    27    25    23
      16    15    20    19    21
   10    13     8    14    17     9
 3     7     6     2    12     5     4
```

<u>Choice of Levels and Pulse-train Characteristics</u>

The block diagram (Fig. 8) of the pulse-train correlator indicates that, depending on the setting of each switch, the signal at the corresponding tap is fed to the adder either via a phase inverter of presumably unity gain, or directly. This scheme, therefore, implies that the two possible values of the stored function $f_1(t)$ are -1 and +1. Furthermore, in the calculation of the signal-to-noise ratio in the adder, it was assumed that the received function $f_2(t)$ has the possible values $0 + N(t)$ and $S + N(t)$. Since, in the most general system, the corresponding levels are a and b for $f_1(t)$, and $c + N(t)$ and

$d + N(t)$ for $f_2(t)$, a justification of the indicated choices is in order. Connected with this problem is the choice of the optimum number of ones in an n-digit pulse train. It will be shown that for best all-around performance half of the digits should be ones.

When considering the general levels given above, it is seen immediately that c, the level of the received function at the "zero" positions (disregarding noise), should equal zero, since it cannot take on a negative value, and since a positive value of c would only decrease the spread between "zeros" and "ones" while at the same time raising the average power requirement of the transmitter.

It is also apparent that no generality is lost if $f_1(t)$ is normalized with respect to b, so that instead of a and b its levels become $x = a/b$ and 1 respectively. Similarly $f_2(t)$ can be normalized with respect to d, thus changing its levels $N(t)$ and $d + N(t)$ to $N_1(t)$ (where $N_1(t) = \frac{N(t)}{d}$) and $1 + N_1(t)$ respectively. (Note that $1/N = \frac{d}{N}$ is the input signal-to-noise voltage ratio, where N and N_1 are defined as the rms values of $N(t)$ and $N_1(t)$ respectively; also that in these terms the system described above has the value $x = -1$.)

It is now possible to calculate $(\Sigma f_1(t)\ f_2(t))_{S+N}$ — the voltage existing in the adder if the correct pulse train, contaminated with noise, was fed into the delay line; subtract from it $(\Sigma f_1(t)\ f_2(t))_N$ — the output of the correlator if only noise was fed in; and divide this difference (representing the output signal) by the latter amount to get the output signal-to-noise voltage ratio. Remembering that in the first case at each of the m taps where a pulse exists we get a contribution $1 \cdot (1 + N_1)$, these contributions adding up to $m + N_1[m]$, (here $N_1[m]$ represents the rms value resulting from the addition of m terms of noise, each of rms value N_1) and that at each of the k taps where no pulse exists the contribution is x, adding up to $x \cdot N_1[k]$, we have:

$$(\Sigma f_1(t)\ f_2(t))_{S+N} = m + N_1[m] + x \cdot N_1[k],$$

and similarly:

$$(\Sigma f_1(t)\ f_2(t))_N = N_1[m] + x \cdot N_1[k].$$

Therefore the output signal $S_o = m$*,

$$\text{and} \quad \left(\frac{S}{N}\right)_o = \frac{m}{N_1[m] + x \cdot N_1[k]}.$$

This expression shall now be considered in connection with pulse jamming, where it must be borne in mind that, regardless of how the jammer times the transmission of jam pulses, they will arrive in essentially random positions of the friendly signal, due to the varying traveling time of the jam and friendly signals. The expected value (in the statistical sense) of the effect of such

* This result can also be obtained by inspection of the normalized levels.

random pulse jam in the adder is zero if x is given the value $-\frac{m}{k}$. For this value of x the expression becomes

$$\left(\frac{S}{N}\right)_o = \frac{m}{N_1[m] - \frac{m}{k} N_1[k]} \qquad \left(\text{if } x = -\frac{m}{k}\right)$$

A relation between m and k can be obtained by analyzing this expression for the case where N_1 is random noise. One obtains

$$\left(\frac{S}{N}\right)_o = \frac{m}{\sqrt{N_1^2 + N_1^2 + \ldots \text{(m such terms)} + \frac{m^2}{k^2} N_1^2 + \frac{m^2}{k^2} N_1^2 + \ldots \text{(k such terms)}}}$$

$$= \frac{m}{N_1 \sqrt{m + \frac{m^2}{k}}} = \frac{1}{N_1 \sqrt{\frac{1}{m} + \frac{1}{k}}} \,.$$

Maximizing this expression, subject to the constraint that n = m + k = constant, yields m = k, from which follows that x = -1. These values, then, have been adopted in the further design of the pulse-train correlator. The problem created thereby, namely that of converting an arbitrary n-place binary number to one having an equal number of ones and zeros, is discussed in some detail in Appendix I.

Derivation of Threshold Formula

In the development of a formula for the threshold voltage the major emphasis was placed on the importance of combatting pulse jamming. Stating this problem more precisely, the probability of obtaining an output when, in addition to pulse jam, there is a "correct" pulse-train present should be maximized, without allowing an output due to the pulse jam in the absence of a "correct" pulse train. (The obvious exception to this latter clause is the case where jam pulses happen to occur at all of the "m" places and at none of the "k" places, thus making the jam indistinguishable from a "correct" pulse train. This exception, however, is the only one that is tolerated.)

These requirements suggest the desirability of a positive contribution to the threshold voltage proportional to the height J of the jam pulses, and of a negative contribution proportional to the height S of the signal pulses, so that jam alone will raise the threshold enough to prevent an output from the threshold device but that the addition of a sufficient amount of "correct" signal will bring the threshold back down enough to allow an output to occur. In symbols, we have, then: $V_T = AJ - BS$, where A and B are positive parameters yet to be determined.

In order to carry out such a scheme it is necessary to obtain reasonably reliable estimates of the magnitudes of S and J from the existing video signal. How this can be accomplished using minimum and maximum tap voltages can be seen from the diagrams in Table I, wherein the variables M and K represent

TABLE I. POSSIBLE JAM CONFIGURATIONS.

K \ M	M = O	O < M < m	M = m
K = O	(no jam) $V_T = -BS$	$V_T = AJ - BS$	(jam indistinguishable from signal) $V_T = -B(S+J)$
O < K < k	$V_T = AJ - B(S-J)$	$V_T = AJ - BS$	$V_T = AJ - BS$
K = k	$V_T = AJ - B(S-J)$	$V_T = AJ - BS$	$V_T = AJ - BS$

$$V = A \max \{k_{max}, m_{max} - m_{min}\} - B \min \{m_{min}, m_{max} - k_{max}\}$$

■ JAM

⊓ SIGNAL

the number of "m" and "k" taps respectively at which at a given instant a jam pulse exists, so that $M = 0$ means that there is no jam pulse at any of the "m" taps, $0 < M < m$ means that there are one or more jam pulses at some (but not all) of the "m" taps, and $M = m$ that there are jam pulses at all of the "m" taps. (Similarly with $K = 0$, $0 < K < k$, $k = k$). It can now be seen that, except in the top row of the table, J can be described as the maximum signal existing at any one of the "k" taps (this value will be represented by the symbol k_{max}), whereas in the top row (except in the first box where no jam exists, and in the last box where the jam is indistinguishable from the signal), J can be represented by $m_{max} - m_{min}$. Since it is considered more important to prevent erroneous outputs from the threshold device than to prevent the occasional loss of correct pulse trains (since, in other words, in the interest of safety, the threshold should be set too high rather than too low), the best estimate of J is the greater one of the two expressions given above, or, symbolically: $\max\{k_{max}, m_{max} - m_{min}\}$.

Referring again to Table I, S is equal to m_{min} everywhere but in the last column, where, however, S can be represented by $m_{max} - k_{max}$ (except again in the highest box which need not be considered). Bearing in mind that S is to yield a negative contribution to the threshold, the "safe" estimate for S is: $\min\{m_{min}, m_{max} - k_{max}\}$. We therefore arrive at the formula for the threshold voltage:

$$V_T = A \max\{k_{max}, m_{max} - m_{min}\} - B \min\{m_{min}, m_{max} - k_{max}\}$$

The block diagram of Fig. 9 shows how such a threshold voltage can be realised.

A condition on the value of A in the above expression can be found by considering the case where a "correct" signal is absent and a pulse jam is introduced which differs from the "correct" signal in only one place, giving rise to an adding bus signal of intensity $(m - 1)$ J, and a threshold voltage AJ. (The two possibilities are shown below.)

"m" places "k" places

$V_T = AJ$

Since no output is allowed in this case, A must be greater than $m - 1$, or $A = m - 1 + \alpha$, where α is a positive constant.

It is expected that the optimum values of α and B will depend on the amount of noise present in the video signal. In the absence of all noise a value of α almost equal to zero and a very large value of B would give very good resistance to constant-amplitude pulse jamming. Conditions on the choice of B (and α) required to combat noise and noise-jamming can in principle be determined by calculating the probability distribution for V_Σ (the adding-bus voltage) and V_T for assumed probability distributions of the noise. Since this calculation, as discussed below under "Behavior of Pulse-Train Correlator in Presence of Noise" appears to be too complex to yield useful results, a working model will be used to obtain the desired information experimentally.

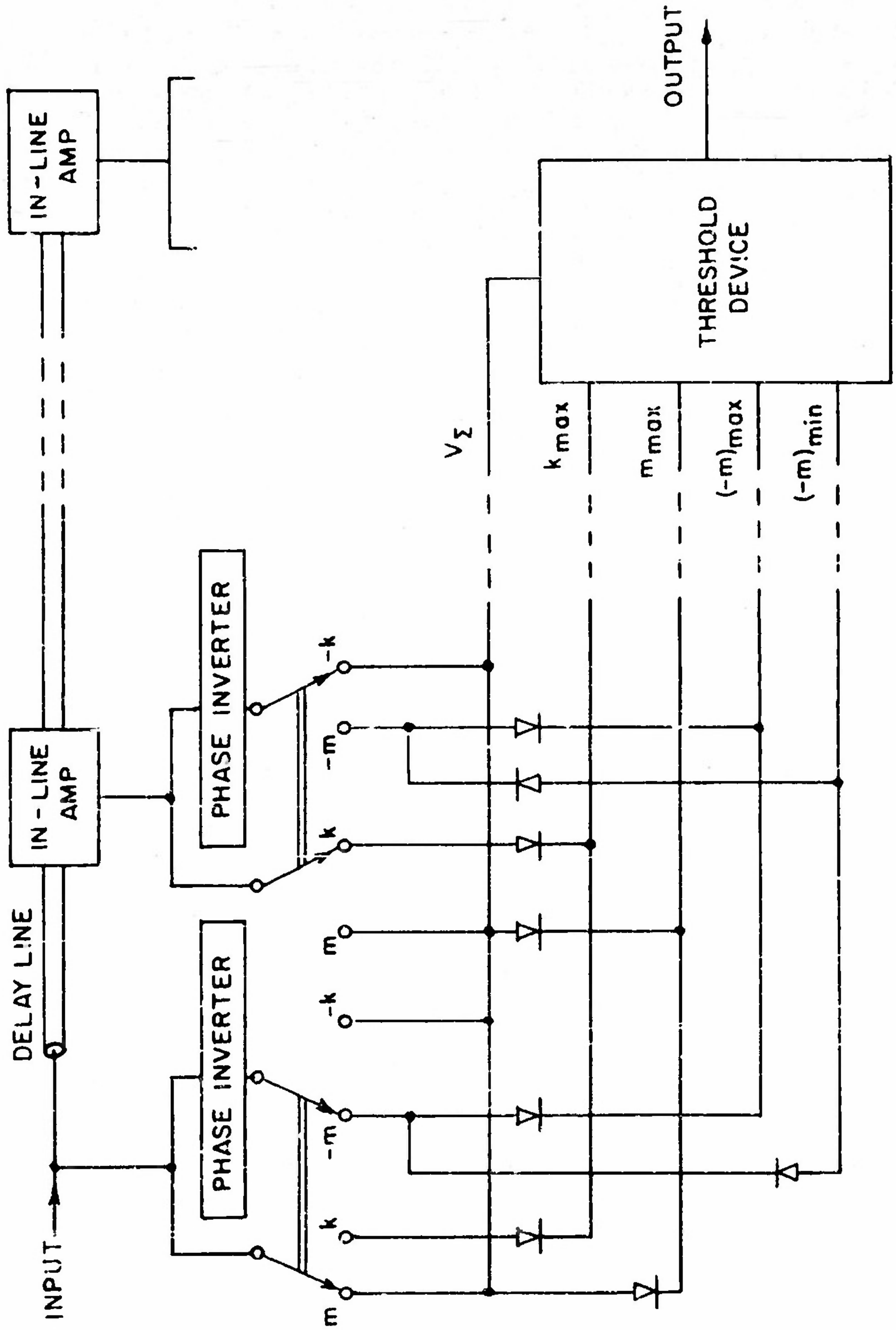

FIG. 9. BLOCK DIAGRAM OF PULSE-TRAIN CORRELATOR.

A more detailed analysis of the behavior of such a correlator in the presence of constant-amplitude pulse jamming has been worked out in Table II, which is laid out in accordance with the values envisioned for the working model under construction. These values are: $m = k = 4$, hence $A = 3 + \alpha$. All possible values of M and K are considered, and the probability of occurrence p of each combination of M and K is calculated for the condition that the probability P, that a jam pulse will coincide with any particular place of the pulse train, is one-half. In this table, then, the first entry in each box is the probability of occurrence p of that box for $P = \frac{1}{2}$; the second entry is the signal V_Σ present in the correlator adding bus in terms of the signal and jam intensities S and J respectively; the third entry is the threshold voltage in terms of S, J, α, and B; and the last entry is the S/J ratio necessary to obtain an output. It should be noted that, except in the first column of the table, α occurs only in the numerator and B only in the denominator of the S/J expressions, indicating that for sufficiently small α and sufficiently large B, S/J ratios appreciably smaller than one will still give satisfactory operation. This can be seen more clearly from the curves in Fig. 10, which, for $\alpha = 1$ and various values of B, show the probability of obtaining an output due to a "correct" pulse-train input in the presence of constant-amplitude pulse jam of signal-to-jam ratio S/J and of probability of occurrence of a jam pulse $P = \frac{1}{2}$.

C. Behavior of Pulse-train Correlator in Presence of Noise

In order to evaluate the reliability of the pulse-train correlator in the presence of noise, and to aid in the choice of values for threshold parameters, it would be desirable to calculate the probability of an output for a given assumed probability distribution of the noise, for the following cases: (1) noise alone, (2) noise combined with a correct signal, (3) noise combined with pulse jamming, and (4) noise plus pulse jamming plus correct signal. An attempt was made to carry out this calculation for the first case, assuming that the noise amplitude x_i at the i-th tap has a probability density $\phi(x_i)$, $0 < x_i < \infty$, and a corresponding cumulative probability distribution $\Phi(x_i) = \int_0^{x_i} \phi(t)\,dt$. The probability of an output from the correlator is $pr\{V_\Sigma - V_T > 0\}$, and since V_Σ and V_T are not independent, this probability depends on their joint density, which for a general $\phi(x_i)$ appears to have a very complicated form. If m and k are large, however, since V_T is calculated from only three of the x_i while V_Σ depends on all m + k of them, it appears that only a small error would result from assuming the independence of V_Σ and V_T. Hence it may be of some interest to write, in multiple integral form, the separate cumulative distribution functions $F_1(V_\Sigma)$ and $G_1(V_T)$:

$$F_1(V_\Sigma) = \int_{\max\{0,-V_\Sigma\}}^{\infty} F_2(V_\Sigma + \eta)\, f_3(\eta)\, d\eta$$

where $F_2(\xi) = \int_0^{\xi} \int_0^{\xi - x_1} \cdots \int_0^{\xi - x_1 - x_2 - \cdots - x_{m-1}} \phi(x_1)\,\phi(x_2)\cdots\phi(x_m)\,dx_m \cdots dx_2\,dx_1$

TABLE II. ADDING-BUS AND THRESHOLD VOLTAGES $(m=k=4, P=\frac{1}{2})$.

K \ M	M=0 $p=(1-P)^4=6.25\%$	M=1 $p=4P(1-P)^3=25\%$	M=2 $p=6P^2(1-P)^2=37.5\%$	M=3 $p=4P^3(1-P)=25\%$	M=4 $p=P^4=6.25\%$
K=0 $p=6.25\%$	$p=.39\%$ $V_\Sigma=4S$ $V_T=-BS$ $V_\Sigma > V_T$ for all $\frac{S}{J}$	$p=1.56\%$ $V_\Sigma=4S+J$ $V_T=(3+\alpha)J-BS$ $\frac{S}{J}>\frac{2+\alpha}{4+B}$	$p=2.34\%$ $V_\Sigma=4S+2J$ $V_T=(3+\alpha)J-BS$ $\frac{S}{J}>\frac{1+\alpha}{4+B}$	$p=1.56\%$ $V_\Sigma=4S+3J$ $V_T=(3+\alpha)J-BS$ $\frac{S}{J}>\frac{\alpha}{4+B}$	$p=.39\%$ $V_\Sigma=4S+4J$ $V_T=-B(S+J)$ $V_\Sigma>V_T$ for all $\frac{S}{J}$
K=1 $p=25\%$	$p=1.56\%$ $V_\Sigma=4S-J$ $V_T=(3+\alpha+B)J-BS$ $\frac{S}{J}>\frac{4+\alpha+B}{4+B}$	$p=6.25\%$ $V_\Sigma=4S$ $V_T=(3+\alpha)J-BS$ $\frac{S}{J}>\frac{3+\alpha}{4+B}$	$p=9.38\%$ $V_\Sigma=4S+J$ $V_T=(3+\alpha)J-BS$ $\frac{S}{J}>\frac{2+\alpha}{4+B}$	$p=6.25\%$ $V_\Sigma=4S+2J$ $V_T=(3+\alpha)J-BS$ $\frac{S}{J}>\frac{1+\alpha}{4+B}$	$p=1.56\%$ $V_\Sigma=4S+3J$ $V_T=(3+\alpha)J-BS$ $\frac{S}{J}>\frac{\alpha}{4+B}$
K=2 $p=37.5\%$	$p=2.34\%$ $V_\Sigma=4S-2J$ $V_T=(3+\alpha+B)J-BS$ $\frac{S}{J}>\frac{5+\alpha+B}{4+B}$	$p=9.38\%$ $V_\Sigma=4S-J$ $V_T=(3+\alpha)J-BS$ $\frac{S}{J}>\frac{4+\alpha}{4+B}$	$p=14.06\%$ $V_\Sigma=4S$ $V_T=(3+\alpha)J-BS$ $\frac{S}{J}>\frac{3+\alpha}{4+B}$	$p=9.38\%$ $V_\Sigma=4S+J$ $V_T=(3+\alpha)J-BS$ $\frac{S}{J}>\frac{2+\alpha}{4+B}$	$p=2.34\%$ $V_\Sigma=4S+2J$ $V_T=(3+\alpha)J-BS$ $\frac{S}{J}>\frac{1+\alpha}{4+B}$
K=3 $p=25\%$	$p=1.56\%$ $V_\Sigma=4S-3J$ $V_T=(3+\alpha+B)J-BS$ $\frac{S}{J}>\frac{6+\alpha+B}{4+B}$	$p=6.25\%$ $V_\Sigma=4S-2J$ $V_T=(3+\alpha)J-BS$ $\frac{S}{J}>\frac{5+\alpha}{4+B}$	$p=9.38\%$ $V_\Sigma=4S-J$ $V_T=(3+\alpha)J-BS$ $\frac{S}{J}>\frac{4+\alpha}{4+B}$	$p=6.25\%$ $V_\Sigma=4S$ $V_T=(3+\alpha)J-BS$ $\frac{S}{J}>\frac{3+\alpha}{4+B}$	$p=1.56\%$ $V_\Sigma=4S+J$ $V_T=(3+\alpha)J-BS$ $\frac{S}{J}>\frac{2+\alpha}{4+B}$
K=4 $p=6.25\%$	$p=.39\%$ $V_\Sigma=4S-4J$ $V_T=(3+\alpha+B)J-BS$ $\frac{S}{J}>\frac{7+\alpha+B}{4+B}$	$p=1.56\%$ $V_\Sigma=4S-3J$ $V_T=(3+\alpha)J-BS$ $\frac{S}{J}>\frac{6+\alpha}{4+B}$	$p=2.34\%$ $V_\Sigma=4S-2J$ $V_T=(3+\alpha)J-BS$ $\frac{S}{J}>\frac{5+\alpha}{4+B}$	$p=1.56\%$ $V_\Sigma=4S-J$ $V_T=(3+\alpha)J-BS$ $\frac{S}{J}>\frac{4+\alpha}{4+B}$	$p=.39\%$ $V_\Sigma=4S$ $V_T=(3+\alpha)J-BS$ $\frac{S}{J}>\frac{3+\alpha}{4+B}$

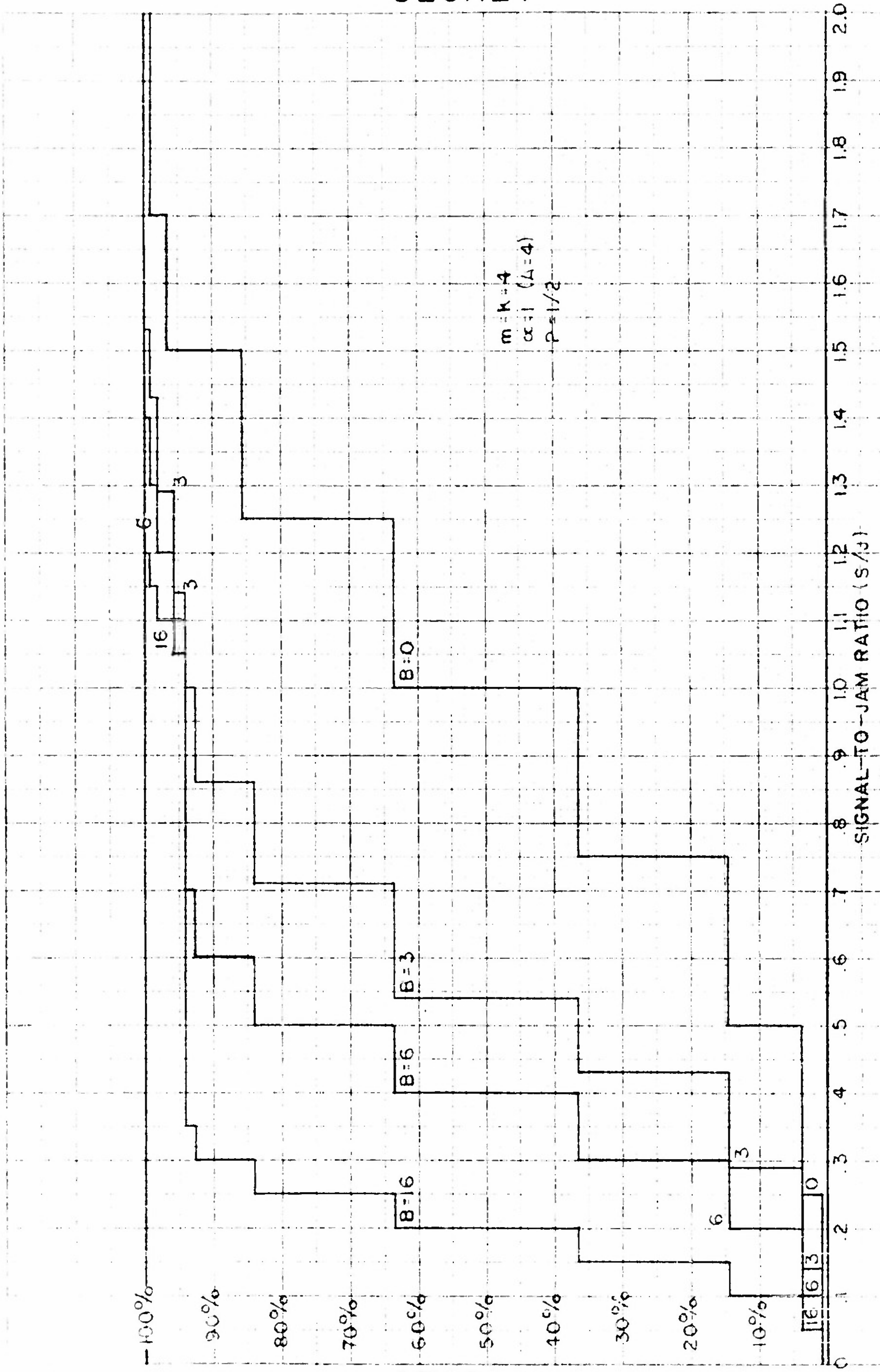

FIG. 10. RELIABILITY OF PULSE-TRAIN CORRELATOR IN THE PRESENCE OF CONSTANT-AMPLITUDE PULSE JAM.

and

$$f_3(\eta) = \frac{d}{d\eta}\left[\int_0^{\eta}\int_0^{\eta-x_{m+1}}\cdots\int_0^{\eta-x_{m+1}-\cdots-x_{m+k-1}}\phi(x_{m+1})\cdots\phi(x_{m+k})\,dx_{m+k}\cdots dx_{m+1}\right].$$

$$G_1(V_T) = \int_{\max\left\{0,-\frac{V_T}{B}\right\}}^{\infty}\int_0^{\frac{V_T+Bv}{A}} g_2(u,v)\,du\,dv + \int_{\min\left\{0,-\frac{V_T}{A+B}\right\}}^{0}\int_{-v}^{\frac{V_T+Bv}{A}} g_2(u,v)\,du\,dv$$

where
$$g_2(u,v) = -\frac{\partial^2}{\partial u\,\partial v}\left[\int_{\max\{0,v\}}^{u+v}\int_{w-v}^{u}\int_{y+v}^{u+w} g_3(y,z,w)\,dz\,dy\,dw\right.$$

$$\left.+\int_{\max\{0,v\}}^{\infty}\int_0^{w-v}\int_w^{u+w} g_3(y,z,w)\,dz\,dy\,dw\right]$$

and
$$g_3(y,z,w) = km(m-1)[\Phi(y)]^{k-1}[\Phi(z)-\Phi(w)]^{m-2}\phi(y)\,\phi(z)\,\phi(w).$$

In these equations, ξ and η represent the sums of the noise voltages at the m taps and the k taps respectively; that is, $\xi = \sum_{i=1}^{m} x_i$ and $\eta = \sum_{j=1}^{k} x_{m+j}$. Also

y, z, and w represent k_{max}, m_{max}, and m_{min} (when noise alone is present) and u and v represent $\max\{y, z-w\}$ and $\min\{w, z-y\}$ respectively, so that $V_T = Au - Bv$.

The above integrals have proved very difficult to simplify for any reasonable choice of the noise probability density $\phi(x)$. However, solutions could undoubtedly be obtained by means of an automatic computer, for specified values of m and k.

D. Circuitry of Pulse-train Correlator Working Model

When implementing the above scheme of a pulse-train correlator, the first question that needed to be decided was what type of coupling should be employed in the amplifiers and computer elements. Three types of coupling circuits were considered: (1) direct coupling, (2) conventional R-C coupling, and (3) R-C coupling with clamping. Of these, direct coupling must be considered to be the most conservative design, there being no question of shift of base level with pulse-repetition frequency or due to a brief instantaneous noise

peak, as would be experienced with coupling circuits (2) or (3) respectively. For the design of this experimental model, therefore, either actual direct coupling or circuits that achieve the results of direct coupling were employed, keeping in mind the possibility of determining the effects of the other coupling methods when the model is operating.

Now consider a length of delay line, followed by an amplifier whose gain is set to just compensate for the attenuation of the line, so that the overall gain is equal to one.

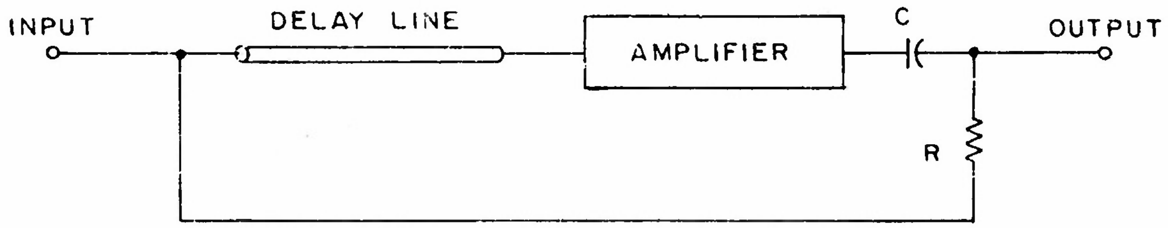

We may obtain the over-all response of direct-coupled circuitry and still use condenser coupling in the amplifier, if we return the resistor of the last coupling circuit to the input instead of to ground, at the same time making the R-C time-constant of that circuit very long compared to the delay time of the line, and making the time-constants of any previous coupling circuits within the amplifier long compared to the last one. (That this circuit will very nearly give the proper response down to zero frequency can readily be seen by analyzing it with a step voltage.) This scheme, then, is used in the design of the working model, thus permitting the in-line amplifiers and the tap phase-inverters to be condenser-coupled. A separate d-c phase inverter of a gain of minus one is used to provide a point to which the output coupling resistors of the tap phase inverters are returned. A schematic of the first half of the correlator is given in Fig. 11 which shows the input tap and phase inverter, a typical in-line amplifier and tap phase-inverter, and the d-c phase-inverter. It should be noted that the connections to the adding bus via the 10-K isolating resistors are the reverse of what would off-hand be expected, i.e. that here the adding bus is connected to the phase-inverted signal at the "m" places, and to the direct signal at the "k" places. The correlated signal on the adding bus is therefore of polarity opposite to that of the input to the delay line. The reason for this will become apparent later.

Figure 11 also shows pulse shaping resistors R_1 - R_8, which in conjunction with the input capacity of the phase inverters in whose grid circuit they are inserted, form single-section low-pass RC filters. Their values are chosen empirically so as to match as closely as possible the distortion of the pulses in the succeeding sections of the delay line, thus bringing about a near match of pulse shapes at the switches.

The formula for the threshold voltage

$$V_T = A \max \left\{ k_{max}, m_{max} - m_{min} \right\} - B \min \left\{ m_{min}, m_{max} - k_{max} \right\}$$

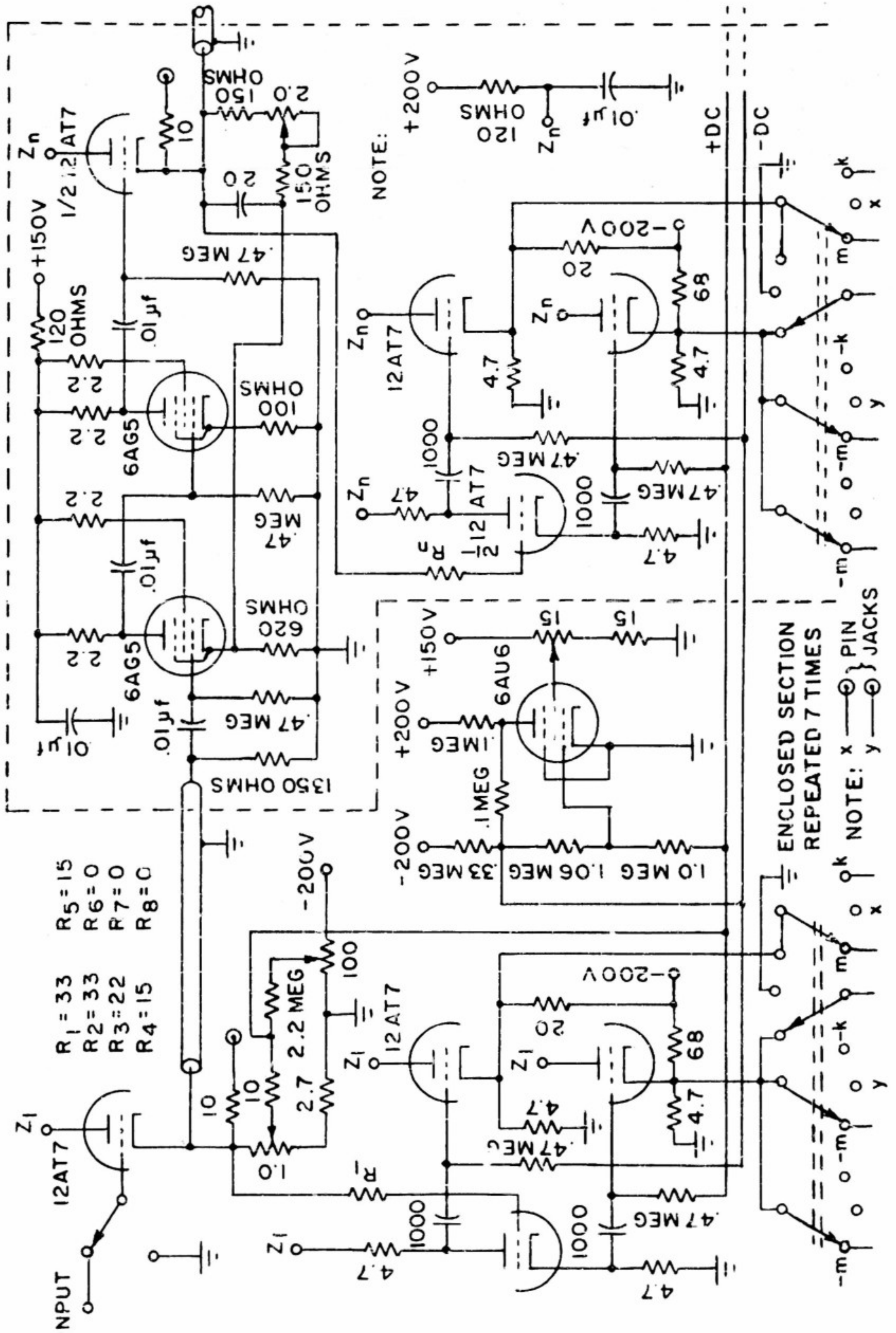

NOTE: ALL RESISTANCE VALUES IN K OHMS AND ALL CAPACITANCE VALUES IN μμf UNLESS OTHERWISE SPECIFIED

FIG. 11. SCHEMATIC OF PULSE-TRAIN CORRELATOR (FIRST HALF).

which was developed previously, implies three subtractions of voltages, which would have to be performed by three direct-coupled phase inverters and adding circuits. This is undesirable since each d-c phase inverter requires a tube with separate gain and zero-setting controls. In the interest of fewer controls it was therefore decided to remove the need for subtraction in the threshold computer by transforming the formula, using the identity $-m_{min} = (-m)_{max}$. We then have:

$$V_T = A \max \left\{ k_{max}, m_{max} - m_{min} \right\} + B \max \left\{ (-m)_{max}, k_{max} - m_{max} \right\} =$$

$$= A \max \left\{ k_{max}, m_{max} + (-m)_{max} \right\} + B \max \left\{ (-m)_{max}, k_{max} + (-m)_{min} \right\} .$$

That this transformation allows for economy of equipment is seen from the fact that the (-m) voltages are available at the tap phase inverters.

Figure 12, which is a schematic of the second half of the correlator, shows how, by means of crystal diodes, the four required voltages k_{max}, m_{max}, $(-m)_{max}$, and $(-m)_{min}$ are produced, and how, by resistive averaging circuits and further crystal rectifiers, the coefficients of A and B are generated. Controllable fractions of these voltages are applied to the adding-bus via cathode followers and isolation resistors. As stated above, the adding-bus signal, before introduction of these "A" and "B" voltages, was given a negative polarity (for positive inputs to the correlator). If the original negative adding-bus signal is powerful enough to override the positive "A" and "B" components, the actual adding-bus voltage will be negative - if not, positive. In principle, then, the threshold operation can be performed by a simple rectifier. Actually, a d-c amplifier has to be used to boost the adding-bus signal to a level where a crystal diode can operate on it.

The photographs of Fig. 13 show the adding-bus signal without and with the addition of the "A" and "B" components, due to a "correct" input (a 0 1 0 1 0 1 0 1 pulse train in this case) and due to an input containing one "error" (0 1 0 1 0 1 1 1). It can be seen in the uppermost trace of each photograph that the "spurious" pulses before and after the negative correlation peak are all of "unit" magnitude (due to the choice of tap spacings) and that the correlation peak is approximately four and three units high respectively. It is also apparent that the addition of the "A" voltage eliminates all spurious negative excursions, and, in the case of the erroneous input, the correlation peak as well.

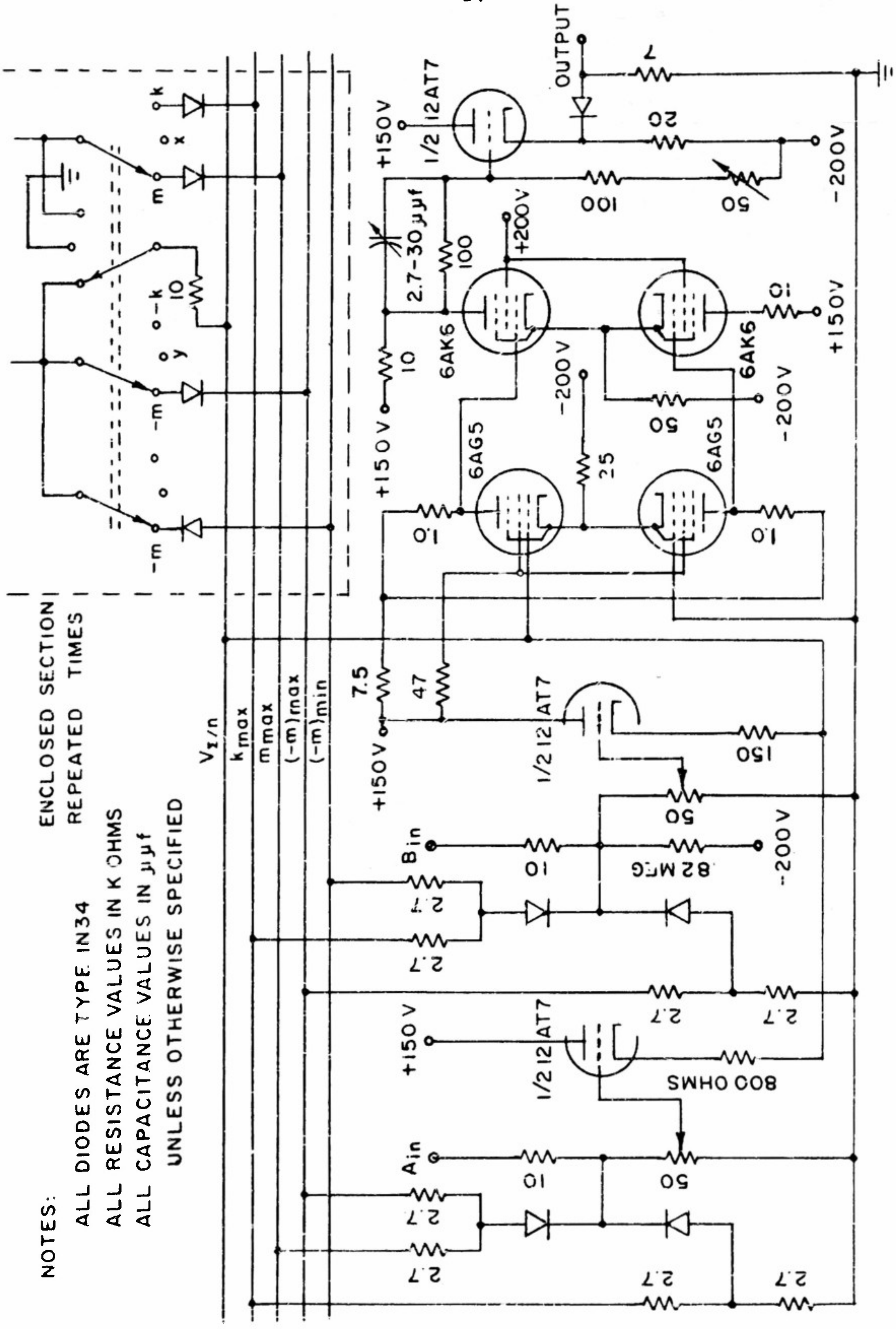

NOTES:

ALL DIODES ARE TYPE IN34

ALL RESISTANCE VALUES IN K OHMS

ALL CAPACITANCE VALUES IN μμf

UNLESS OTHERWISE SPECIFIED

FIG. 12. SCHEMATIC OF PULSE-TRAIN CORRELATOR (SECOND HALF).

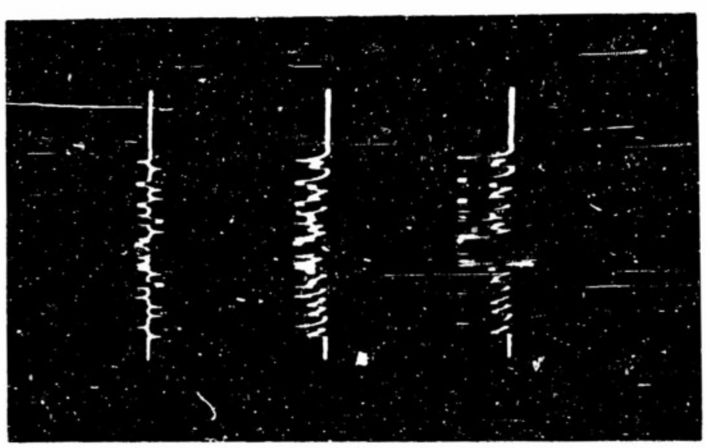

"CORRECT" PULSE TRAIN

A:0, B:0

A:4, B:0

A:4, B:3

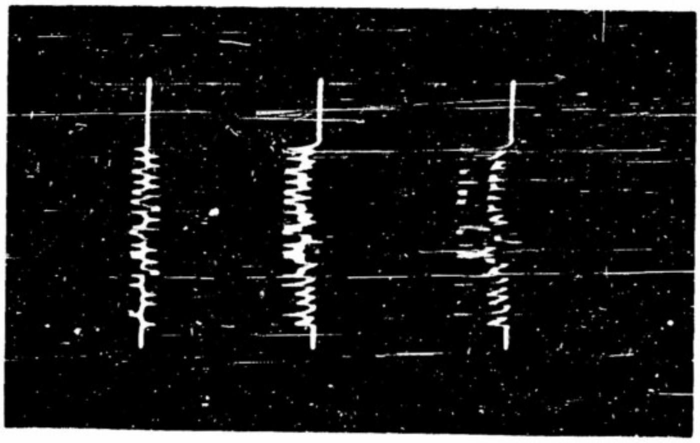

PULSE TRAIN CONTAINING ONE "ERROR"

FIG. 13. OSCILLOGRAPH TRACES OF ADDING-BUS VOLTAGE.

CHAPTER IV

MOCK-UP SYSTEM

A. Introduction

Most of the work on this item has been concerned with the development of a mock-up of the air-to-ground link of the IFF system assumed in Chap. I. Its purpose is to provide a means for checking experimentally the usefulness of the matched-filter and pulse-train correlator techniques as noise- and pulse-jam countermeasures.

Figure 14 is a block diagram of the mock-up system. The system employed is of the carrier type, the frequency assumed being 30.6 mc for practical reasons. The signal generator, whose output represents the reply from the transpondor, provides a pulse train in which the individual pulses are non-uniformly spaced, as discussed in Chap. III. The jamming-pulse generator and the two noise sources allow for the simulation of random-pulse and low- and high-frequency noise jam. Three separate modulators are used to ensure that phase agreement does not exist between the three carriers. The adder, used to combine the pulse-train signal with the artificial jamming signals, simulates the transmission path. Both the matched filter and the pulse-train correlator have been completely covered previously (see Chaps. II and III, respectively), and in the mock-up system represent the receiver at the responsor unit. All of the blocks, with the exception of the detector which will be of conventional design, have been completed and tested as individual units. At this writing, the various units are being combined, and the system made to operate as a whole. The following sections give practical details of the units and, where possible, operating data are included.

B. Components

Pulse-Train Generator

A pulse-train generator has been constructed to simulate the IFF signal. It generates an eight-digit number consisting of 0.6-μs pulses spaced at intervals of 1.8, 4.2, 3.6, 1.2, 7.2, 3.0 and 2.4 μs, respectively. The repetition rate of the number is variable from approximately 2 to 11 kc. Provision is made to trigger the generator from an external source.

The block diagram, shown in Fig. 15, subdivides the pulse-train generator into four functional groups: the pulse-train initiator, the digit generators, the output generator, and the synchronising-pulse generator.

The pulse-train initiator, shown in Fig. 16, consists of a free-running multivibrator (V2). The free-running multivibrator is of the conventional type with the grid-bias return variable from zero to plus 200 volts for a frequency variation from approximately 2 to 11 kc. A DPDT switch allows either internal triggering or triggering from an external source. The free-running multivibrator is made inoperative during triggering from an external source by returning the grid bias to minus 200 volts by the aforementioned switch.

SECRET

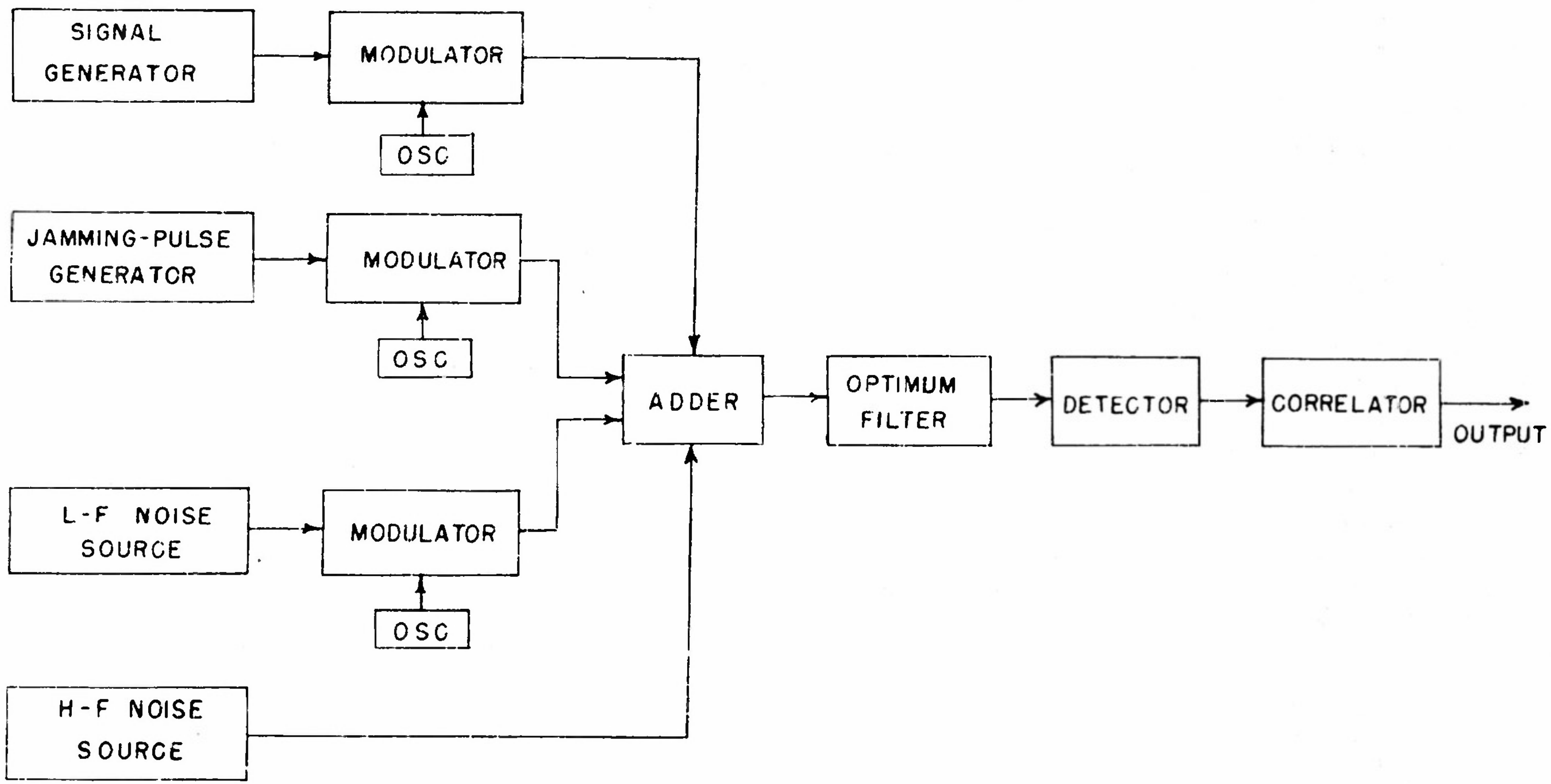

FIG. 14. BLOCK DIAGRAM OF PROPOSED TEST SET-UP.

SECRET

SECRET

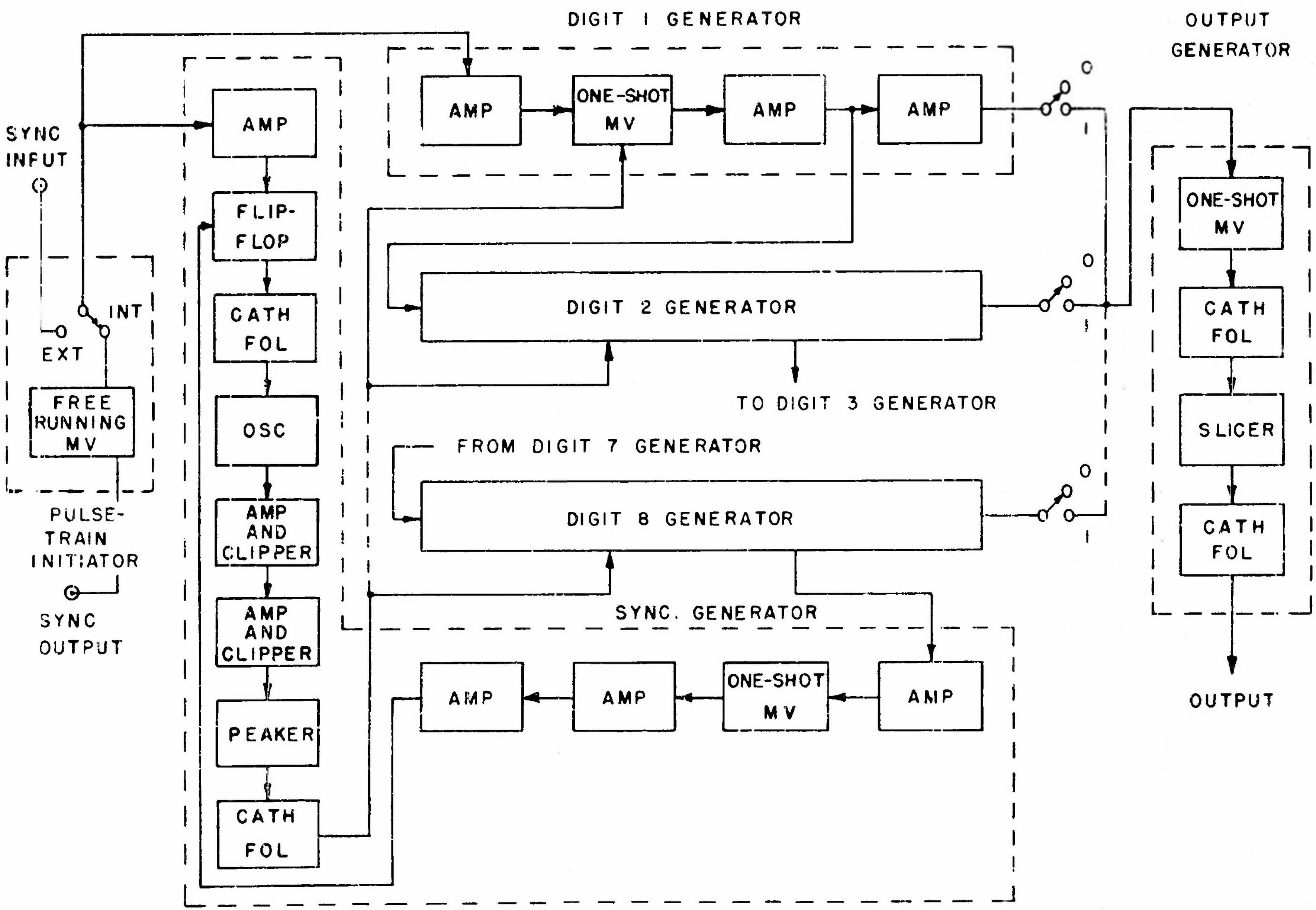

FIG. 15. PULSE – TRAIN GENERATOR

SECRET

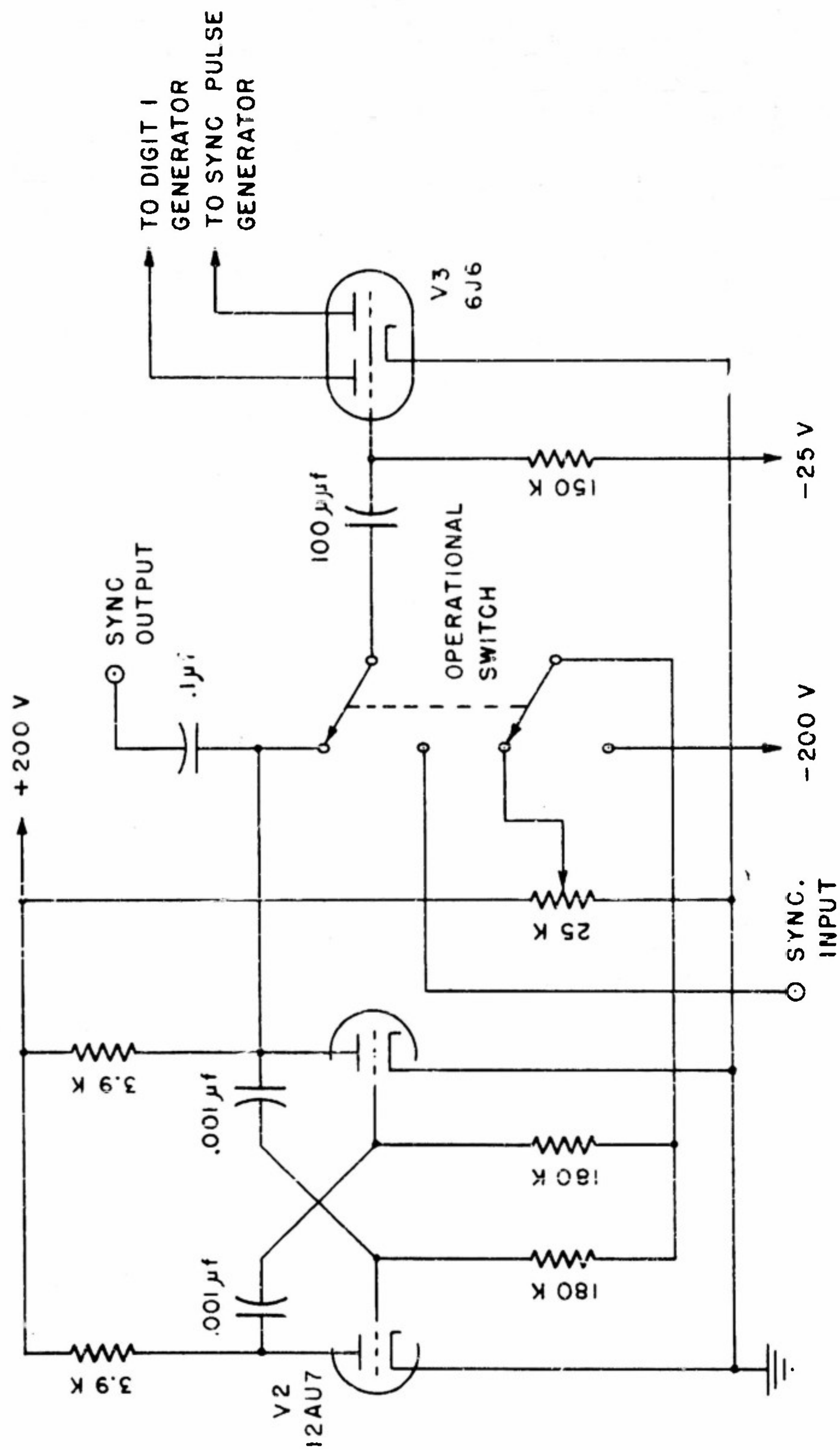

FIG. 16. PULSE—TRAIN INITIATOR.

A typical digit generator is shown in Fig. 17. Tube V1 is an amplifier used to plate-trigger the conventional one-shot cathode-coupled multivibrator V2. The input to V1 is from the pulse-train initiator in the case of the digit-1 generator, and from the preceding digit generator in the case of digit-2 to 8 generators. The output from the normally conducting plate of the multivibrator is differentiated at the input of amplifier V3. A positive pulse is generated at the plate of V3 when the plate of the multivibrator returns to its normally low level. Amplifier V3 then feeds into pulse amplifier V4 to obtain a pulse at its plate which is tied through the digit switch and the adding bus to the output generator. Amplifier V3 also feeds into the pulse amplifier at the input of the following digit generator, thus initiating its one-shot multivibrator to generate the pulse for the next digit. The delay of the one-shot multivibrator in the digit-1 generator can be set to an arbitrary number of pulse widths to delay the start of the train from the initiating pulse, but the delay of the one-shot multivibrators in the digit-2 through 8 generators must be set for 3, 7, 6, 2, 12, 5, and 4 pulse widths respectively by means of their delay capacitors. The presence or absence of a pulse on the adding bus to the output generator is controlled by the setting of the digit switches. Synchronizing pulses spaced at one pulse width are fed to each of the digit one-shot multivibrators so that they can only generate delays that are integral multiples of one pulse width.

The output generator, shown in Fig. 18, is made up of a conventional one-shot cathode-coupled multivibrator (V1), two cathode followers (V2 and V3), and a crystal-diode slicing circuit. The one-shot multivibrator generates a positive pulse of 0.6-μs duration at its normally low plate each time a pulse appears on the adding bus. The final output is coupled from the multivibrator through a cathode follower (V2) to a crystal-diode slicing circuit to cut out any noise at the base line and at the peaks of the pulses due to the synchronizing pulses. The slicing circuit feeds the output cathode follower (V3). The output pulse obtained is 20 volts in amplitude with a rise and fall time of 0.1 μs when feeding a capacitive load of 100 μμf.

A synchronizing-pulse generator, shown in Figs. 19 and 20, is incorporated in the pulse-train generator in order to insure time stability. The initiating pulse from V3 of Fig. 16 plate triggers a conventional type flip-flop (V1). The left plate of the flip-flop drops enough to cut off the cathode-follower switch circuit (V2), allowing the transitron oscillator (V3) to operate. The variable L-C tank circuit in the cathode of V2 is adjusted to oscillate at a period of 0.6 μs. The potentiometers in the cathode of the oscillator control the stability and amplitude of the oscillations. Tubes V7 and V8 of Fig. 20 are clipper amplifiers, the output of V8 being differentiated at the input of peaker V9. The negative pulses generated at the plate of peaker V9 feed a cathode follower V10 used to distribute the synchronizing pulses to the various one-shot multivibrators. Tubes V4, V5, and V6 comprise a unit similar to the digit generators. The function of this unit, which is triggered from the digit-8 generator, is to return flip-flop V1, thereby making the synchronizing-pulse generator inoperative after some arbitrarily fixed delay (about 5 pulse widths) of one-shot multivibrator (V5). Therefore, synchronizing pulses are generated only for a time shortly preceding, to a time shortly following the pulse train.

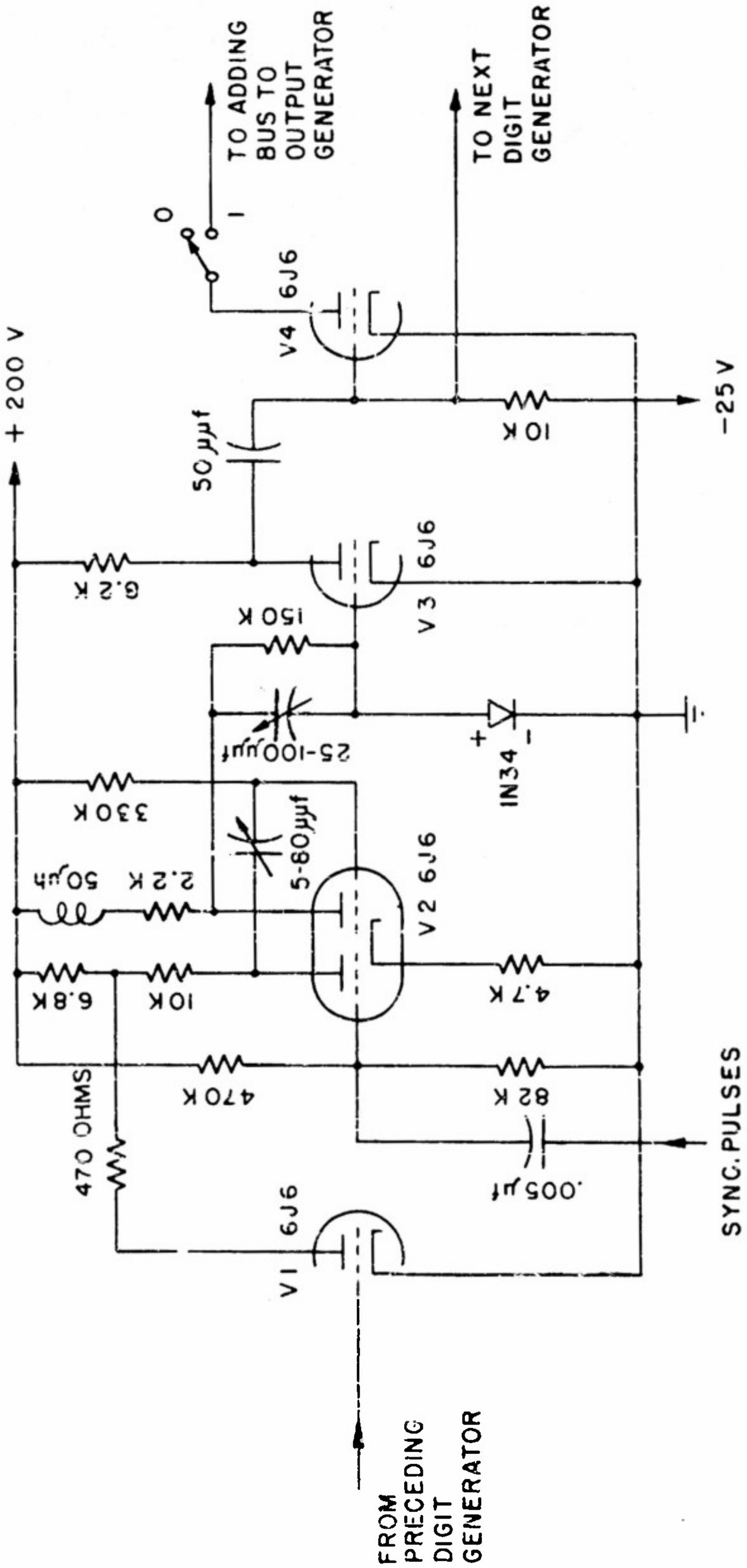

FIG. 17. TYPICAL DIGIT GENERATOR

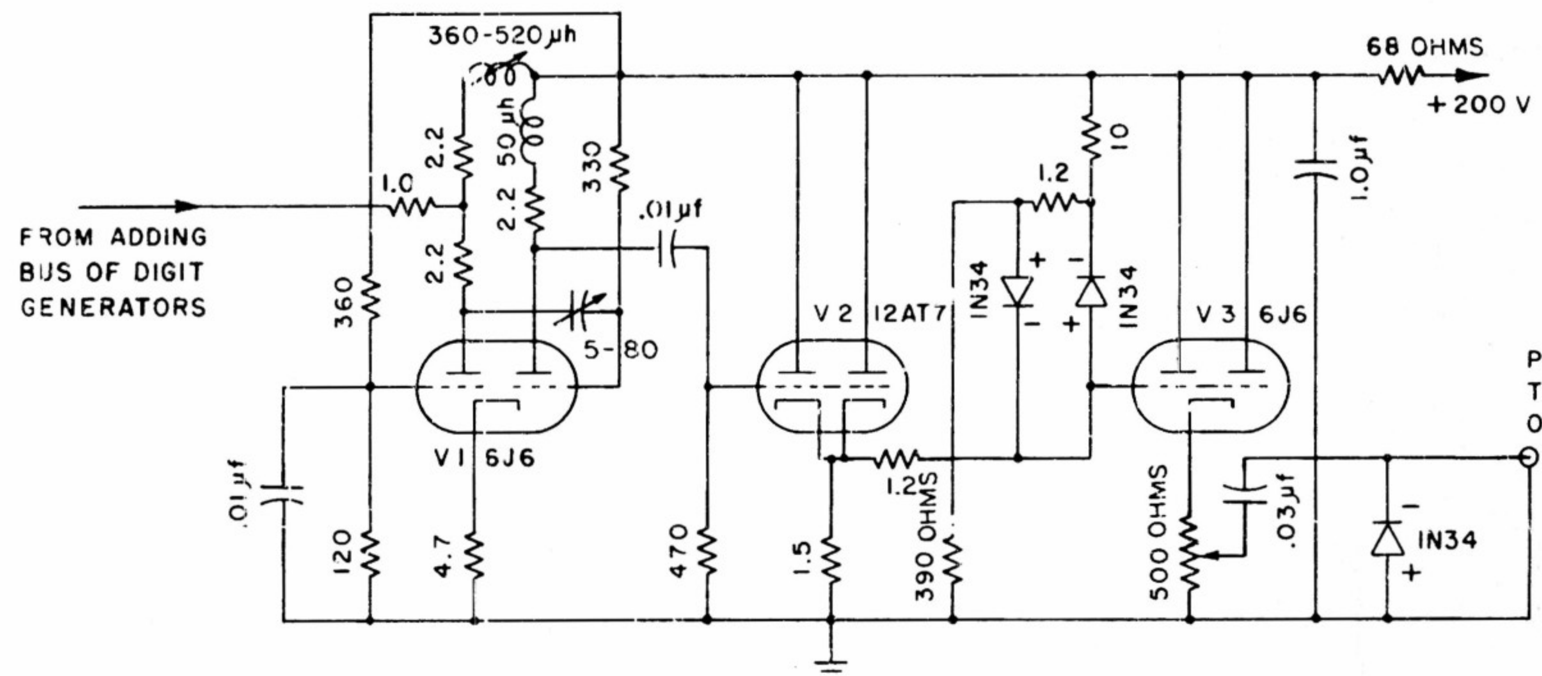

NOTE: ALL RESISTANCE VALUES IN KΩ AND ALL CAPACITANCE VALUES IN µµf UNLESS OTHERWISE SPECIFIED.

FIG. 18. OUTPUT GENERATOR.

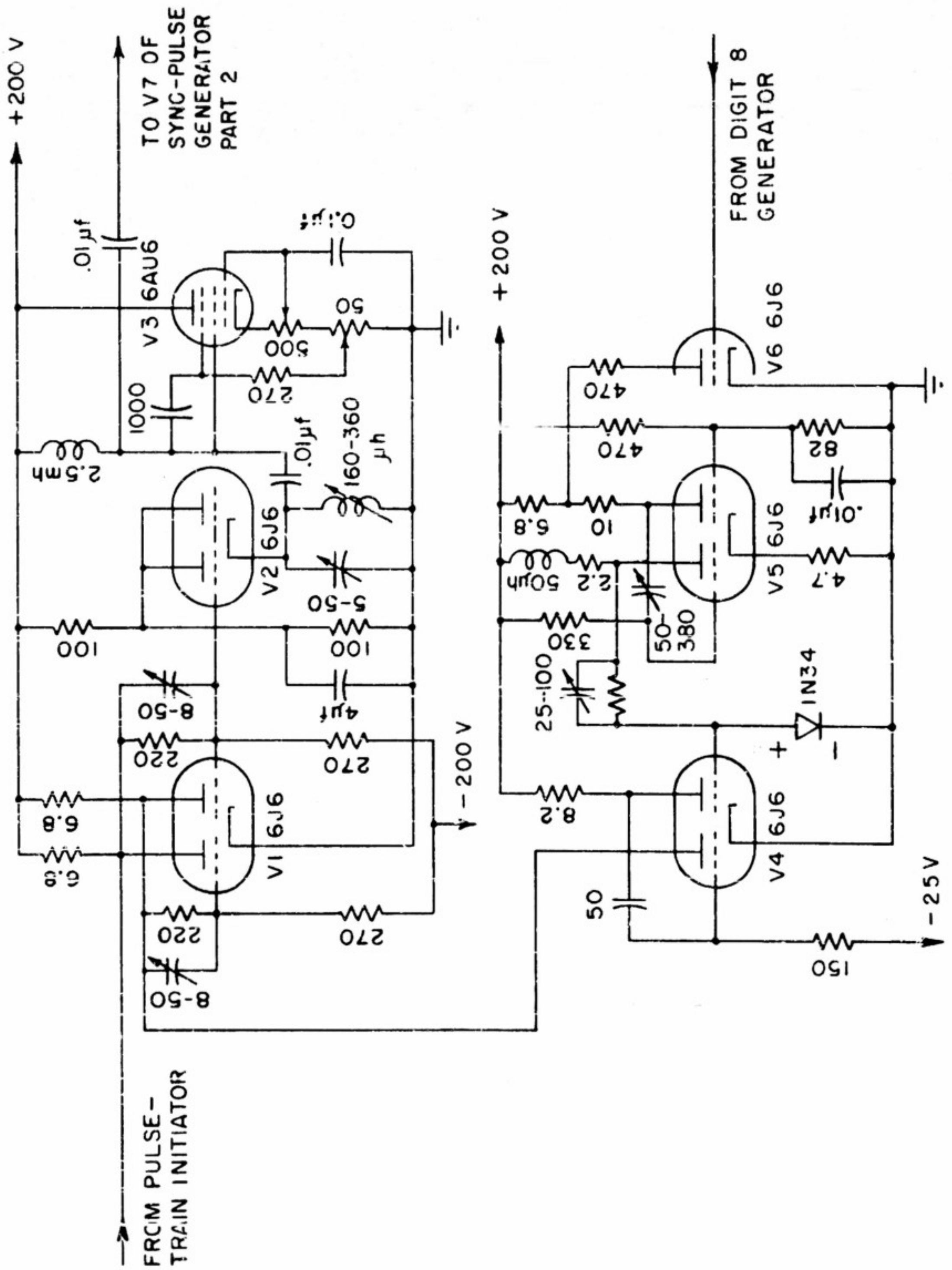

NOTE: ALL RESISTANCE VALUES IN KΩ AND ALL CAPACITANCE VALUES IN µµf UNLESS OTHERWISE SPECIFIED.

FIG. 19. SYNCHRONIZING-PULSE GENERATOR.
PART I

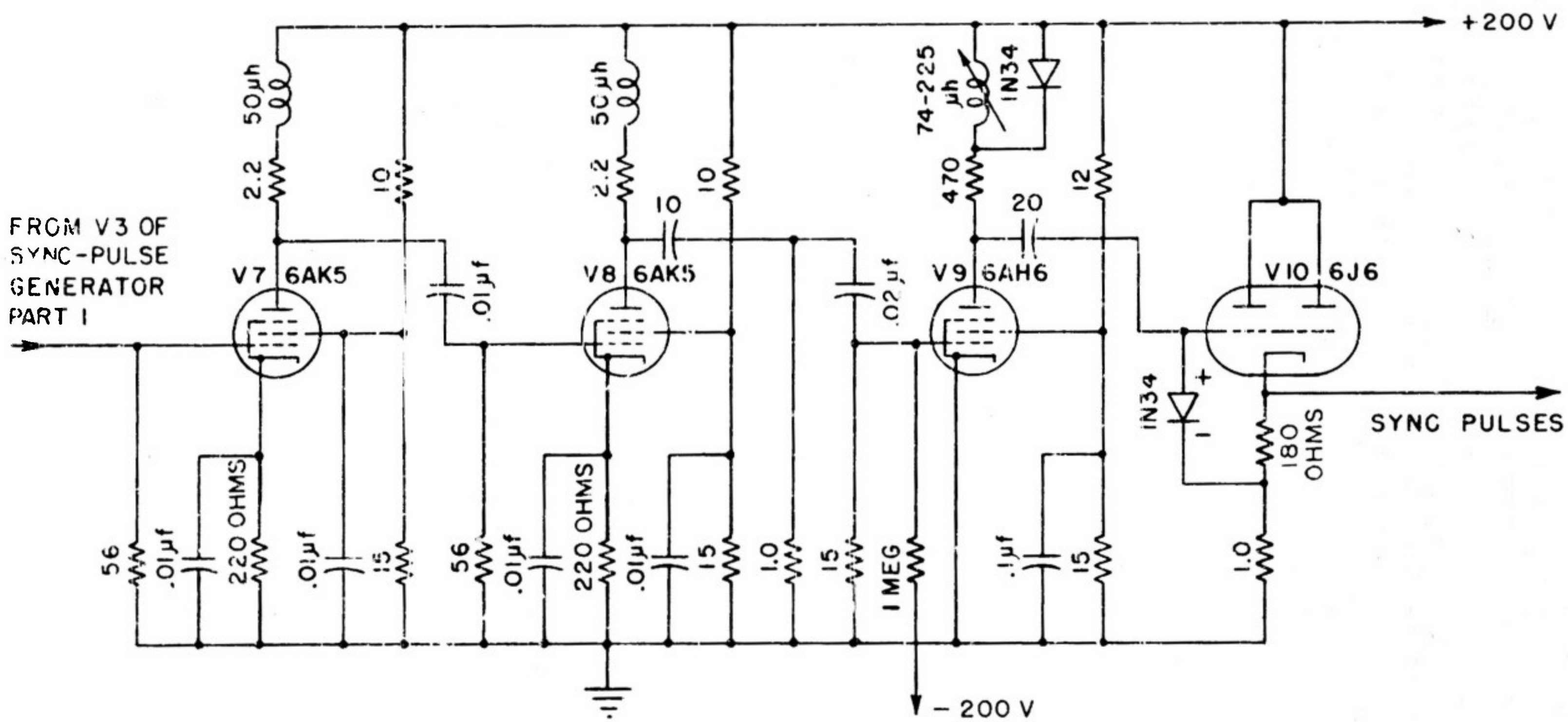

NOTE: ALL RESISTANCE VALUES IN KΩ AND ALL CAPACITANCE VALUES IN µµf UNLESS OTHERWISE SPECIFIED

FIG. 20. SYNCHRONIZING-PULSE GENERATOR.
PART 2

Random-Pulse Generator

The random-pulse generator shown schematically in Fig. 21 has been designed to produce randomly spaced constant-amplitude 0.6-μs pulses when a commercial noise source is connected to its input. The generator consists of two stages of amplification and clipping, and a differentiator, which produce randomly spaced pulses. These pulses are further amplified and used to trigger a one-shot cathode-coupled multivibrator followed by a cathode-follower output stage. A plot of frequency versus the minimum sinusoidal rms voltage required to produce an output is shown in Fig. 22.

Pulse Modulator

The pulse modulator shown in Fig. 23 consists of a phase inverter V1, a ringing circuit V2 and a driver tube V3. The high-Q tank circuit is normally loaded down due to tube V2 conducting heavily. A negative pulse from the phase inverter cuts off V2 and causes the high-Q tank circuit to ring. The driver tube V3 is a cathode follower using a low-Q tank circuit as its cathode impedance. Over a limited frequency range, this type of driver circuit can tolerate a moderate amount of capacitive loading since the shunting capacity can be made a part of the low-Q tank circuit. For a video pulse input having an amplitude of 20 volts and a rise time of .01 μs, the r-f pulse output is greater than 10 volts peak-to-peak with an envelope rise time that is less than 0.1 μs.

Noise Modulator

This unit shown schematically in Fig. 24 consists of an oscillator of the Hartley type and a modulator tube. The carrier frequency is variable from 20 to 60 mcps and can be modulated up to 100 percent. A filter consisting of a loaded tank circuit prevents the modulation frequencies from appearing in the output.

Noise Sources

These units are available in the laboratory as pieces of commercial equipment. The General Radio Type 1390A Random Noise Generator is used to provide low-frequency noise, and the Kay Electric Mega-Node Noise Diode supplies the high-frequency noise.

Adding Circuit

The adding circuit shown schematically in Fig. 25 consists of four cathode followers using a common cathode resistor. If linear operation is desired, the peak-to-peak signal applied to each input must not exceed 2.5 volts. The output impedance is approximately 50 ohms and the gain for each input is about 0.2 with a half-power point at 45 mc.

C. Test Procedure

The mock-up system was constructed to evaluate the performance of the matched i-f filter and the pulse-train correlator under conditions closely approximating those which may be encountered in actual operation. The

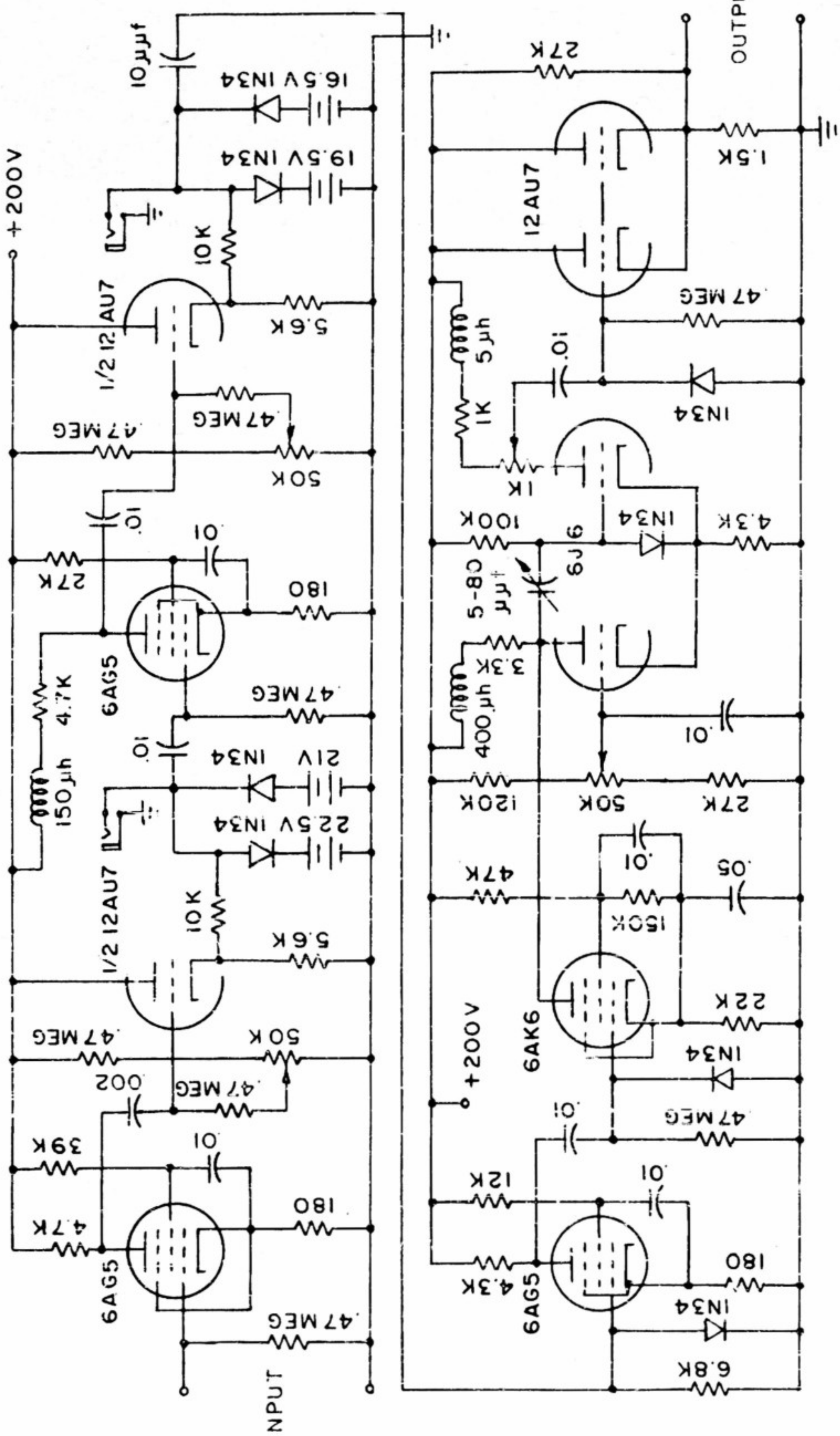

NOTE: ALL RESISTANCE VALUES IN OHMS AND ALL CAPACITANCE VALUES IN μf UNLESS OTHERWISE SPECIFIED.

FIG. 21. CIRCUIT DIAGRAM OF RANDOM PULSE GENERATOR.

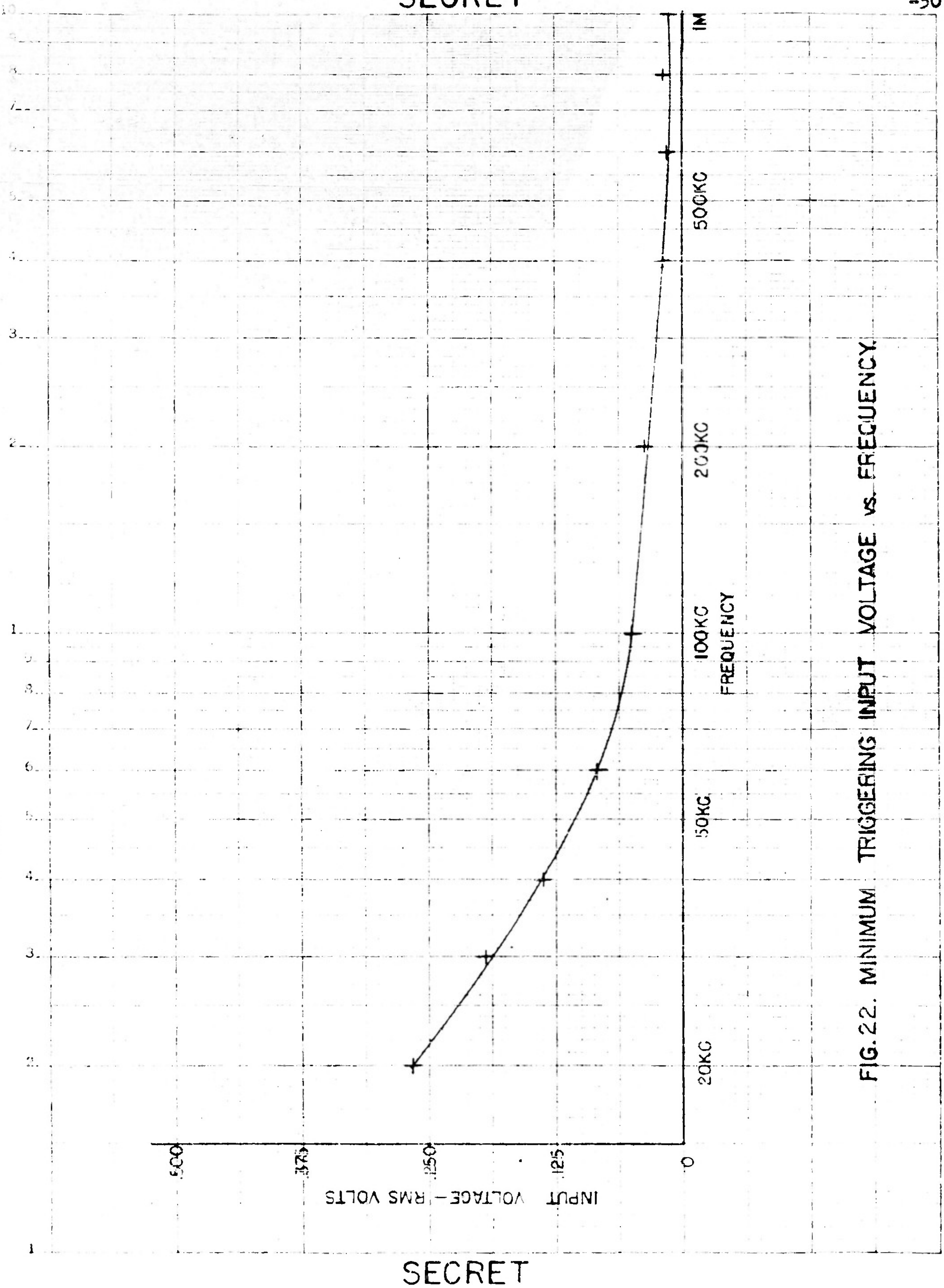

FIG. 22. MINIMUM TRIGGERING INPUT VOLTAGE vs. FREQUENCY.

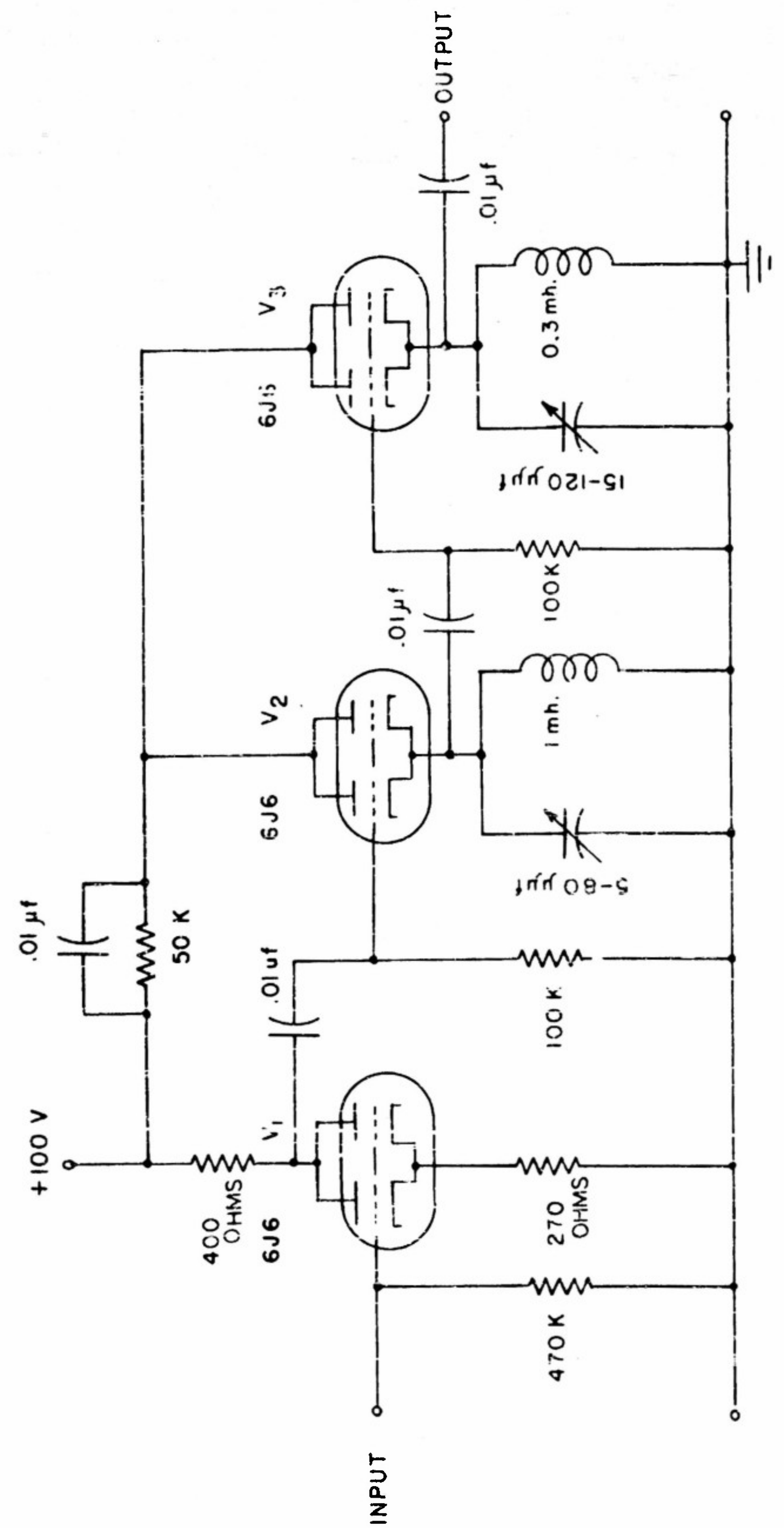

FIG. 23. PULSE MODULATOR.

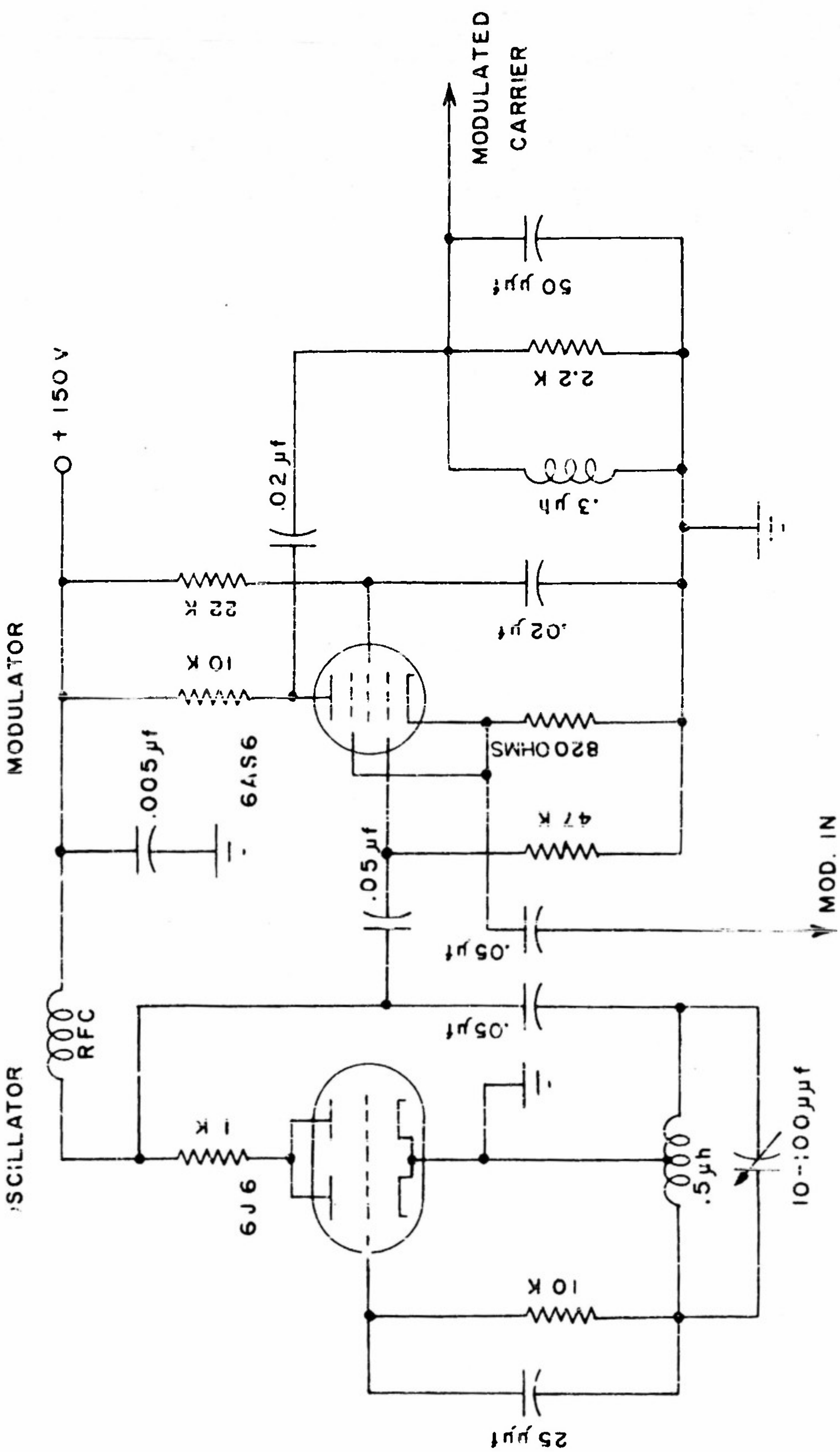

FIG. 24. NOISE MODULATOR

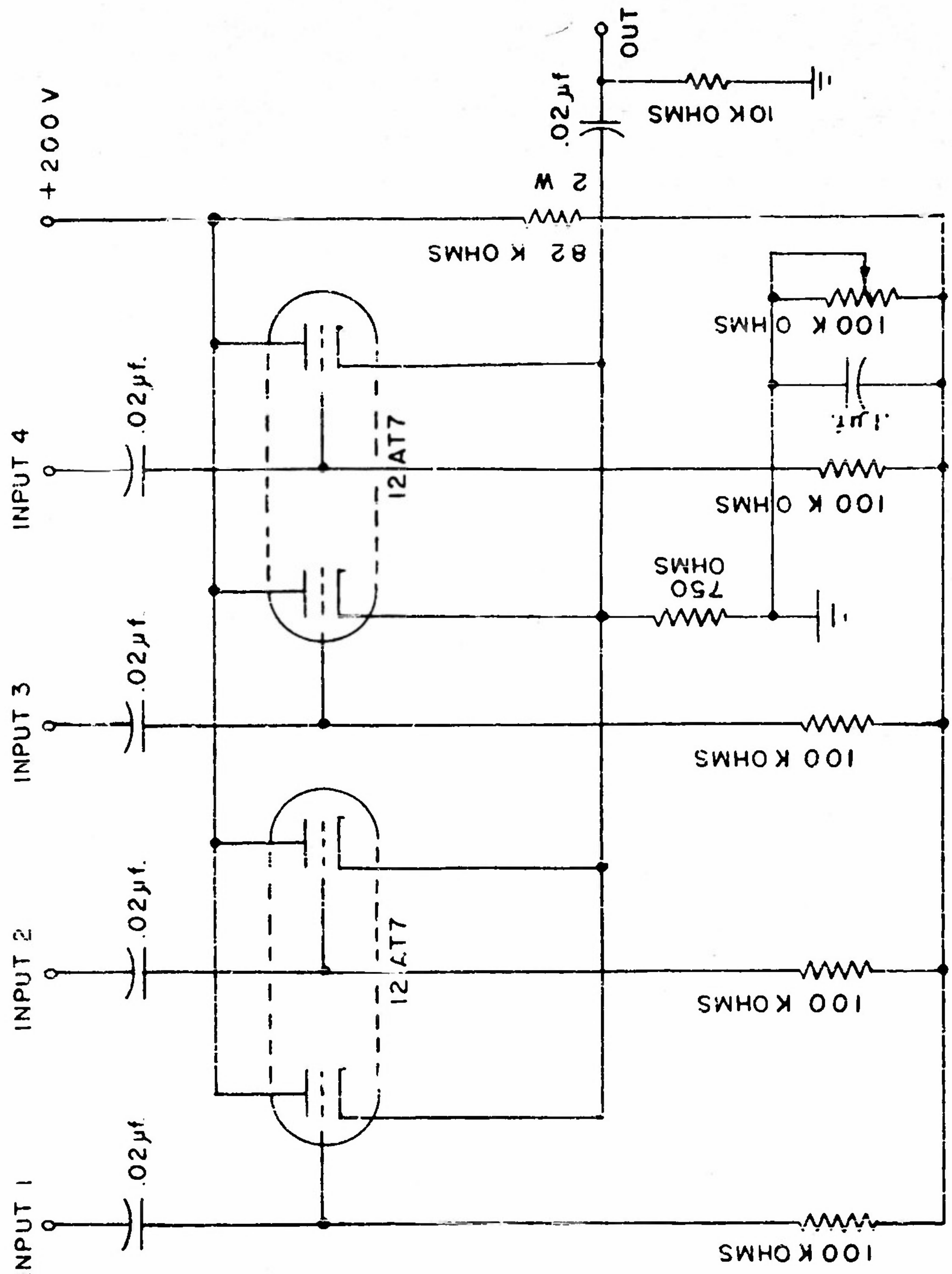

FIG. 25. ADDING CIRCUIT.

receiver at the ground terminal of the IFF system can be represented by the cascade combination of the matched i-f filter, a detector, and the pulse-train correlator. The receiver at the air terminal of the system can be represented by the cascade combination of the matched i-f filter, a detector, and a threshold device. The reliability of either receiver in the presence of jamming can be expressed in terms of the probability of a miss (the probability that the signal will not be detected) and the probability of a false alarm (the probability that the jamming signal will be interpreted as the "correct" signal). For a given type of jamming, these probabilities will be a function of the signal-to-jam ratio at the input to the receiver undergoing testing. Consequently specification of the type of jamming and input signal-to-jam ratio will determine the reliability and vice-versa.

The above-mentioned probabilities can be determined, for a given type and strength of jamming, by comparing the signal waveform with the output waveform. High-speed film strips taken of signal and output waveforms would serve this purpose well but would require a considerable amount of labor to process the data. Perhaps initially this method would be justified since unforeseen difficulties arising from equipment reliability and the like might become apparent. However, once confidence in the equipment is justified, instrumentation similar to that indicated below would considerably simplify data taking.

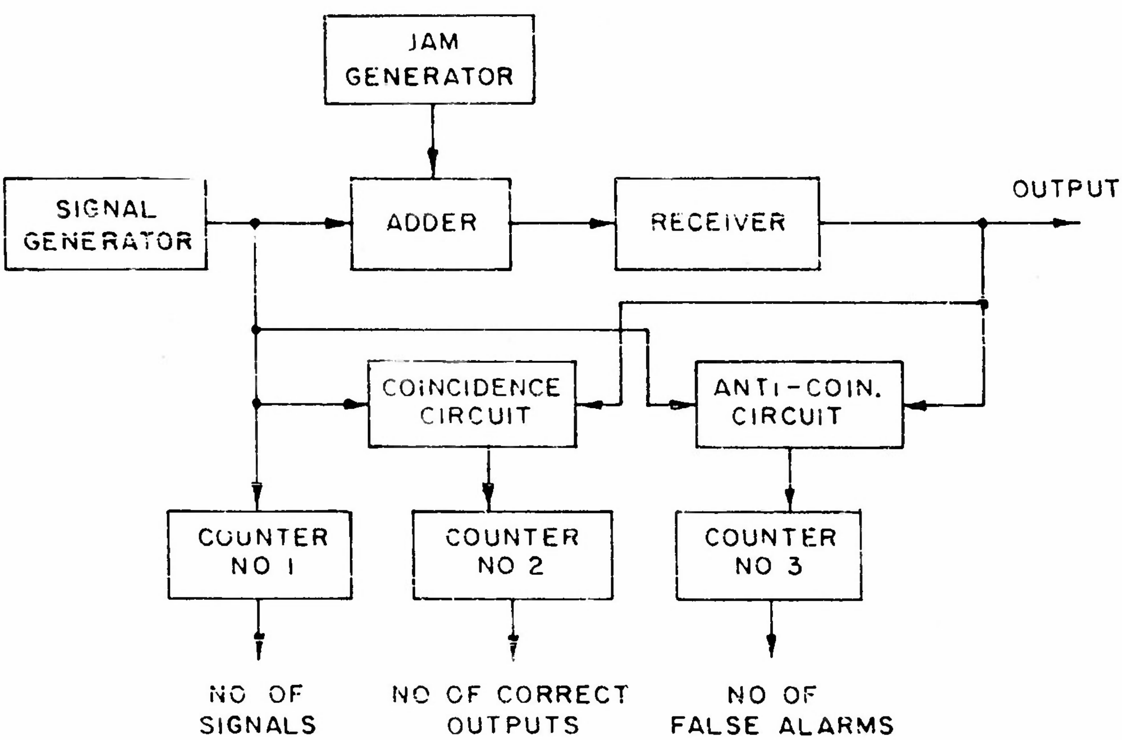

The number of misses can be easily calculated by subtracting the output of counter No. 2 from that of counter No. 1. The number of false alarms

will be available at the output of counter No. 3. Consequently the miss probability and false-alarm probability can be easily obtained by dividing the appropriate quantity by the output of counter No.1.

Further simplification in the above instrumentation could be obtained if the counters were replaced by suitable analogue computers. A possible analogue device could consist of a voltage-to-current converter followed by a low-pass filter and an ammeter. If the integrating time were long enough, the ammeter reading would be proportional to the reading hitherto given by a counter.

The jamming signal would differ depending on the receiver undergoing testing. In the case of the airborne receiver, only noise-like jamming signals should be used as the matched i-f filter is not expected to yield improvement in the presence of pulse jamming. In the case of the ground-terminal receiver, both noise and pulse jamming would be employed. For the purpose of determining the performance of the pulse-train correlator alone, video pulse trains and jamming signals would be employed.

CHAPTER V

REDUNDANCY AS A MEANS OF IMPROVING SYSTEM RELIABILITY

Considerable of the contract research has dealt with the application of various means of employing redundancy to improve the reliability of the IFF system in the presence of interfering signals. Methods studied include the use of additional digits in the pulse train to theoretically match the channel capacity for given assumed noise conditions, and the use of integration over repeated challenges. The first method assumes that a decision is made separately at each position, while in the second the decision is made either at the end of each pulse train or at the end of the repetition period depending upon the type of integration employed.

A. Coding to Match Channel Capacity

In the first method, the objective has been to achieve a high degree of reliability with a minimum amount of redundancy. Information theory[23] provides a means of calculating, in terms of the channel capacity, the theoretical minimum redundancy, but does not specify, except in special cases, a coding method to approximate the ideal values. Some calculations of channel capacities for assumed noise conditions are presented in this section along with some sample codes developed by trial and error. The assumptions are that a pulse train, representing an IFF challenge or reply, is to be detected by making a separate decision at each position of the pulse train. Furthermore, it must be assumed that the noise and/or random jamming acts in such a way that there is a constant independent probability of an erroneous decision at every position, which may, however, depend on what was transmitted in that position.

It was found that the possible situations could be separated into essentially three different cases, according to the method of pulse transmission and the nature of the noise. The first two cases arise when the pulse train consists of pulses and gaps; that is, when nothing is transmitted to indicate the binary digit zero. If the characteristics of the interference and of the corresponding threshold device are such that errors occur only in the gap positions while pulses are always received correctly, this is called Case (1). If the interference can cause errors in either pulses or gaps but with different probabilities, this is called Case (2). If, on the other hand, the binary digits one and zero are indicated by transmitting pulses of equal power but coded in some manner, such as by P.P.M., this is called Case (3). In this case, it is logical to assume equal probabilities of error for the two types of pulse.

To formulate these assumptions in the notation of information theory[23], let p_{ij} be the probability, if symbol i is sent, that symbol j will be received, and let subscripts 1 and 2 indicate pulse and gap respectively - or pulses of types 1 and 2 in the case of P.P.M. coding. Then the matrix $\{p_{ij}\}$ will be one of the following three types according to which of the three cases applies:

$$\begin{bmatrix} 1 & 0 \\ a & 1-a \end{bmatrix} \qquad \begin{bmatrix} 1-b & b \\ a & 1-a \end{bmatrix} \qquad \begin{bmatrix} 1-a & a \\ a & 1-a \end{bmatrix}$$

The channel capacity in bits/symbol can be obtained by the formula

$$C = \log \sum_{k=1}^{n} \exp \left[\sum_{i=1}^{n} \left\{ h_{ik} \sum_{j=1}^{n} p_{ij} \log p_{ij} \right\} \right]$$

where $\{h_{ij}\}$ is the transpose of the inverse of $\{p_{ij}\}$ and the base 2 is understood for all logarithms and exponentials. This formula for C, which was derived under this contract, can be obtained either from the formula for Q_t given on page 18 of reference 24 or from the formula for P_k given on page 46 of reference 23. P_k represents the probability of using the k-th symbol in an ideal code which matches the channel capacity, and Q_t represents the probability that the t-th symbol will be received, using such a code. In either case the derivation can be completed by making use of the identity

$$\sum_{i=1}^{n} h_{ij} = 1 \qquad j = 1, \ldots, n.$$

This in turn can be proved by noting that from the nature of conditional probabilities,

$$\sum_{j=1}^{n} p_{ij} = 1 \qquad i = 1, \ldots, n.$$

and that, by definition of the matrix $\{h_{ij}\}$,

$$\sum_{j=1}^{n} p_{ij} h_{sj} = 1 \qquad \text{if } s = i$$

$$= 0 \qquad \text{otherwise.}$$

Letting $a_j = \sum_{s=1}^{n} h_{sj}$, we obtain by addition

$$\sum_{j=1}^{n} p_{ij} a_j = 1 \qquad i = 1, \ldots, n.$$

But these are a set of n linear equations in the n quantities $a_1, \ldots, a_n$ and hence there is exactly one simultaneous solution since we have assumed that the determinant $|p_{ij}| \neq 0$ by assuming an inverse for $\{p_{ij}\}$. But $a_1 = a_2 = \cdots = a_n = 1$ is obviously a solution of each equation, and therefore it is the only solution.

Applying the formula for C to the three types of matrices, we obtain respectively

$$C = \log\left\{1 + \exp\left[\frac{a}{1-a}\log a + \log(1-a)\right]\right\} = \log\left\{1 + (1-a)\, a^{\frac{a}{1-a}}\right\}$$

$$C = \log\left\{(1-b)\left(\frac{b}{1-a}\right)^{\frac{b(1-a)}{1-a-b}}\left(\frac{1-b}{a}\right)^{\frac{ab}{1-a-b}} + (1-a)\left(\frac{a}{1-b}\right)^{\frac{a(1-b)}{1-a-b}}\left(\frac{1-a}{b}\right)^{\frac{ab}{1-a-b}}\right\}$$

$$C = 1 + a\log a + (1-a)\log(1-a)$$

For Case (1), two numerical solutions are given for illustration:

Example I: If $a = \frac{1}{2}$, then $C = .32$, $P_1 = .60$, $P_2 = .40$

Example II: If $a = \frac{1}{4}$, then $C = .56$, $P_1 = .57$, $P_2 = .43$

In Example I, the probabilities that pulse and no pulse will be received are $Q_1 = .80$ and $Q_2 = .20$ respectively, and the various entropies for the ideal coding are $H(x) = .97$, $H(y) = .72$, $H_y(x) = .65$, and $H_x(y) = .40$, where x and y indicate transmitted (coded) message and received (coded) signal respectively.

Although a very long coding period is required to approximate errorless transmission at a rate equal to C, the following illustrations for 8-place codes give about 15% probability of error for both of these examples. No original uncoded messages are shown; the coded messages are numbered and can be considered as a catalogue of permissible 8-place pulse trains. A received signal would be identified as that permissible message having the smallest number of gaps including those received.

Example I. Rate of transmission .323 bits per symbol
Probability of error .148 (for 8-place message)
($P_1 = .52$)

Coded Messages

1. P P P P P P P P
2. P P P P P G G G
3. G G G P P P P P
4. P P G G G G P P
5. G G P P G P G G
6. G G G G G G G G

(P = pulse, G = gap)

Example II: Rate of transmission .557 bits per symbol
Probability of error .149 (for 8-place message)
(P_1 = .53)

Coded Messages

1.	P P P P P P P P	12.	P G P P G P G P
2.	P P P P P P G G	13.	G P P P P G P G
3.	P P P P G G P P	14.	G G G G G P P P
4.	P P G G P P P P	15.	P P P G G G G G
5.	G G P P P P P P	16.	G G G P P P G G
6.	P G P G P G P P	17.	G P G G P G G P
7.	P G G P P P P G	18.	P G G P G G P G
8.	G P P G P P G P	19.	G G P G G P G G
9.	G P G P G P P P	20.	P G G G G G G P
10.	P P P G G P P G	21.	G P G G G G P G
11.	P P G P P G G P	22.	G G G G G G G G

It is possible to reduce the probability of error by reducing the rate of transmission. In Example I, the following simple 8-place code yields a rate of transmission of .25 bits per symbol with .062 probability of error:

P P P P P P P P
P P P P G G G G
G G G G P P P P
G G G G G G G G (P_1 = .50)

These four coded messages can be thought of as encoded versions of the four possible two-place messages, PP, PG, GP, and GG; where the code consists merely of repeating each symbol four times.

Some numerical results were also calculated for Case (2) where the values selected for a and b were determined by assuming for the noise a Rayleigh distribution

$$p(N) = \frac{N^2}{\sigma^2} e^{-\frac{N^2}{2\sigma^2}}$$

where σ is the rms value of the noise before detection.* It was further assumed for the sake of a numerical illustration that signal and noise would be additive, and that a threshold T for detecting the presence of a pulse would be set in such a way as to maximize $p_{11} + p_{22}$ (i.e. the sum of the conditional probabilities of correct decisions when a pulse is present or not present). The following values were calculated for three choices of σ in terms of S, the signal amplitude:

σ	T	p_{11}	p_{12}	p_{21}	p_{22}	C	P_1	P_2	Q_1	Q_2
.5S	1.10S	.98	.02	.09	.91	.71	.52	.48	.56	.44
S	1.54S	.86	.14	.30	.70	.25	.52	.48	.59	.41
2S	2.50S	.76	.24	.46	.54	.07	.54	.46	.62	.38

* See page 61 of reference 25.

No sample codes were constructed for this case.

To determine conditions for the optimum code in Case (3) suppose that the coding period is selected so that the coded signal consists of blocks of n pulses each, where each block is to be decoded as a unit. In other words, the problem is to select, for use in transmission, a subset $A_1, \ldots, A_M$ out of the 2^n possible pulse trains of length n. The selection should be such that under the assumed conditions of noise or of random jamming, it is highly probable that the pulse train transmitted will be perturbed by the noise or jamming in such a way that it will still be decoded as that pulse train which was actually transmitted rather than some other pulse train of the subset. From this subset or catalogue of pulse trains, $A_1, \ldots, A_M$, one is chosen at random for transmission at any time; thus the entropy of the transmitted pulse train is $H = \frac{\log_2 M}{n}$ bits/symbol.

Since every pulse has the same probability, a, of being received incorrectly, the probability, $pr(B_j/A_i)$ that pulse train A_i will be received as B_j depends only on the number of places in which A_i and B_j differ, or, representing the 2^n possible pulse trains as vertices of an n-dimensional hypercube, the number of coordinates in which A_i and B_j differ. This number of differing coordinates will be referred to as the "distance" between A_i and B_j. Two intuitively evident principles can now be stated for the design of the code: (1) A received train B_j should always be decoded, or identified, as that A_i from which its "distance" is least. (2) For a given M, the subset $A_1, \ldots, A_M$ should be selected in such a way as to maximize the minimum "distance" between pairs A_i, A_j; that is, using Hamming's[26] terminology, the points $A_1, \ldots, A_M$ should be the centers of non-overlapping spheres of as nearly equal radius as possible which among them include, as nearly as possible, all of the 2^n points.

This leads us to the type of coding considered by Fano[27] who considered the problem of determining the maximum number M of such spheres which can be found for a given n, and a given radius n - k. A quantitative statement of what can be achieved by this type of coding can be obtained following Fano's analysis and results, if specific values are assumed for the constant involved. Suppose, for example, that a = .1. This corresponds in the case of video transmission to a signal-to-noise power ratio of 2.16 db, if the noise x is Gaussian, with mean value 0 and mean square value N; that is, if

$$f(x) = \frac{1}{\sqrt{2\pi N}} e^{-\frac{x^2}{2N}}.$$

We are assuming here a signal consisting of equally probable positive and negative pulses with amplitude $\pm\sqrt{S}$, so that

$$a = .1 = \frac{1}{\sqrt{2\pi N}} \int_{\sqrt{S}}^{\infty} e^{-\frac{x^2}{2N}} dx$$

which yields the solution $\sqrt{\frac{S}{N}} = 1.28$ or $\frac{S}{N} = 2.16$ db.

The channel capacity C corresponding to $a = .1$ is

$$C = \log_2 2 + .9 \log_2 .9 + .1 \log_2 .1 = .531 \text{ bits/symbol.}$$

If a 16-digit pulse-train is transmitted without coding under these conditions, the probability that it will be received correctly is $(.9)^{16} = .18$, indicating a definite need for improvement in reliability. The choice of the coding period n and of the rate of transmission of information H will determine the reliability, and, according to Shannon's theorem, if $H < C$, the probability of error can be made arbitrarily small by choosing n sufficiently large. In Fig. 3 of reference 27 the reliability, measured by the "per-unit equivocation" or fraction of transmitted information which is lost due to noise, is plotted against C for several values of n, but for fixed $H = .2$ bits per symbol. From the point of view of the value $a = .1$ assumed above, and the consequent value of $C = .531$, it would be of interest to plot reliability against H for this fixed C, for several values of n. A few such calculations have been made, as follows, where the measure of reliability, R, is approximately the probability that 16 bits of information will be received correctly; that is, a figure comparable to the value .18 given above for the case of no coding:

n = 2	H = .5	R = .18
n = 3	H = .67	R = .18
	H = .33	R = .64
n = 4	H = .75	R = .18
n = 6	H = .50	R = .54
n = 7	H = .57	R = .52
n = 32	H = .52	R = .79
	H = .44	R = .89
	H = .37	R = .95
	H = .31	R = .98

The first five of these codes will correct an error in at most one digit out of n, and the code for n = 7 is Hamming's single-error-correcting code. The four codes for n = 32 will correct up to 4, 5, 6, and 7 errors respectively. If one of these codes is to be used in an IFF system, it would be desirable to use one of Hamming's "systematic" codes, such as the single-error-correcting code for n = 7 which provides a convenient procedure for correcting the errors. The procedure is to add certain combinations of digits in the received message and to use the resulting sums to locate which digit or digits are in error.

In this study of redundancy coding, it has been assumed that the transmitting equipment is operating at maximum peak power but not at maximum average power. In other words, it has been assumed that additional digits can be added for redundancy without decreasing the amplitude of each pulse, and furthermore that the gain in reliability being achieved by the use of redundancy could not have been achieved by simply increasing the amplitude of each pulse. The value of redundancy in an IFF system will depend on the extent to which these assumptions apply to the transmitting equipment used in the system.

B. Repeated-Challenge System

Early work under the contract gave attention to the problem of optimum detection of the signals received at the airplane. It was tacitly assumed that crosscorrelation would provide the optimum means of detection, and this would require storage of the correct challenge at the airplane. Calculations were made to show that punched tape could provide a practical solution to the mechanization of such a scheme. The scheme was not pursued further due to the operational difficulties entailed in the distribution and control of the tapes. It is expected that equivalent transmission reliability will be obtained, however, if all possible challenges are stored at the airplane, the transmitted challenge is repeated a number of times, and each challenge upon arrival at the airplane is crosscorrelated against all stored challenges - the stored challenge showing maximum correlation over a number of tries being chosen as the one that was transmitted. In this section, consideration is given to such a system in which the pulse-train challenge is stored by means of weighting networks attached to the taps on a delay line. In this treatment, attention is first given to a suggested practical system, and a qualitative operational analysis is included to indicate its expected performance in the presence of various types of interference. A supporting analysis in the next section attempts to show quantitatively the degree of reliability improvement that may be expected from such a scheme in the presence of Gaussian-noise interference. The method is also applied to an analysis of the ground end of the link. In these analyses, the system has been idealized to what is probably an impractical extent in order to permit the evaluation to be made.

All of the schemes referred to in the above, and discussed in detail in later sections, make use of integration over successive repetitions of the same challenge in order to obtain improvement in reliability. The numerical analyses have been made on systems wherein this integration has been performed on a digital basis - i.e. by the method commonly called binary integration. It has been shown by Harrington[28] that while this method is slightly poorer in principle than the analogue method, the non-ideal characteristics (such as finite memory) of the analogue integrator make the two about equivalent in the final analysis. An important advantage gained by the use of binary integration stems from its allowing the use of pulse circuitry instead of the less stable linear circuitry demanded by the analogue method. The types of circuits required are those for which reliable transistorized versions are either presently available, or seem possible.

Outline of a Suggested Airborne System

In this system the same n-digit challenge is transmitted repeatedly (perhaps fifty times) and with random spacing before a reply is elicited. As shown in the sketch below, after detection at the airplane the pulses are fed to a delay line with n taps, feeding n phase inverters. 2^n adding-busses are connected to the taps (directly and via the phase-inverters) in such a way that each adding-bus corresponds to one of the 2^n possible different challenges. (The sketch shows this for n = 2)

Those outputs of adding-busses which exceed a certain value (first threshold) are time-integrated over the interval between synchronizing

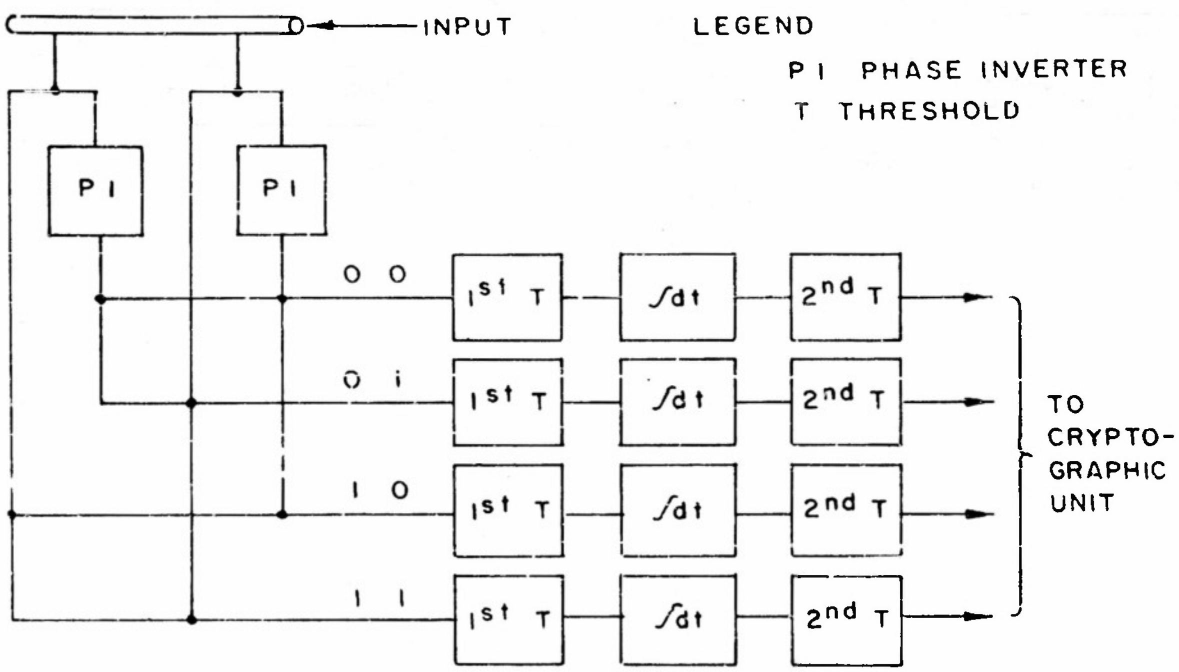

(perhaps radar) pulses, whose spacings are randomized within certain limits. Upon reception of a synchronizing pulse, those integrators whose voltages exceed a (second) threshold value cause the cryptographic unit to produce the corresponding replies, which are then transmitted in turn in rapid succession (interlaced?). At the same time the integrators are cleared, and a time-gate prevents any further synchronizing pulses from affecting the unit for a length of time equal to the minimum interval between synchronizing pulses. The first threshold may be set such that at maximum range a challenge will almost certainly cause its adding-bus voltage to exceed the threshold. The second threshold is set so that under the same transmission conditions a string of identical challenges will cause the proper integrator voltage to exceed the threshold.

Philosophy

In this section the repeated-challenge system will be considered in greater detail, and reasons for its various features will be given. It is easily seen that the additions in the adding-busses and the time integrations in the integrators will result in very good cancellation of random noise and random pulse jamming, so that the attention in this section is focused on the operation of the system in the presence of planned enemy interference.

In accordance with the design of the pulse-train correlator (discussed previously in Chap. III), the spacings of the pulses of each challenge will be staggered according to a fixed scheme to avoid multiple coincidences of pulses and taps prior to and subsequent to the instant of exact superposition.

The spacing between successive challenges is to be randomized within limits, in order that periodic pulse jamming cannot be employed to jam the same digit in each challenge. It is realized, on the other hand, that a jammer might achieve this result by sending out a jam pulse as soon as he receives the first pulse of a challenge. It is necessary, however, for this jam pulse to arrive at the target plane while the same challenge is still being received, that the difference in transmission times from the ground station to the target plane (1) via the jammer, and (2) directly, must be less than the duration of the challenge. For a challenge of reasonable size this method of jamming would therefore be effective only for a limited region and with the jammer located such as to be quite vulnerable to elimination.

The first threshold has the purpose of keeping the integrators from responding to anything but a correctly lined-up challenge. In the absence of such a threshold, each incoming pulse would yield a certain contribution to an integrator, and different challenges with the same number of pulses would not be differentiated between.

In the absence of enemy interrogation (and if only one ground station is received by the plane) only one integrator voltage will increase to more than the second threshold. In this case, then, only one reply will be triggered off by the arrival of the synchronizing pulse, and accurate range information can be obtained at the ground station from the round-trip transmission time. An enemy who attempts to upset the system by barrage interrogation will find that, to exceed the second threshold, each interrogation will have to be sent a great number (perhaps 50) of times within one synchronizing period. There will then not be time enough within that period to send many (say more than 5) different interrogations, each that many times. The transpondor then will reply to these enemy interrogations and to the friendly challenge, one after the other. Since, among others, it has produced the correct reply, the airplane will still be regarded as a friend (especially after several rounds). Since, however, the reply to the friendly challenge is not necessarily the first one to be sent upon arrival of the synchronizing pulse, somewhat different round-trip times will result for successive rounds, in other words, the accuracy of the obtainable range information is reduced by enemy interrogation.

In the event the enemy duplicates the synchronizing pulse the transpondor will be triggered by the enemy's pulse at least some of the time. Due to the time-gate in the synchronizing-pulse receiver, the replies will not be sent at an excessive rate, so that enough time still is available for the friendly challenges to integrate and exceed the second threshold. Due to the random timing of the friendly synchronizing pulses, no consistent range information will be obtained from the replies due to the enemy's synchronizing pulse. The replies due to the friendly synchronizing pulses can therefore be recognized by the relative constancy of the round-trip time.

A limiter at the input to the delay line can be provided to prevent strong individual pulses (at close range from the ground station, or due to powerful jamming) from exceeding the first threshold.

It is hoped that the number of digits that need to be included in a correlation interval can be kept small (say not to exceed eight). It is felt that, with proper miniaturization, seventy adding busses and associated

circuits can be readily accommodated in the airborne unit. For cryptographic reasons it is expected that challenges having a much larger number of digits will be required. It is hoped that a way can be found to break the challenges up into six- to eight-digit groups and to treat each group individually, thus making the size of the equipment increase at most linearly with the number of digits instead of exponentially. One promising-looking approach to this problem involves the use of a recycling delay line as storage and adding device. A tentative block diagram showing this modification to the receiver is shown below. It is intended that the tap switch periodically sweep the integrator

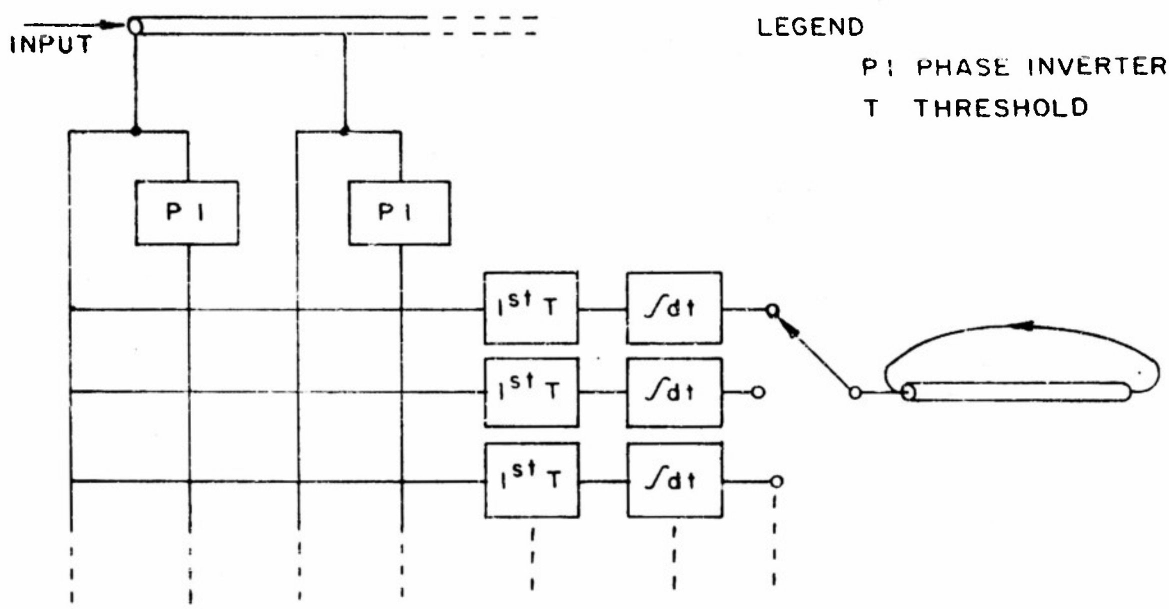

outputs fairly rapidly, allowing considerable inactive periods between sweeps. The recycling delay line, which is fed from the switch, has a delay equal to R times the period of the switching sweeps, where R is the number of groups in one challenge. The spacings between these challenge groups are made random but greater than the switching period, so that only one group at a time will be read off by the switch to produce a pulse on the recycling delay line. It can now be seen how every repetition of the R challenge groups will enhance the height of the recycled pulses, which by their timing relative to the switching sweep will indicate which challenge was received. It is realized that the system as outlined here is vulnerable to pulse-train jamming. While it is hoped that further refinement will remove or reduce this drawback, considerable recent effort toward this end has not proved successful.

C. Binary Integration of Repeated Challenges

Binary integration of repeated signals embedded in noise is ideally suited for application in the repeated-challenge system as a means for improving the

system reliability. Harrington[28] has shown the details of the application of this procedure in the case of the repeated radar signal. During the contract period his methods have been appropriately modified and applied to the theoretical analyses of the ground and air terminals of the IFF link (assuming, of course, the use of repeated challenges). In the beginning, it has been necessary to make certain (possibly unrealistic) assumptions concerning the form of the pulse-code symbols, the type of modulation, and the interference, in order that the analyses be manageable by presently understood techniques. It is felt that the results obtained indicate the order-of-magnitudo improvement that is possible through the use of a repeated-challenge system employing pulse-train correlation, and serve to suggest avenues for future work in this general direction. The procedures employed, and results obtained to this writing, are outlined in the two sections below where the work is divided to show application at the ground terminal and air terminal, respectively, of the IFF link.

System for Application at the Ground. Consider the block diagram of Fig. 26. It is assumed that the input to the correlator is connected to the output of the i-f amplifier of the IFF responsor and that the signal being received is immersed in Gaussian noise and consists of a train of pulses properly coded to correspond to the switch positions of the correlator. In this system it is assumed that a sinusoidal carrier is shifted 180 degrees to differentiate between the ones and zeros of the binary code. The bandwidth of the i-f amplifier is assumed to provide an appropriate match to the pulse width of a code symbol, i.e. the signal is assumed to reach its peak amplitude during the time of the pulse. The pulse recurrence period is sufficiently long for the given i-f bandwidth that independent samples of noise can be assumed during adjacent pulse periods, and the digit and space lengths are equal.

For a case covered by the above assumptions, Rice[29] has shown that the envelope distribution density of the output voltage of the i-f amplifier can be given by

$$p(R) = \frac{R}{\psi_o} \exp\left[-\frac{R^2 + P^2}{2\psi_o}\right] I_0\left(\frac{RP}{\psi_o}\right) \qquad (5\text{-}1)$$

where

R = envelope amplitude

P = peak value of the sinusoidal signal

ψ_o = noise power at the output of the amplifier.

$I_0\left(\frac{RP}{\psi_o}\right)$ = value of the modified Bessel function of the first kind and order zero for argument $\frac{RP}{\psi_o}$.

Assuming an ideal correlator for an n-place code, the envelope probability density of the adding-bus voltage V_Σ can be written as

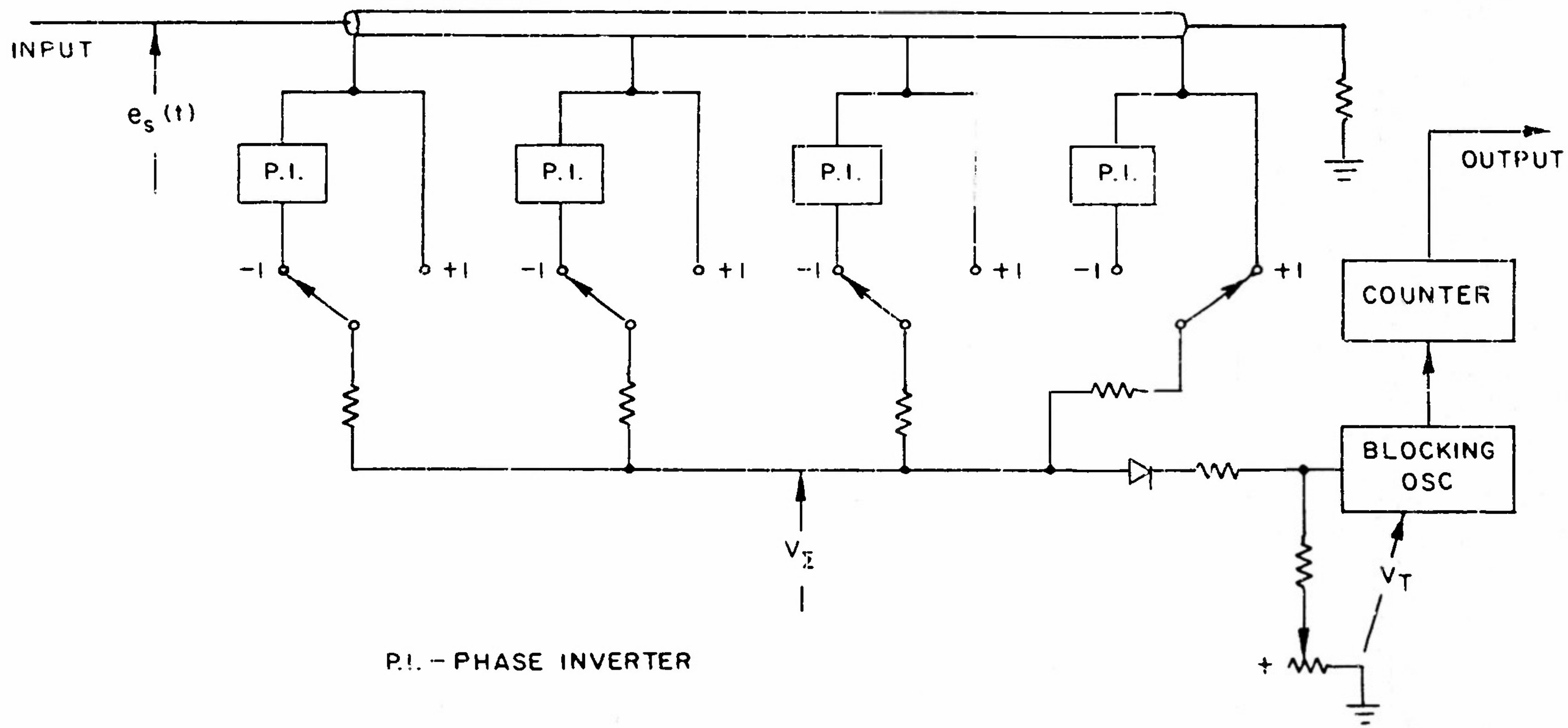

FIG. 26. BLOCK DIAGRAM SHOWING SCHEME ASSUMED IN MAKING THE ANALYSIS OF THE PERFORMANCE OF THE PULSE-TRAIN CORRELATOR.

$$p(R) = \frac{R}{n\psi_o} \exp[-\frac{R^2 + n^2P^2}{2n\psi_o}] \; I_o\left(\frac{RP}{\psi_o}\right) \tag{5-2}$$

and the corresponding probability distribution P(R) is p(R)dR. A more convenient form for future use is obtained if the following normalized parameters are introduced:

$$v = \frac{R}{\sqrt{n\psi_o}} \qquad a = \frac{\sqrt{n}\,P}{\sqrt{\psi_o}} = \sqrt{n}\,\rho$$ where ρ is the input signal-to-noise ratio.

$$\text{Thus, } p(R)dR = v\,dv\,\exp[-\frac{v^2 + a^2}{2}]\,I_o(av). \tag{5-3}$$

The blocking oscillator produces one pulse when the voltage V_Σ exceeds the threshold voltage V_T. It is assumed that the specifications on the system are such that this can happen only once during a digit, or during the space between digits.

The probability of the blocking oscillator producing a pulse due to signal and noise during the signal period is

$$P_S = \int_{V_T}^{\infty} p(R)dR = \int_{V}^{\infty} v\,dv\,\exp[-\frac{v^2 + a^2}{2}]\,I_o(av) \tag{5-4}$$

where $V = \dfrac{V_T}{\sqrt{n\psi_o}}$

and due to noise alone during the space period,

$$P_N = \int_{V}^{\infty} v\,dv\,\exp[-\frac{v^2}{2}] = \epsilon^{-\frac{V^2}{2}}. \tag{5-5}$$

Equation (5-5) has been obtained from (5-4) by noting that when the signal is zero, a = 0.

Optimum reliability, in one sense, is obtained if the threshold voltage is adjusted to a value that minimizes the probability of error. For this system, errors are produced when the signal amplitude is interfered with by the noise so that the threshold is not reached (called a "miss"), and when the noise during the space periods is sufficient to exceed the threshold (called a "false alarm"). Letting the probability of a miss be represented by P_M, and noting that the false-alarm probability is the P_N previously defined, then the problem becomes one of determining the value of V_T that makes (P_N + P_M a minimum).

Harrington has shown that equations (5-4) and (5-5) can be combined to eliminate v and yield

$$P_S = 1 - \varepsilon^{-\frac{a^2}{2}} \int_{P_N}^{1} I_0(a\sqrt{-2\log p})\,dp. \qquad (5\text{-}6)$$

By using a series expansion for I_0, it can be shown that

$$P_S = 1 - \varepsilon^{-\frac{a^2}{2}} \sum_{n=0}^{\infty} \frac{1}{n!} \lambda_n \left(\frac{a^2}{2}\right)^n$$

$$\text{where } \lambda_n = [1 - \sum_{k=0}^{\infty} \frac{1}{k!} P_N(-\log P_N)^k] \qquad (5\text{-}7)$$

$$\text{and } P_N = \varepsilon^{-\frac{V^2}{2}}.$$

Note that

$$P_M = 1 - P_S$$

so that $2P_e$, the probability* of error, is

$$2P_e = 1 - P_S + P_N. \qquad (5\text{-}8)$$

Figure 27 shows plots of P_M and P_N vs V (the normalized threshold voltage) for a = 1 and a = 2. Figure 28 shows curves of $2P_e$ vs. V obtained by using eq. (5-8) and the data plotted in Fig. 27. For a 16-digit correlator, the curves for a = 1 and a = 2 correspond to input signal-to-noise ratios of 1/4 and 1/2, respectively. Inspection of the curves indicates that, for a = 1, the optimum value of V is 1.5; and for a = 2, it is 1.75. The corresponding figures for the error probabilities are given in the table below.

a	P_N	P_M	P_e
1	.33	.51	.42
2	.22	.30	.26

* It should be mentioned that P_e is not a true probability in the statistical sense, but an arbitrary function (i.e. half the sum) of two probabilities derived from two different sets. As such, in the following the term average probability will be used to represent P_e.

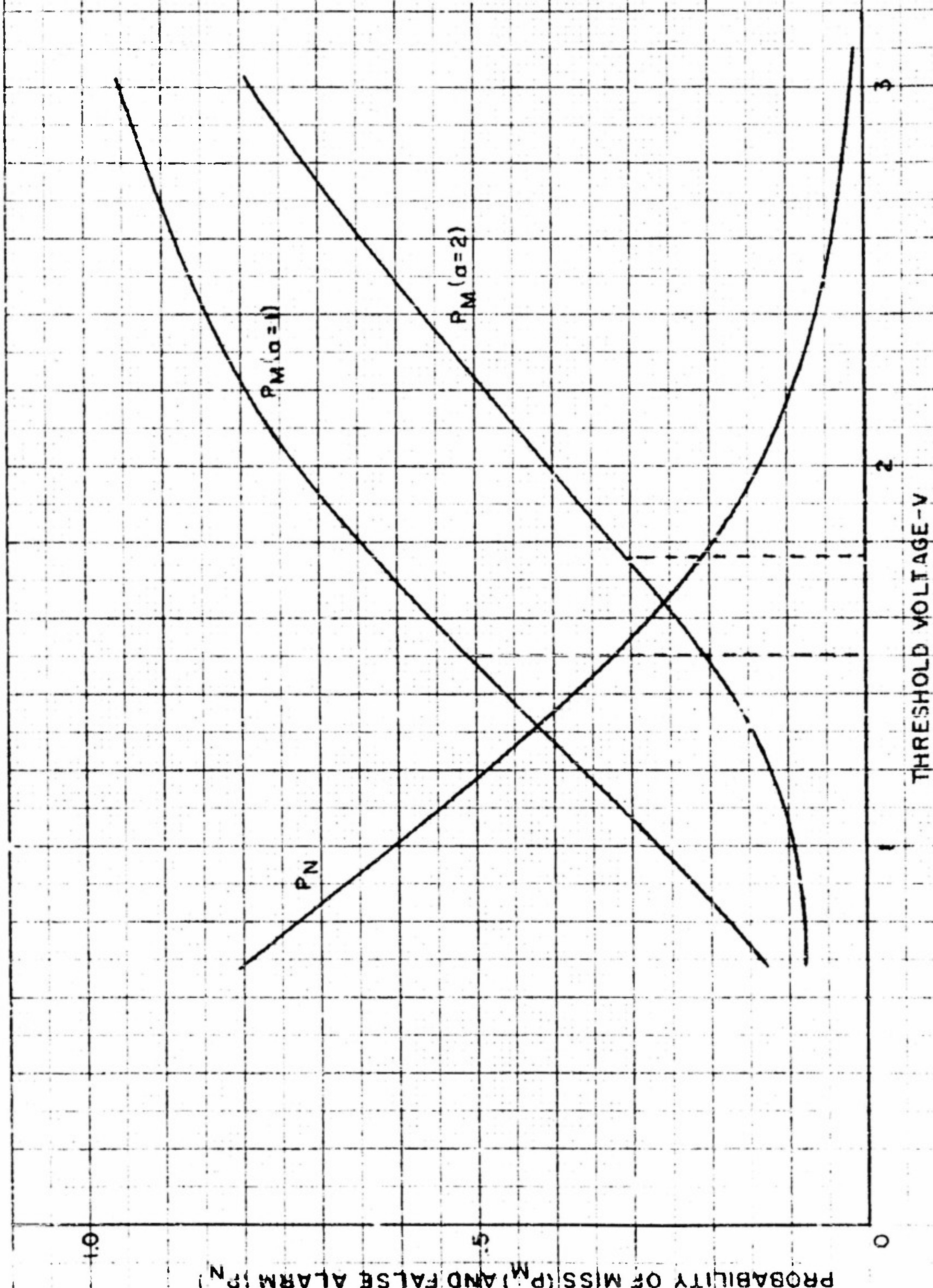

FIG. 27. PROBABILITIES OF MISSES AND FALSE-ALARMS VS. THRESHOLD VOLTAGE.

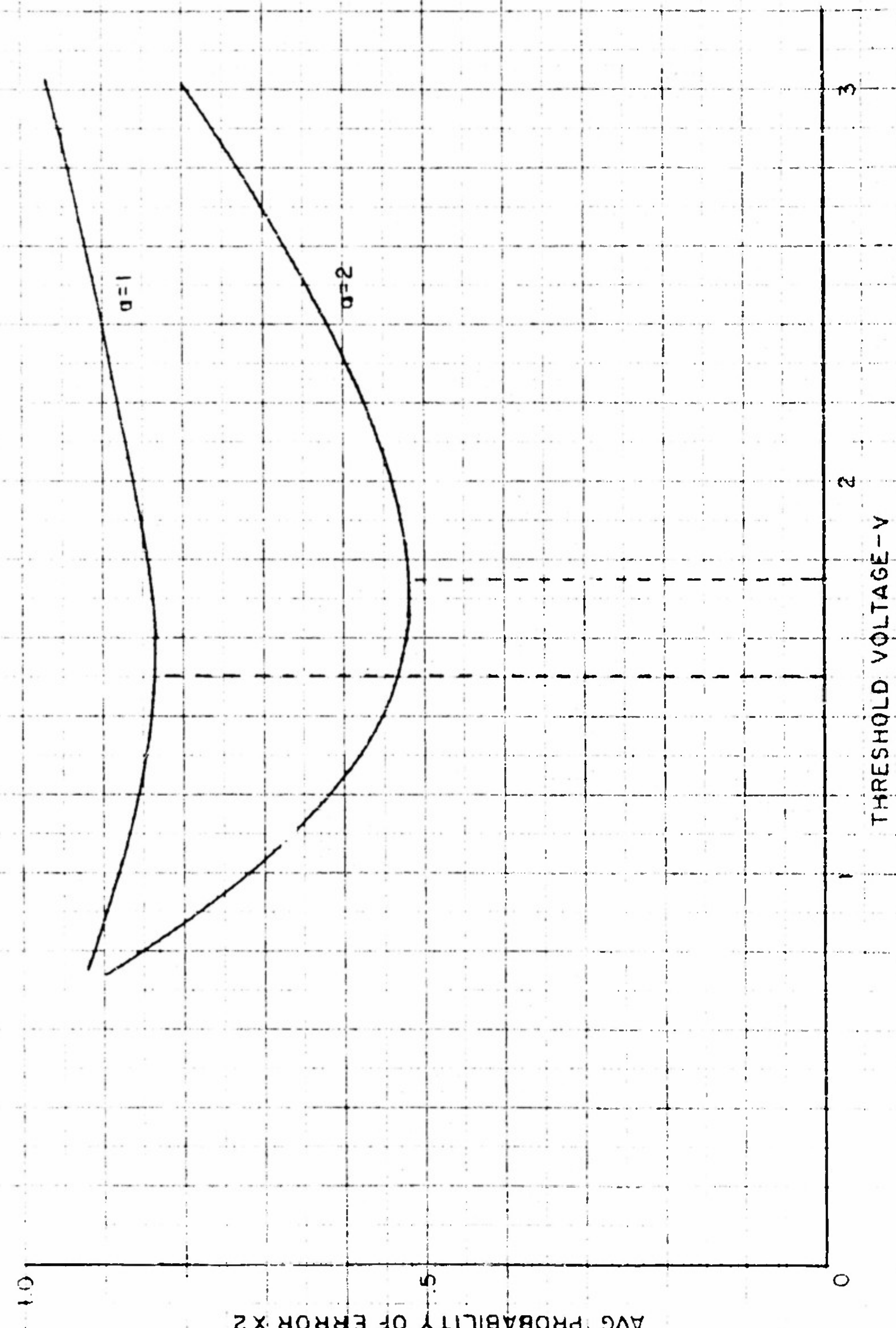

FIG. 28. PROBABILITY OF ERROR vs. THRESHOLD VOLTAGE FOR PULSE-TRAIN CORRELATOR.

In addition to serving to fix the value of V_T, the results of the preceding analysis can be interpreted to provide a quantitative figure for the reliability improvement resulting from the use of the pulse-train correlator. For example, if $\rho = 1$, then the average probability of error values give the relative improvement gained by using a four-place correlator. Likewise, for $\rho = 1/2$, the same figures give the improvement gained by using sixteen places compared to four places.

In the system assumed for this analysis (see Fig. 26), the challenges and replies are repeated m times in rapid succession, and binary integration used following the threshold device to provide further improvement in reliability. The final decision as to whether or not the correct reply has been received is based upon whether or not a threshold count k is exceeded in the m trials. Here two new error probabilities can be defined. The first is a "miss" probability P_m which increases with k; and the second, a false-alarm probability P_n due to noise during the space intervals that increases with a decrease in k. It is desired, therefore, to find the value of the threshold count that minimizes $(P_m + P_n)$.

The probability P_S is the probability of a correct pulse train being registered at the counter. The probability of obtaining a count of x due to correct pulse trains (in a set of m repetitions of the same reply) is given by the binomial distribution $C_x^m P_S^x (1 - P_S)^{m-x}$, and the probability of obtaining a counter reading of k or more, by

$$P_s = \sum_k^m C_x^m P_S^x (1 - P_S)^{m-x}. \qquad (5\text{-}9)$$

This expression can be readily handled, as shown by Harrington, if the Edgeworth series approximation to the binomial distribution is employed. This gives

$$P_s = 1 - \phi^{(-1)}(Y) - \frac{a_3}{3!}\phi^{(2)}(Y) + \frac{a_4 - 3}{4!}\phi^{(3)}(Y) + \frac{10}{6!}a_3^2\,\phi^{(5)}(Y)\cdots \qquad (5\text{-}10)$$

where $Y = \dfrac{k - \bar{K} - 1/2}{\sigma}$

$$\bar{K} = m P_3 \qquad\qquad \phi(y) = \frac{1}{\sqrt{2\pi}}\epsilon^{-\frac{y^2}{2}}$$

$$\sigma = \sqrt{\bar{K}(1 - P_S)} \qquad\qquad \phi^{(-1)}(Y) = \int_{-\infty}^{Y}\phi(y)dy$$

$$a_3 = \frac{1 - 2P_S}{\sigma} \qquad\qquad \phi^{(n)}(Y) = \frac{d^n}{dy^n}\phi(y)\Big|_{y = Y}$$

$$(a_4 - 3) = \frac{6P_S^2 - 6P_S + 1}{\sigma^2}$$

In a similar way, the probability P_n of obtaining a counter reading of k or more due to noise can be computed by using P_N in place of P_S. The miss probability P_m is evidently $1 - P_s$, and the problem resolves itself to one of plotting P_n and P_m vs. k, and determining the value k which makes $(P_n + P_m)$ a minimum.

The curves of Fig. 29 show results of such plotting for the case of $a = 2$, $m = 25$, V_T at optimum value. The curve of average error probability need not be plotted in this case, since it is evident from the steepness and curvature of the curves that the minimum point will occur practically at the intersection point where $k = 11.7$* and each of the error probabilities has a value of 0.00085. The average probability of error P_e, then, is also 0.00085. This figure is correspondingly reduced with an increase in m; however, computational difficulties arise in attempting a quantitative analysis for large values of m due to the need for the use of more terms in the Edgeworth series.

The equation for the probability density of the envelope of V_Σ (eq.5-2) used in the above analysis is only applicable when no detector is used ahead of the correlator. For the more practical system, where a detector is desirable due to difficulty in cutting the lengths of delay line, a new formula is required. Equation (5-1) is still applicable for the voltage at the output of a linear detector of the envelope-tracer type, and the problem becomes one of finding the probability density of the sum of n random variables each having the probability density p(R) given by eq. (5-1). This can be readily accomplished through the use of the characteristic function of p(R), $\psi(s)$, since

$$\mathcal{F}[p(V_\Sigma)] = [\psi(s)]^n \tag{5-11}$$

and $p(V_\Sigma)$ is, then, the "n"th convolution of p(R) with itself, or, for $n = 4$,

$$p(V_\Sigma) = p(R) * p(R) * p(R) * p(R). \tag{5-12}$$

The pulse-train signal assumed in the above analysis used a 180-degree phase shift to indicate the difference between ones and zeros. In a more practical system, a dual-frequency transmission system would be employed, so that a frequency p would be used to represent a one, and a frequency q for a zero, and the detector would take the form of a frequency discriminator. The equation for the envelope probability density required in this case in place of eq. (5-1) is given by Rice[29] as

$$p(R) = R \int_{r=0}^{\infty} r\, J_0(Rr)\, [J_0(Pr)]^2 \exp\left[\frac{-\psi_0 r^2}{2}\right] dr. \tag{5-13}$$

The criterion used in setting the counter threshold has been that which minimizes the sums of the unweighted probability that noise (or an incorrect signal) will appear as the correct signal and the unweighted probability that the correct signal will be lost (or called noise), this minimization being

* In practice, k would be made equal to either the nearest integer or the nearest power of two, depending upon the type of binary counter.

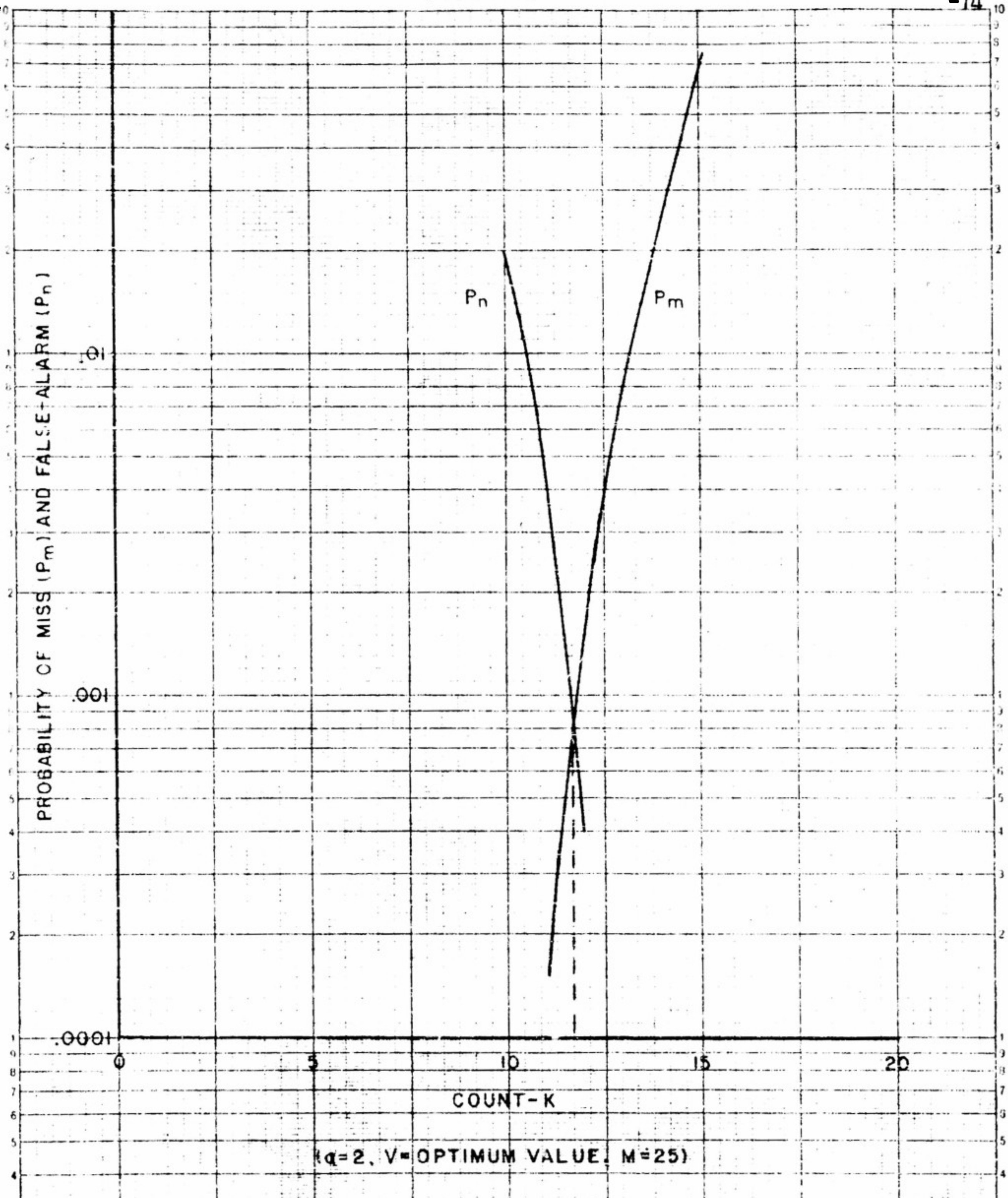

FIG. 29. PROBABILITIES OF MISSES AND FALSE-ALARMS vs. COUNT.

made for a fixed input signal-to-noise ratio by varying the number of repetitions over which the counter output is integrated. This is essentially the case of the "ideal observer" described by Middleton[30]. Whether or not this is the best criterion has not been studied.

System for Application at the Airplane. The block diagram of Fig. 30 shows the components which may be used in a transpondor receiver in the airplane if pulse-train correlators are employed to provide the advantages of crosscorrelation in improving the reliability of the IFF system. Each of the branches including a pulse-train correlator, threshold device, and binary counter can be assumed to be the same as the system considered in the previous section. With an n-place binary code, there will be 2^n possible different codes, and each of the correlators would be set to a different code. A different criterion would be used for setting the threshold voltages V_T than in the previous analysis, however; the most critical interfering signal for a given channel now is not noise, but the signals intended for correlators set for adjacent numbers. Insofar as the output decision device is concerned, three possibilities are presented. First, at the end of the challenge period (during which m challenges have been received) the counter showing the highest count is selected by a maximum-voltage measuring circuit to indicate the pulse train having the highest probability of being correct. In the second method, the 2^n counters are successively sampled after each pulse train has been received, and any which have received no pulse during the preceding interval are made inoperative for the remainder of the challenge interval. This is continued until only one channel remains in operation. It can be shown[31] that with high probability this is the channel corresponding to the correct pulse train. In the third scheme, a counter threshold K ($K < m$) is set, and the counter reaching this count first identifies the correct pulse train. Because of its relative mechanical simplicity, the system considered in the following will assume the last-mentioned type of decision circuit.

The main purpose of this section is to describe the method of an analysis currently being made to determine for this system the optimum settings for the voltage threshold V_T and counter threshold K; and, coincidently, the expected (average) probability of error for specified received signal-to-noise ratios will be obtained. Unless otherwise indicated, the same assumptions stated in the previous analysis will be made in the present analysis. Since detection occurs before summation, it will be necessary to use the method of eqs. (5-11 and 5-12) to find the probability density of the adding-bus voltage (V_Σ). Assuming for purposes of illustrative example that n = 4, the following equation can be written for the probability density of V_Σ, $p_0(V_\Sigma)$, for a correlator receiving a correct pulse train

$$p_0(V_\Sigma) = p(R)*p(R)*p(R)*p(R) = [p(R)*p(R)]*[p(R)*p(R)] \qquad (5\text{-}14)$$

where p(R) is given by eq. (5-1).

For a correlator receiving a signal differing by one digit from its correct pulse train, it can be easily shown that

$$p_1(V_\Sigma) = p(R)*p(R)*p(R)*p(-R) \qquad (5\text{-}15)$$

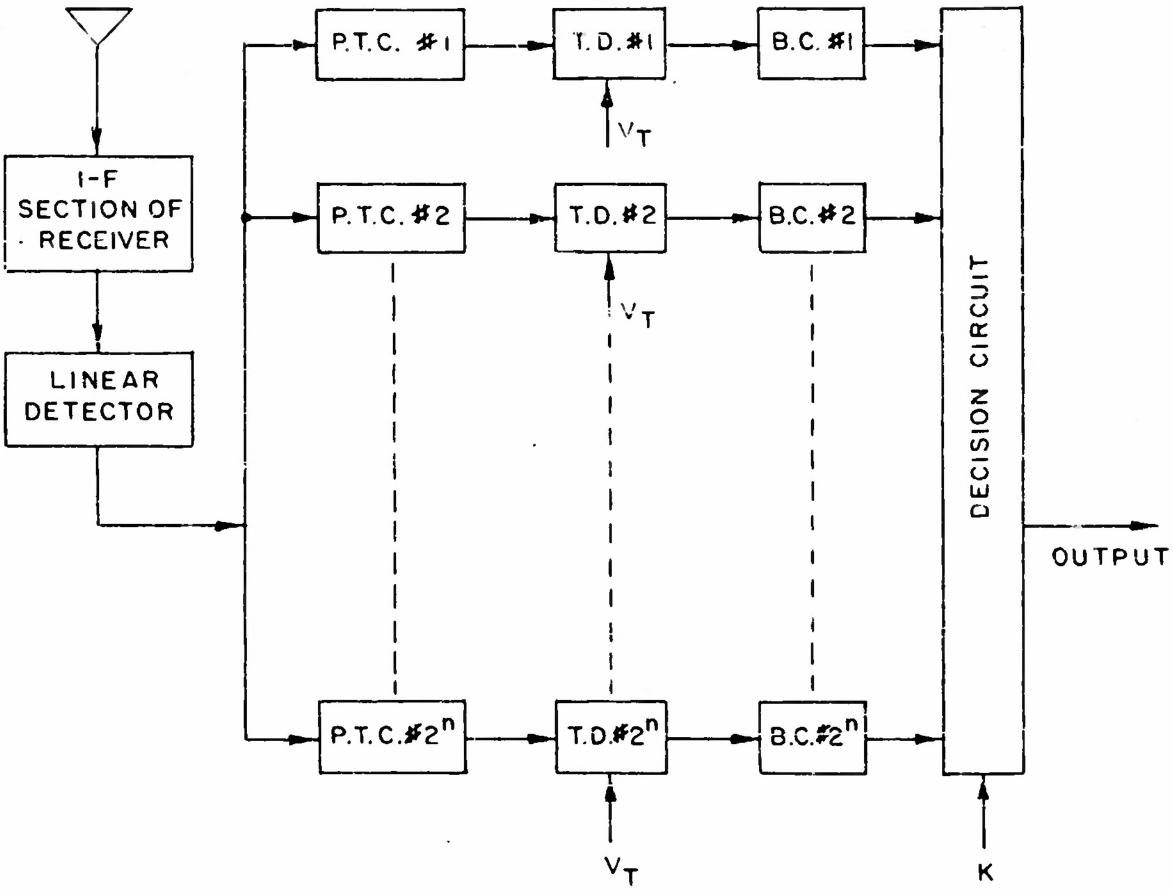

LEGEND

P.T.C. PULSE-TRAIN CORRELATOR

T.D. THRESHOLD DEVICE

B.C. BINARY COUNTER

FIG. 30. AIRPLANE END OF THE GROUND-TO-AIR LINK ASSUMED FOR ANALYSIS.

Likewise,

$$p_2(V_\Sigma) = p(R)*p(R)*p(-R)*p(-R) \tag{5-16}$$

$$p_3(V_\Sigma) = p(R)*p(-R)*p(-R)*p(-R) \tag{5-17}$$

$$p_4(V_\Sigma) = p(-R)*p(-R)*p(-R)*p(-R) \tag{5-18}$$

Equation (5-1) can be put into a form more convenient for the present analysis if the variables are normalized by letting

$$v = \frac{R}{\sqrt{\psi_o}} \qquad \rho = \frac{P}{\sqrt{\psi_o}} = \text{input signal-to-noise ratio.}$$

Then,
$$p(v) = v\,\varepsilon^{-\frac{v^2+\rho^2}{2}}\, I_o(v\rho)\ . \tag{5-19}$$

With the above probability densities defined, the first step in the analysis can now be described. It involves determining for a given ρ, the value of the normalized threshold $V(= V_T/\sqrt{\psi_o})$ which provides at the output of the threshold device a minimum average probability of error P_e as defined by

$$2\,P_e = P_M + P_F \tag{5-20}$$

$$\text{where } P_M = \text{probability of a miss} = 1 - \int_V^\infty p_o(V_\Sigma)dV_\Sigma \tag{5-21}$$

$$\text{and } P_F = \text{probability of a false alarm}^* = \int_V^\infty p_1(V_\Sigma)dV_\Sigma\ . \tag{5-22}$$

The analysis described above has been made using graphical techniques to evaluate $p_o(V_\Sigma)$, $p_1(V_\Sigma)$, the integrals of eqs. (5-21) and (5-22), and to effect the minimization of P_e. The curves of Fig. 31 show P_M and P_F vs. V_Σ, and their sum, $2P_e$, gives a minimum at the optimum threshold value of $V = 4.55$. The corresponding values (for $\rho = 1$) of P_M, P_F, and P_e are approximately .18, .14, and .16, respectively.

The above represents the extent to which the analysis being described has been so far carried out. The following outlines the procedure to be used in completing the analysis.

* In the present analysis, an approximation is being made in that the effect of noise occurring during the spaces within the pulse train is being neglected. It seems reasonable to assume that the false-alarm probability will be controlled by the adjacent-channel V_Σ. In any case, at the expense of considerable complication, this effect of noise can be included as will be discussed later.

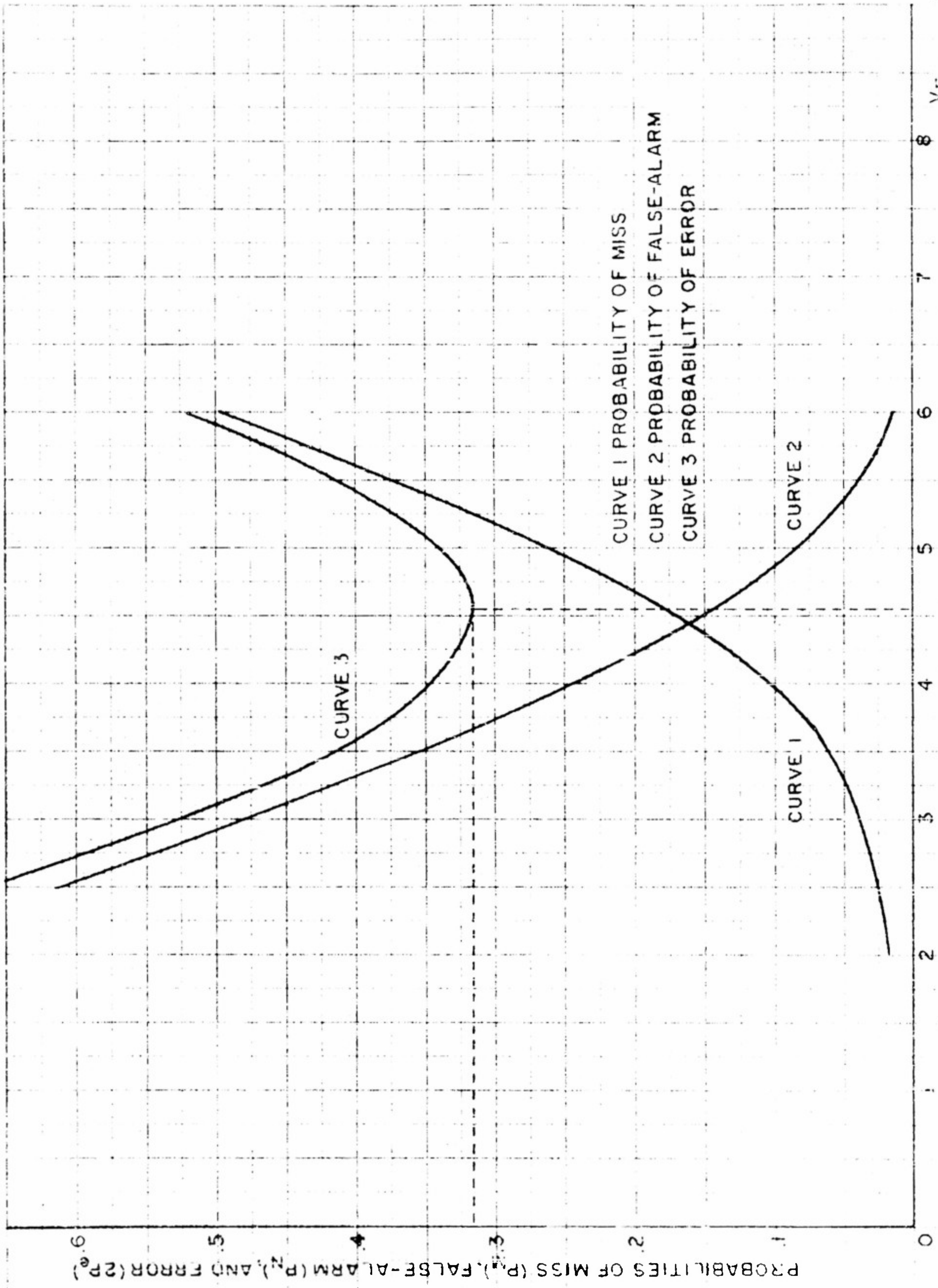

FIG. 31. PROBABILITY CURVES.

After determination of the optimum voltage threshold, attention can be given to the calculation of the optimum counter threshold, K. This is the setting that maximizes the probability that the counter connected to the channel receiving its correct pulse train reaches the threshold first. Or, in other words, it minimizes the sum of the probabilities of no channel count reaching the threshold at all and of some other channel count reaching it first. The first probability is the probability of a miss, $P_{M'}$, and the second is the probability of a false alarm, $P_{F'}$.

For n = 4, there are four component false-alarm probabilities for incorrect signals that are required in the determination of $P_{F'}$. They are:

P_{F_1}, the false-alarm probability when one digit is wrong

$$P_{F_1} = \int_V^\infty p_1(V_\Sigma)dV_\Sigma \tag{5-23}$$

(where V is the fixed threshold value)

P_{F_2}, the false-alarm probability when two digits are wrong

$$P_{F_2} = \int_V^\infty p_2(V_\Sigma)dV_\Sigma \tag{5-24}$$

where $p_2(V_\Sigma)$ is given by eq. (5-16)

P_{F_3}, the false-alarm probability when three digits are wrong

$$P_{F_3} = \int_V^\infty p_3(V_\Sigma)dV_\Sigma \tag{5-25}$$

and P_{F_4}, the false-alarm probability when all four digits are wrong

$$P_{F_4} = \int_V^\infty p_4(V_\Sigma)dV_\Sigma. \tag{5-26}$$

After noting that the probability P_s that the correct correlator produces a count of one at the counter is

$$P_s = \int_V^\infty p_0(V_\Sigma)dV_\Sigma, \tag{5-27}$$

the probability $\theta(k)$ that the correct counter will reach a count of k first can be written as

$$\theta(k) = \sum_{i=k}^{m} \theta_i(k), \tag{5-28}$$

where $\theta_i(k)$, the probability that the "correct" counter reaches a count of k first on the i-th trial, is given by

$$\theta_i(k) = [C_{k-1}^{i-1} p_s^k (1 - P_s)^{i-k}] \cdot [\sum_{x=0}^{k-1} C_x^i P_{F_1}^x (1 - P_{F_1})^{i-x}]^4 \cdot$$

$$[\sum_{x=0}^{k-1} C_x^i P_{F_2}^x (1 - P_{F_2})^{i-x}]^6 \cdot [\sum_{x=0}^{k-1} C_x^i P_{F_3}^x (1 - P_{F_3})^{i-x}]^4 \cdot$$

$$[\sum_{x=0}^{k-1} C_x^i P_{F_4}^x (1 - P_{F_4})^{i-x}] . \qquad (5\text{-}30)$$

The first factor in eq.(5-30) gives the probability of the correct counter reaching a count of k on the i-th trial. The product of the last four factors gives the probability that none of the other $2^n - 1$ correlators will reach the count of k on or before the i-th trial. Thus, $\theta_i(k)$ as written gives the probability that the correct counter reaches a count of k <u>first</u> on the i-th trial. By use of eq.(5-28), we obtain $\theta(k)$, the probability of a "success" in the process of determining which challenge was transmitted.

The probability $\mu(k)$ that none of the counters will reach k can be written as

$$\mu(k) = [\sum_{x=0}^{k-1} C_x^m P_s^x (1 - P_s)^{m-x}] \cdot [\sum_{x=0}^{k-1} C_x^m P_{F_1}^x (1 - P_{F_1})^{m-x}]^4 \cdot$$

$$[\sum_{x=0}^{k-1} C_x^m P_{F_2}^x (1 - P_{F_2})^{m-x}]^6 \cdot [\sum_{x=0}^{k-1} C_x^m P_{F_3}^x (1 - P_{F_3})^{m-x}]^4 \cdot$$

$$[\sum_{x=0}^{k-1} C_x^m P_{F_4}^x (1 - P_{F_4})^{m-x}] . \qquad (5\text{-}31)$$

Equations (5-30) and (5-31) can now be used to write an expression for the false-alarm probability $P_{F'}$. This is

$$P_{F'} = 1 - [\theta(k) + \mu(k)] . \qquad (5\text{-}32)$$

The probability $P_{M'}$ that no channel count will reach k is $\mu(k)$ as given by eq.(5-31).

All of the information required to determine the optimum value of the counter threshold, K, is now available. The problem becomes one of finding the value of k for which the sum of $P_{F'}$ and $P_{M'}$ (as given by eqs. 5-31 and 5-32) is a minimum. It is to be noted that the different forms of the

functions involved have all been handled before in the numerical analyses described in this and the preceding sections.

The preceding has assumed that there is no noise during the space interval, such as would be true if a synchronous system employing some scheme of gating off the noise during the space interval were used. In the more practical system where this is not true, the computations necessary in the determination of the new threshold count become unwieldy unless the use of automatic computing machines is assumed. The symbolism of formulating the analysis is relatively simple, however, and for completeness an outline of the procedure is given in Appendix II.

Commentary

As pointed out previously, the analyses just described are to be considered to be of an exploratory nature. Their purpose has been to provide experience in the use of statistical tools for quantitatively studying the reliability of relevant transmission systems. In some cases the idealizations have in obvious ways tended toward the impractical, a freedom which was taken in order to make possible the selection of a mathematical model under which analytical solutions would be possible. It is hoped that future work under this item will include the extension of the methods used in these preliminary analyses to cover more practical examples, and also provide information relating to operation at other values of input signal-to-noise ratio. It is hoped also that it will be possible to check the results of at least some of the analyses by experimental tests. Some of these may be performed on the model of the pulse-train correlator.

CHAPTER VI

CONSIDERATION OF ALTERNATIVE SCHEMES

A. Airborne Storage

The IFF system assumed in the previous sections of this report and shown in Fig. 1 precludes the storage of the successive challenges in the airplane. That such storage would entail the severe operational problem of secure distribution of the sequence of challenges to all airplanes is fully realized. On the other hand, with the promising development of the pulse-train correlator, the possible improvement in ground-to-air transmission reliability seems to warrant a certain amount of speculation about a system based on the storage of challenges in the airplane. Such a system would have the additional advantage of making it impossible for an enemy to elicit replies from our airplanes.

Aside from the operational problem referred to above, the realization of such a system poses the problem of storage of a large number of binary numbers in the airplane, and that of synchronization to within a challenge period between airplane and ground station. Analyzing the latter problem first, consider a system where a 2^{o} beam of the ground station rotates at 6 rpm. A target will be in the beam for one eighteenth of a second, and, if two hits per revolution are specified, a challenge rate of 36 per second will be needed. A sortie time of 72 hours then contains more than 10^7 challenge periods, and a timing accuracy of better than one part in 10^7 would have to be maintained to have available in the plane the information as to which challenge to expect next. Such accuracy cannot be realised practically. The synchronization problem can, however, be broken up into two parts, coarse synchronization, and fine synchronization, each part requiring an accuracy of about one part in $\sqrt{10^7} \approx 3 \times 10^3$.

Coarse synchronization can be achieved with mechanical clocks of a required accuracy of $\pm$ 30 seconds in 72 hours, so that the clock determines the minute of the day. Once a minute the ground station transmits omni-directionally a synchronizing pulse train (a different one every minute, not necessarily utilizing the same channel as the directional IFF beam), whose pulse-and-gap assignment is available at both plane and ground (stored on punched tape or the like). This pulse train can therefore be detected in the airplane by crosscorrelation, and is used to lock in the fine synchronization equipment. As soon as one correct synchronizing pulse train has been received, the lock-in equipment is gated off until the mechanical clock changes the code for the next minute.

Fine synchronization between synchronizing pulse trains is possible with a crystal-controlled or tuning-fork-controlled oscillator. (Required accuracy: one part in 10^4.)

The problem of challenge storage can probably be greatly reduced by evolving a scheme for generating, reproducibly yet unpredictably, a large number of challenges from one or a very few stored "challenge-generating" numbers. For example, one challenge-generating number for each minute could be stored

along with the synchronizing pulse train. That number and all its successive multiples are fed to an encoder to produce the challenges used during that minute. If the challenge-generating number has considerably more digits than the challenges to be produced, the encoder performs a many-to-one transformation which may be irreversible enough to afford sufficient security even with a fixed encoder (which then must be assumed to be available to the enemy). With this system of crosscorrelation by synchronization, the reply could be generated independently of the challenge by an identical process.

Care would have to be taken with this system to prevent the enemy from throwing off the lock-in of the fine-synchronization equipment by generating all possible pulse trains during each minute. This can be accomplished by making the synchronizing pulse trains long enough so that even with interlacing of pulse trains the enemy can transmit only a small fraction of all possible pulse trains in one minute.

B. Rotating Airborne Antenna

None of the countermeasures discussed so far appear to be completely reliable in the presence of pulse jamming. One obvious solution to this difficulty would be found in a system where it would be impossible for enemy jamming signals to be received by a transpondor simultaneously with the reception of a challenge. This condition can be nearly fulfilled with a line-of-sight communication system. If both ground station and aircraft were to have narrow-beam antennas which were directed along the line of sight connecting the two throughout the challenge-reply time, then neither transpondor nor responsor could be jammed by any enemy station except one situated within their respective antenna beams. Obviously, the probability of an enemy airborne jammer being located within these regions is quite low and consequently this type of system would be a close approach to a jam-free communication system.

A system possessing these qualities could be realized if each friendly aircraft were equipped with a rotating antenna as shown in Fig. 32. The IFF ground station at the center of Fig. 32 would contain the I-R unit and might very well be located at a vital target. The search antenna associated with the ground station rotates at a speed of S_g revolutions per minute and produces a beam which is θ_g degrees in azimuth and wide-angle in elevation. In the absence of enemy jamming, the ground station is capable of reliably identifying aircraft at all ranges up to R land miles from the installation and consequently identification of aircraft is usually accomplished in the "identification zone". Figure 32 also shows a number of friendly aircraft and airborne enemy jammers located throughout the search volume. All friendly aircraft are equipped with antennas which rotate at a speed of S_a revolutions per minute and produce beams which are θ_a degrees in azimuth and wide-angle in elevation.

Since the I-R antenna rotates with a speed S_g and has a beam-width of θ_g degrees in azimuth, any particular target will be within the beam angle for $\frac{\theta_g}{6S_g}$ seconds. In order to make it possible for a friendly aircraft to be able to receive a challenge during this time, the airborne antenna must make

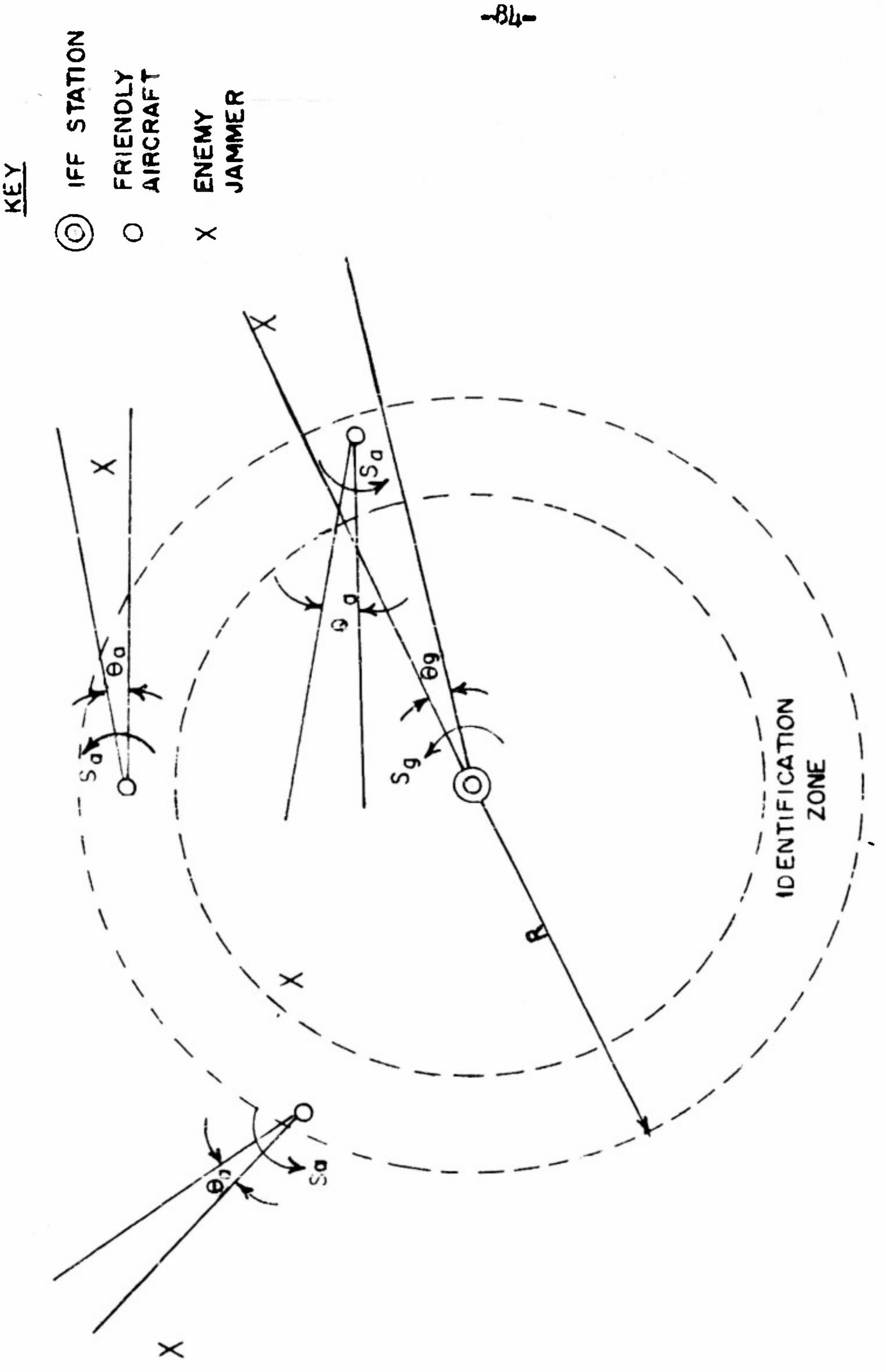

FIG. 32. OPERATING SKETCH OF IFF SYSTEM USING ROTATING AIRBORNE ANTENNA.

one revolution within this time and thus

$$S_a = \frac{360\ S_g}{\theta_g} \text{ rev. per min.}$$

Since the airborne antenna rotates at a speed S_a, the ground station will only be within its beam angle for $\frac{\theta_a}{6S_a}$ seconds. Therefore, in order that the transpondor may receive at least one challenge during this time, the ground station must transmit two challenges during this time and thus the challenge period must be

$$\tau_r = \frac{10^6\ \theta_a}{12\ S_a} \text{ microseconds.}$$

Furthermore, the maximum length of time between the transmission of a challenge and the receipt of its associated reply will be
$T = [10.73\ R + (\text{Time required for transpondor to encode reply})]$ microseconds. In all practical cases this time T will be much larger than τ_r and therefore there is the possibility of $\frac{T}{\tau_r}$ challenges being transmitted before the first reply is received. Therefore, two frequency channels will be required (one for transmitting challenges and one for receiving replies), a T-R switch will be required in the transpondor, two antennas will be necessary at the I-R unit, and the I-R unit will have to provide storage for the correct replies associated with a number of challenges sent in the past. (The number of challenges in storage should be equal to the smallest integer above $\frac{T}{\tau_r}$.)

In order to discuss the equipment required at the I-R unit, consider an IFF system which has R = 200 miles, S_g = 6 rpm, and $\theta_g = \theta_a = 4°$.

From previous equations, S_a = 540 rpm and τ_r = 617 µs. Assuming a reasonably short time for the transpondor to produce the reply from the challenge, it is evident that four storage units will be required at the I-R unit. The block diagram of Fig. 33 indicates the equipment (with the exception of r-f, i-f, and video stages) which might very well be used in a working system.

The challenge initiator would either work in conjunction with the search radar (and initiate challenges whenever aircraft were detected) or operate on a fully automatic basis. This latter case will be considered here and consequently the challenge initiator would put out triggers at intervals of 617 µs. These trigger pulses would be fed in parallel to three units: the challenge generator, the routing switch, and the ring counter.

Upon the arrival of a trigger pulse, the challenge generator would put out an n-digit challenge. The challenge itself would be transmitted to the aircraft whereas the correct reply would be obtained from the encoder.

The function of the routing switch would be to pass replies from the encoder to the storage unit in the appropriate correlator. Each trigger

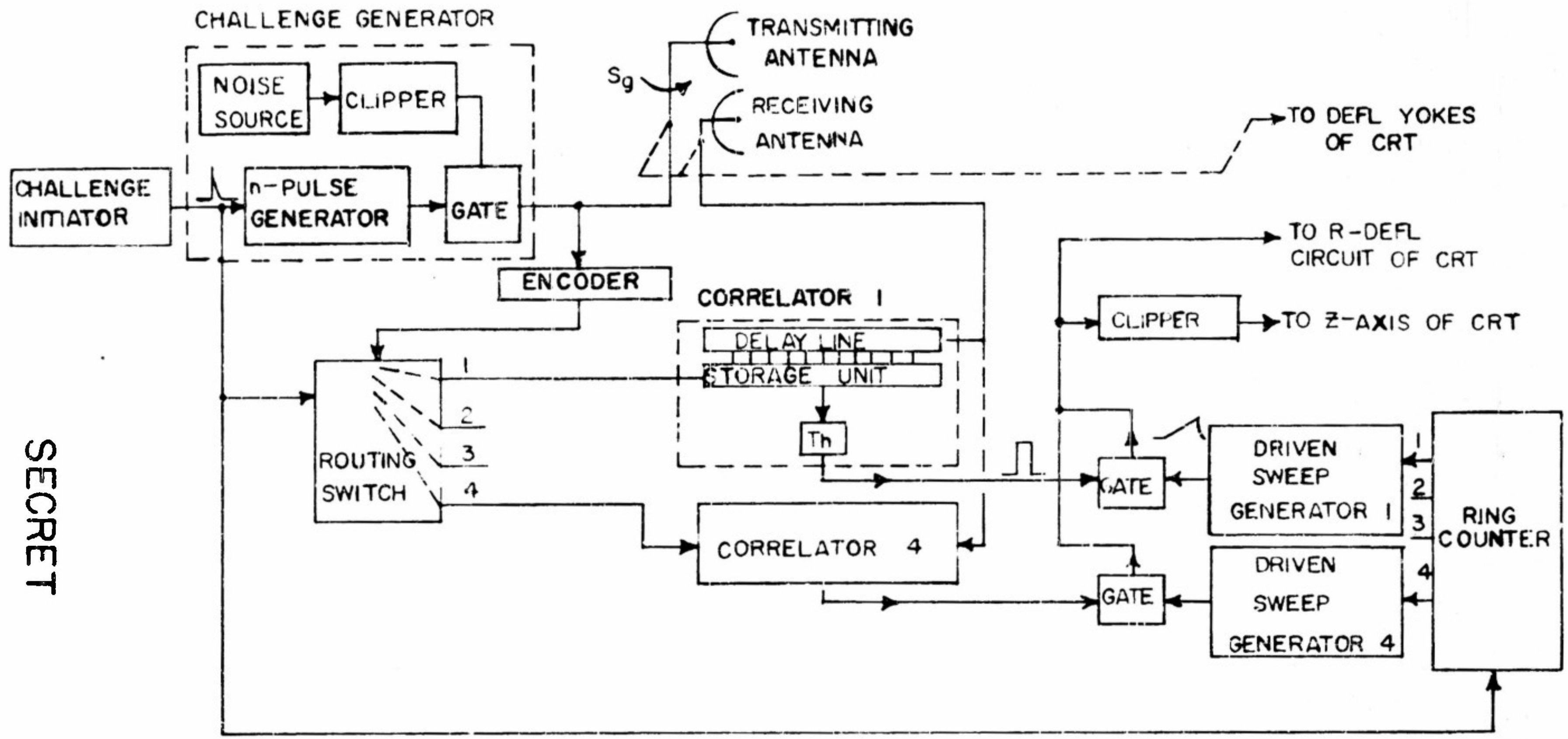

FIG. 33. I-R UNIT OF IFF SYSTEM USING ROTATING AIRBORNE ANTENNA.

from the challenge initiator would step the routing switch and thus the output of the encoder would be connected in sequence to the storage units of correlators 1, 2, 3, and 4. The fifth trigger would reset the routing switch to position #1 and hence the fifth reply would take the place of reply #1 in the storage unit of the first correlator. Each correlator is considered to be of the type described in Chap. III and thus storage of replies would be accomplished by setting the switches associated with the phase inverters.

In order to correlate replies with radar echoes, bearing and range must be known. Bearing can be obtained from the orientation of the antennas (which will rotate in synchronism). The range requirement, however, makes it necessary to measure the time elapsed between the transmission of a challenge and the receipt of its associated reply. In order to accomplish this end, triggers from the challenge initiator are fed to a third unit, the ring counter.

The outputs of the ring counter are connected to four driven sweep generators. Upon being triggered each sweep generator would generate a saw-tooth sweep of T microseconds duration. Since the ring counter would be stepped by triggers from the challenge initiator, a sweep would commence at the transmission of each challenge.

Replies are fed in parallel to all correlators. Upon receipt of a reply it would be crosscorrelated with the correct replies associated with the four challenges sent in the immediate past. The correct reply from a friendly aircraft would cause the threshold device (indicated by T_h in Fig.33) in one of the correlators to produce an output pulse. This pulse would drive the gate tube associated with the correlator and thus sample the saw-tooth sweep voltage. The amplitude of the pulse resulting at the output of the gate tube would be proportional to the range of the identified aircraft.

A PPI type of presentation, indicating all identified aircraft, could be readily obtained with the information now available. Azimuth information can be obtained by rotating the deflection yokes of the CRT in synchronism with the antennas. Range pulses would be fed from the outputs of the gate tubes to the deflection coils and the z-axis of the CRT. The information from the screen of the CRT could now be combined by optical means with the echoes on the screen of the search radar CRT so that friends could be indicated by green spots and unidentified aircraft by red spots.

All parts of the airborne unit could consist of conventional equipment with the exception of the narrow-beam rotating antenna. It is realized that the development of such an antenna might prove to be a difficult task. Size and weight considerations would probably make an X-band system mandatory. The problem of antenna design is being considered by the Antenna Laboratory of AFCRC.

The need for a rotating antenna arises from the assumption that an airplane, irrespective of its course, might be challenged by any interrogator within range. However, for certain applications (ADC for example) where it appears feasible that airplanes would be required to approach interrogators along certain prescribed courses[32], a rotating airborne antenna would not be necessary. A narrow-beam antenna mounted in the nose of the airplane

would suffice for this purpose and thus considerably simplify the antenna development problem.

C. Use of Noise-like Signal as Challenge

For a fixed average power and a fixed bandwidth the maximum entropy is possessed by an ensemble which is white Gaussian noise[23]. The use of such noise as a challenging signal makes it possible to fill an assigned channel capacity more efficiently and therefore to compete favorably with man-made jamming or natural interference. One example demonstrating efficiency in filling the channel capacity is given by multi-channel considerations. Also the ability to resist jamming and interference is conjectured in a proposed IFF system using noise-like signals. Both points are considered below.

Multi-channel Transmission

The question often arises as to what is the relative merit of sending a signal through a single channel or through n channels. This question, in general, cannot be answered in simple terms, because the transmission efficiency of any system depends, among other things, upon the properties of signal and interference, and the threshold effect of the system. If the amplitudes of both signal and interference are of Gaussian distribution and if the threshold effect is discounted, then there is always an increase in the average entropy if the same amount of signal power is divided into n frequency channels (each of bandwidth W_1) and when the interference noise power in each channel remains the same.

For a single channel with bandwidth W_1 and an average signal-to-noise power ratio r_1^2, the ideal capacity is

$$C_1 = W_1 \log_2 (1 + r_1^2) \text{ binits/sec.}$$

When the signal power is divided equally into n channels, the total capacity is

$$C_n = n W_1 \log_2 \left(1 + \frac{r_1^2}{n}\right) \text{ binits/sec.}$$

When both signal and noise belong to random Gaussian processes having flat spectra up to W_1, the number of degrees of freedom is $2W_1$ per second, and the maximum received entropies which the ideal channels are supposed to be able to transmit are

$$H_{R1} = \frac{C_1}{2W_1} = \frac{1}{2} \log_2 \left(1 + \frac{r_1^2}{n}\right) \text{ binits/degree of freedom}$$

$$H_{Rn} = \frac{C_n}{2W_1} = \frac{n}{2} \log_2 \left(1 + \frac{r_1^2}{n}\right) \text{ binits/degree of freedom}$$

and

$$\lim_{n \to \infty} H_{Rn} = \frac{1}{2} r_1^2 \log_2 e \quad \text{binits/degree of freedom}$$

These are plotted in Fig. 34.

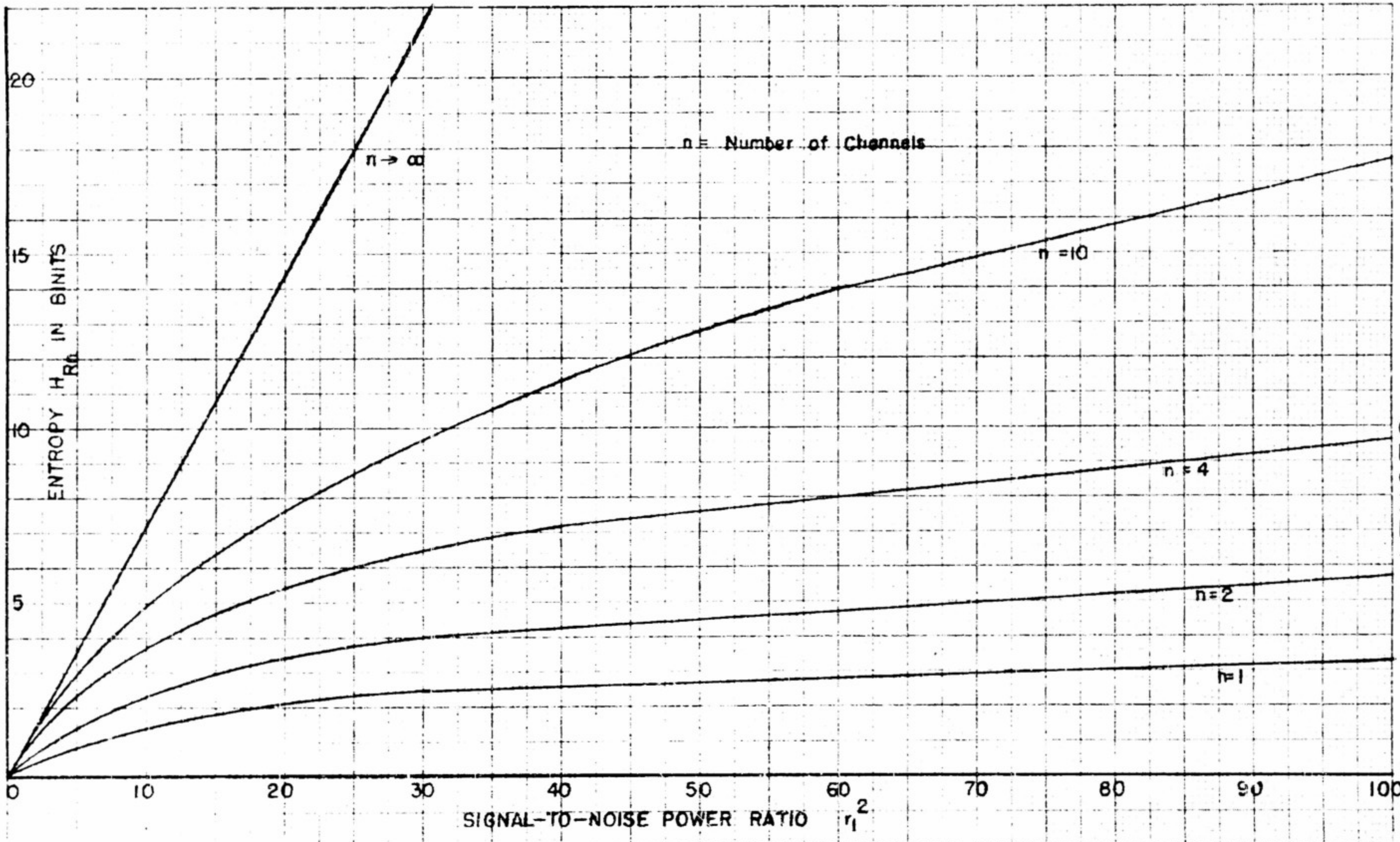

FIG. 34. ENTROPY IN MULTI-CHANNEL TRANSMISSION.

The advantage of multiple-channel over single-channel transmission depends upon how efficiently the ideal channel capacities are utilized. In practical systems, there is always a threshold value for r_1^2. Any multiplexing which tends to make the ratio less than the threshold results in rapid deterioration of the transmission.

As stated in the beginning paragraph of this section, the multi-channel consideration merely demonstrates the ability of signals resembling white Gaussian noise to fill the capacities provided by the increased number of channels. The main concern here is to propose a possible scheme for an IFF system using that kind of noise as the challenging signal.

Conjecture on Using Noise as the Signal

The use of a white Gaussian signal would be impractical if correlation methods were not available. A filter of lumped or distributed elements designed to select one such signal among the ensemble in the same band will be highly complicated if not impossible. Fortunately, in the IFF system, the signal sent to the plane is also available at the receiver of the ground station, and correlation techniques may be used. The principal features of the proposed scheme are analogous to those of the main scheme under consideration except that a continuous noise source replaces the randomized discrete binary digits, as shown below:

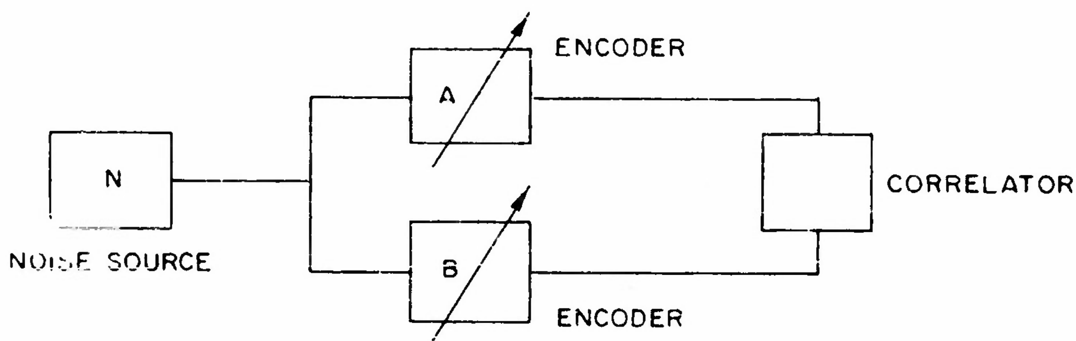

Path A represents the transpondor in the plane to be identified and path B represents a local simulating link. The two encoders can either be linear or non-linear, but they must be as nearly identical to each other as possible. The correlator under consideration is a simple analog computer using the polar portrayal of the joint distribution of the signals from the two paths. Such a correlator is discussed in detail in a recent report* of an unclassified project. It is deemed especially applicable to Gaussian signals. A brief description of the correlator follows:

Correlator of Gaussian Signals. When two Gaussian signals of zero mean and equal variances are applied to the x- and y-axes of an oscilloscope the distribution follows a pattern of elliptical symmetry. It is found that the distribution of intensity of illumination with respect to the polar angle θ

* Quarterly Progress Report No. 16, Contract No. AF 19(122)-7 Item 1. Visual Message Presentation, Feb. 8, 1953 to May 8, 1953, Northeastern University, pp 10-16.

is given by the equation:

$$p(\theta) = \frac{\sqrt{1 - r^2}}{2\pi(1 - r \sin 2\theta)}$$

where $p(\theta)$ is the distribution density and r is the normalized correlation coefficient of the two signals. It is to be noted that when $r = 1$ (or -1), the pattern becomes a straight line making an angle $45°$ (or $135°$) with the x-axis. When $r = 0$, the pattern has a circular symmetry and the polar distribution is uniform. For intermediate values of r, maximum density M is observed at $\theta = 45°$ and minimum density m at $\theta = 135°$, or vice versa in case r is negative. These two densities are sufficient to determine the particular value of r, by the following formula,

$$r = \frac{M - m}{M + m}$$

An alternative method is to determine the total illumination (call it P_1) of the first quadrant and that of the second quandrant (call it P_2). Because of symmetry the illumination of the third and fourth quadrants are also equal to P_1 and P_2 respectively. Then the correlation coefficient can be computed from the formula

$$r = \sin^{-1} \frac{\pi(P_1 - P_2)}{2(P_1 + P_2)}.$$

P_1 and P_2 may also be determined by infinitely limiting the x and y signals and measuring the intensity of the two beam spots in the first and second quadrants respectively.

One main advantage of this correlator is that no high-speed function multiplier is needed, and the calculations involved are simple addition and division to be performed at low speed. It is hoped that simple photoelectric and mechanical devices can be made to perform this task.

Linear vs. Non-linear Encoders

The purpose of the encoder is to distort and scramble the incoming signal in a prearranged way so that it is impossible for the foe to detect and thereby imitate its function within the sortie period. A linear encoder has several advantages: (1) It is simple to design the networks involved in each encoder of the two paths. Also, if necessary, it is feasible to design a direct encoding network in one path and an inverse network in the other. (2) Although the amplitude and phase spectrum of the incoming signal can be drastically changed by the encoding networks, the Gaussian amplitude distribution is still preserved in the output signal. (3) The additive interferences or jamming at the input will remain as additive in the output, thus facilitating their rejection by correlation. A fundamental limitation of the linear encoder lies in the possibility that the enemy can design an approximating network and pose as a friendly plane. A more critical evaluation of this situation is studied in a subsequent paragraph. It is also deemed possible that if the noise-like signal is packed in the form of bursts or pulses, the non-linear encoding technique used in the pulsed C.W. signals is

then applicable to increase the security against deception.

Possible Networks for Linear Encoder

Many methods are available in the design of linear networks of arbitrary characteristics. It is preferable, however, that the network be composed of simple units, connected in parallel and/or in cascade. It is also preferable that the number of isolating devices such as vacuum tubes or transistors should be reduced to a minimum. The elements of the component units may be adjusted separately to produce necessary codes for security.

One simple scheme to produce systematic codes of various degrees of complexity is to divide the spectrum into a number of complementary bands, each band to be phase-distorted by several stages of all-pass networks. The outputs of these bands are combined again to form the output of the encoder. A block diagram of such an encoder is shown as follows:

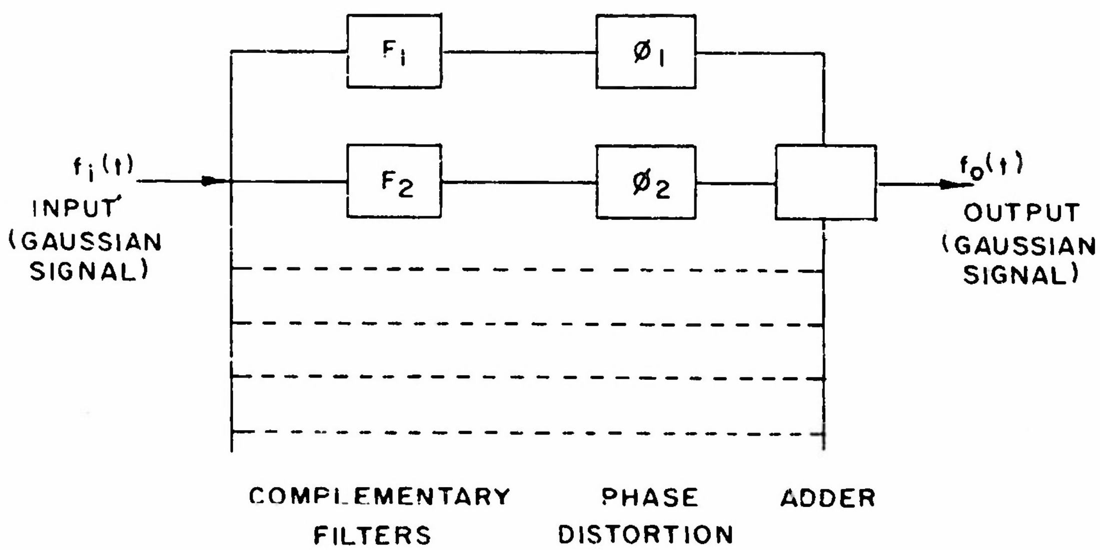

Designs of complementary filters of various classes and all-pass phase-distorting networks are available elsewhere and need not be discussed here.

The overall performance of the linear encoder can be described by the transfer characteristic H(s) or its equivalent, the unit impulse response, h(t). It is theoretically[33] possible that the enemy can, by cross-correlating the input and output signals of the encoder installed in a friendly plane, determine the transfer characteristic H(s) or h(t); he may thereby design an approximating network and pose as a friendly plane. This, indeed, is a fundamental limitation of the linear encoder. An analysis to find a measure of the closeness of imitation is shown on page 93.

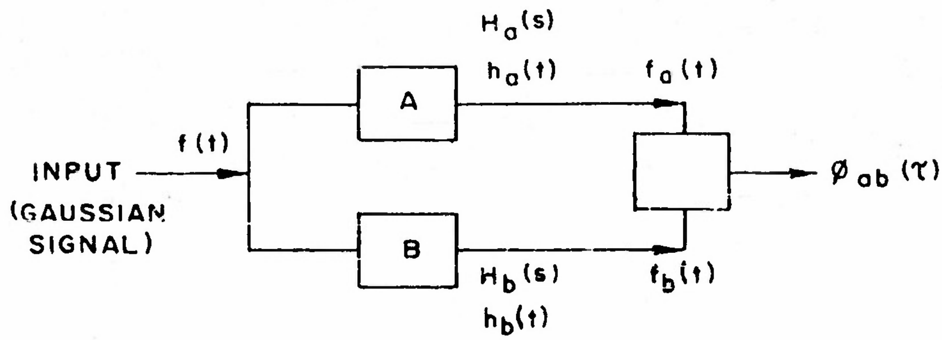

The transfer characteristics of the encoders of the two paths are expressed as $H_a(s)$ and $H_b(s)$, or alternatively as the unit impulse responses $h_a(t)$ and $h_b(t)$. Path B is the local link while path A may be the plane of a friend or foe. It can be shown that the cross-correlation $\phi_{ab}(\tau)$ between $f_a(t)$ and $f_b(t)$, as a function of $h_a(t)$, $h_b(t)$ and the autocorrelation function of $f(t)$, $\phi_{11}(\tau)$, is

$$\phi_{ab}(\tau) = \lim_{T\to\infty} \frac{1}{2T} \int_{-T}^{T} f_a(t) f_b(t+\tau)\,dt$$

$$= \int_{-\infty}^{\infty}\int_{-\infty}^{\infty} h_a(\xi) h_b(\eta)\,d\xi\,d\eta\,\phi_{11}(\tau - \eta + \xi).$$

When $\tau = 0$,

$$\phi_{ab}(0) = \int_{-\infty}^{\infty}\int_{-\infty}^{\infty} h_a(\xi) h_b(\eta)\phi_{11}(\xi - \eta)\,d\xi\,d\eta.$$

In case $f(t)$ belongs to a white noise ensemble, then

$$\phi_{11}(\xi - \eta) = \delta(\xi - \eta)$$

which is a delta function. This means that

$$\int_{-\infty}^{\infty} h_a(\xi) h_b(\eta)\phi_{11}(\xi - \eta)\,d\eta = \int_{-\infty}^{\infty} h_a(\xi)\, h_b(\eta)\,\delta(\xi - \eta)\,d\eta$$

$$= h_a(\xi) h_b(\xi)$$

and hence,

$$\phi_{ab}(0) = \int_{-\infty}^{\infty} h_a(\xi) h_b(\xi)\,d\xi.$$

By changing the variable of integration ξ into t and by using Parseval's theorem,

$$\phi_{ab}(0) = \int_{-\infty}^{\infty} h_a(t)h_b(t)dt = \frac{1}{2\pi}\int_{-\infty}^{\infty} H_a(\omega)H_b^*(\omega)d\omega.$$

In the case of a friendly plane, $h_a(t)$ should be almost identical to $h_b(t)$ and the value of $\phi_{ab}(0)$ is comparatively high. If this value is used as a standard, then one measure of the closeness of imitation is expressed as the ratio

$$\frac{\phi_{ab}(0)}{\phi_{aa}(0)} = \frac{\int_{-\infty}^{\infty} h_a(t)h_b(t)dt}{\int_{-\infty}^{\infty} h_a^2(t)dt} = \frac{\int_{-\infty}^{\infty} H_a(\omega)H_b^*(\omega)d\omega}{\int_{-\infty}^{\infty} |H_a(\omega)|^2 d\omega}$$

The success of the enemy plane in posing as a friendly plane will depend upon how closely this ratio approximates unity.

Additional Non-linear Encoding of Discrete Type

The scheme described above involves the use of a noise-like signal as challenge, a linear encoder, a transpondor and a special correlator for Gaussian signals. This scheme will be relatively immune to natural interference or artificial jamming but the possibility of deception is high especially if the sortie time is long. Additional security may be obtained by adopting techniques similar to those used in the main scheme as described in this report, namely, non-linear encoding of the discrete type.

Consider, for example, that the noise-like signal is packed in a sequence of pulses which represents an 8-place binary digit. It is further assumed that only 4 places contain pulses. These four packages of noise, after passing through the linear encoder, are recorded in a suitable storage device. The digital positions of these packages can then be scrambled by a discrete, non-linear encoder. The recorded noise packages are then assigned the new digital positions and retransmitted after a certain necessary delay. They are decoded at the ground station through the use of a Gaussian correlator (for the linear encoding part) and the pulse-train correlator (for the non-linear encoding part). To reduce the chance of jamming of the information continued in the digital positions of the pulses, the latter information may also be sent through auxiliary channels of much narrower bandwidth. As an added precaution, a number of pulse-train correlators may also be installed in the plane, based upon the same principle as proposed in the main scheme.

Briefly speaking, the attempt in this scheme is to depend upon the noise-like signal in achieving reliability against jamming and to depend upon the non-linear coding of the discrete type in achieving reliability against deception. More studies are needed to determine the theoretical and practical feasibility of the scheme and to reach a best compromise of the two component parts, continuous and discrete.

D. Use of Enemy Jam as the Challenge

The preceding chapters have outlined some relatively straightforward approaches to the problem of reducing the detrimental effects of enemy jam. In this section of the present chapter, a revolutionary scheme that reduces the advantages of jamming to the enemy will be suggested. Detailed work on this method has not been performed because of the unique procedures and equipment complexity involved. The principle, however, is quite simple as will be seen from the following.

Consider the presently conceived IFF system as it was shown in Fig. 1. The two encoders, call them A and B, are simultaneously "challenged" by random-digit numbers generated by the random-digit generator located at the ground with encoder A. If the replies are the same (as determined by the comparator) then the ground encoder A knows that encoder B is located in a friendly airplane. Let it now be assumed that a jamming signal is sent out from a source C, so that the encoder B is now challenged by the sum of the two signals from A and C. Without crosscorrelation techniques available at the airplane, B is unable to distinguish between the challenge from A and the jamming signal, provided they are sufficiently alike so that ordinary linear filtering cannot be used to differentiate between them. Encoder B then responds to the sum, and the friendly airplane is identified as an enemy. However, the error is made for the fundamental reason that the system requires that the two encoders operate on the output of a random-function generator located at the ground base. Note also that the enemy's effectiveness in jamming the signal increases with his ability to duplicate the friendly challenge. The suggestion then, is to force him to this point in jamming technique, and to then turn off the friendly random-digit generator and use the jamming signal in its stead as the input to the two encoders. The revised system is compatible with the basic idea of the original approach, the only requirement on the two encoders in either approach being that they answer <u>any</u> and <u>all</u> questions in the same manner.

It is of course necessary that the ground station be equipped with a jam-analyzing receiver, and that some provision be made in the system for determining the exact location of the jammer. Also, an automatic means would be required to switch the operation between "self" and "enemy" interrogation as the strength and type of jamming is varied - either due to natural causes, or by intent of the enemy. The enemy would attempt to keep his signal at the threshold where it is sufficient to partially disrupt the communication, but not sufficient to be used as the challenge. The uniqueness of the problem is interesting - here is an unusual case, unusual in that the operation of a communications link is definitely controlled by the principles of military strategy.

This approach has not been carried beyond the point of its initial consideration. To perform experimental research would require a complete turn-about in the direction in which work had been started. Also, there are several fundamental problems involved, some of which have been indicated above, which promise extreme difficulty in their solution for a practical system to result. It may be, however, that work on future IFF systems might well make use of this suggested scheme.

CHAPTER VII

CODING CIRCUITRY

A. Introduction

Item III on coding circuitry has involved, in general, the design, construction, test, and evaluation of reliable circuits for use in the final IFF system. The first circuit studied in this way was a transistorized shift register for use in the encoder units of the system. Later, the work was narrowed to cover the reliability evaluation by marginal-checking procedures of a particular transistorized flip-flop circuit.* A supporting unit of work under this item has been a transistor-testing program.

B. Transistorized Dynamic Delay-line Storage Cell

As indicated above, work under Item III began with the study of a reliable shift register. The fact that several of these are required in the final IFF system, and that some are involved in airborne equipment, makes it necessary that weight be reduced to a minimum. Hence, the use of transistors, instead of vacuum tubes, has been assumed for use in the components of the register.

For the purpose of the intended application, the following specifications were set: (1) the input to the register will consist of 16-digit binary numbers, each pulse having a width of 0.1 to 0.3 μs, and the pulses spaced by 1 μs, (2) the register is to be arranged for either serial or parallel read-in, and either serial or parallel read-out, and (3) the effects of loading the register should be investigated, since the registers in practice will be connected to such devices as matrix switches.

The first shift register considered was one in which a dynamic delay-line storage cell is used for each digit register. A block diagram and schematic of this storage cell is shown in Fig. 35. Several of these cells were built and gave satisfactory performance individually. A slight improvement in stability was obtained by introducing a small positive bias voltage (about 0.8 volts) in the base circuit of the amplifier included in the storage-cell unit. Certain transistors used (Transistor Products Type 2C and 2D), which tended to oscillate in the amplifier circuit, were made stable by the addition of this bias voltage.

However, when several of these digit registers were cascaded through amplifiers and shift gates in building up a shift register, satisfactory operation could not be obtained. Time delays, introduced by the transistor amplifiers and diode gate circuits, prevented the coincidence of pulses at the inputs of the shift gates, resulting in a stored "one" being lost as a "zero".

* This circuit was designed by A. W. Carlson[34] of the Air Force Cambridge Research Center.

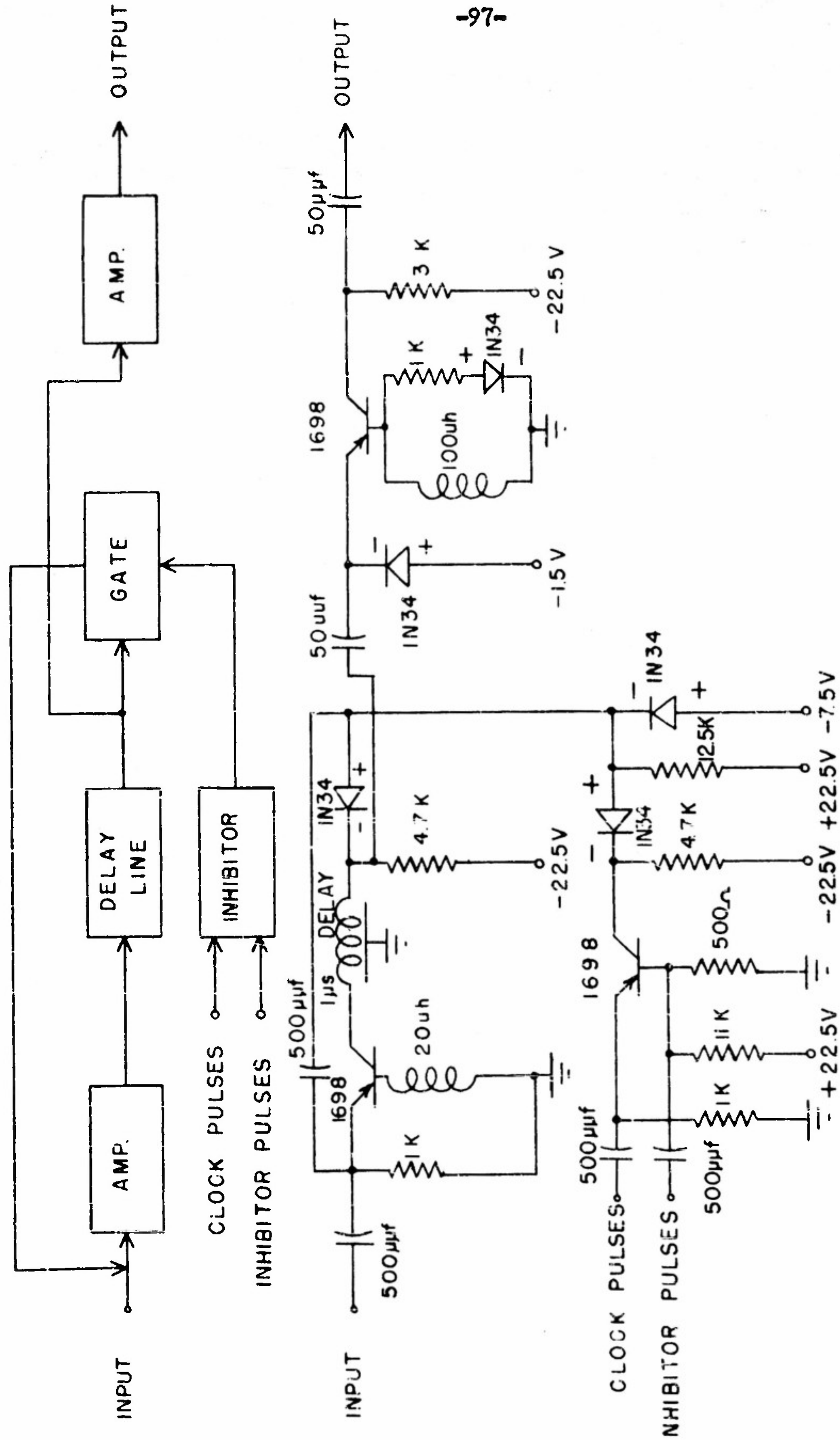

FIG. 35 TRANSISTORIZED DYNAMIC DELAY - LINE STORAGE CELL.

C. Dynamic Transistor Storage Cell Using Two Monostable Circuits

The appearance of the undesirable time delays in the dynamic delay-line storage cell led to the consideration of a second type dynamic storage cell using two monostable transistor circuits. This type of storage cell, including an inhibitor circuit and an "and" gate, is shown in the block diagram below.

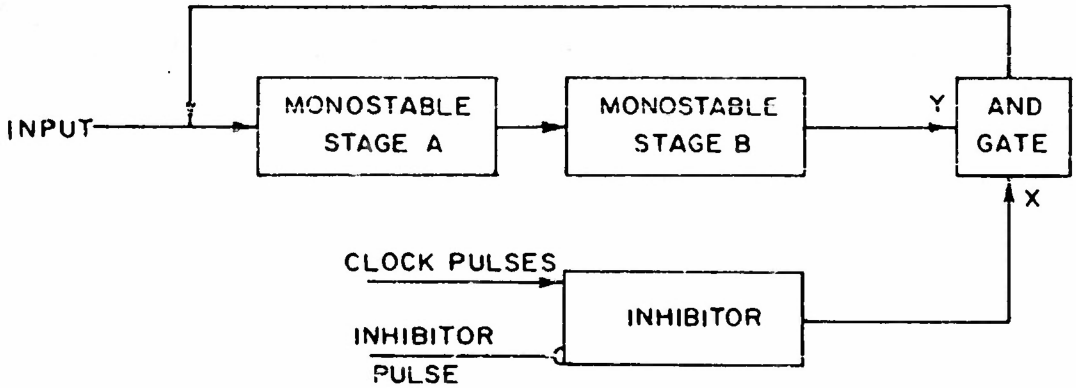

Clock pulses applied to the input of the inhibitor also appear at the "x" input of the gate circuit, provided that no inhibitor pulse is present. A pulse at the input of the storage cell initiates monostable stage A. The return of stage A initiates stage B. The combined delay of stages A and B must be greater than the time interval between clock pulses but less than two times the time interval between clock pulses. In this manner, the gate circuit is made operative by having pulses at the "x" and "y" inputs simultaneously. The output pulse from the gate circuit again initiates the stage A causing the continuous repetition of the above cycle. The timing diagram for this type storage cell is shown below. A storage cell of this type has been made to operate continuously for several hours at a time.

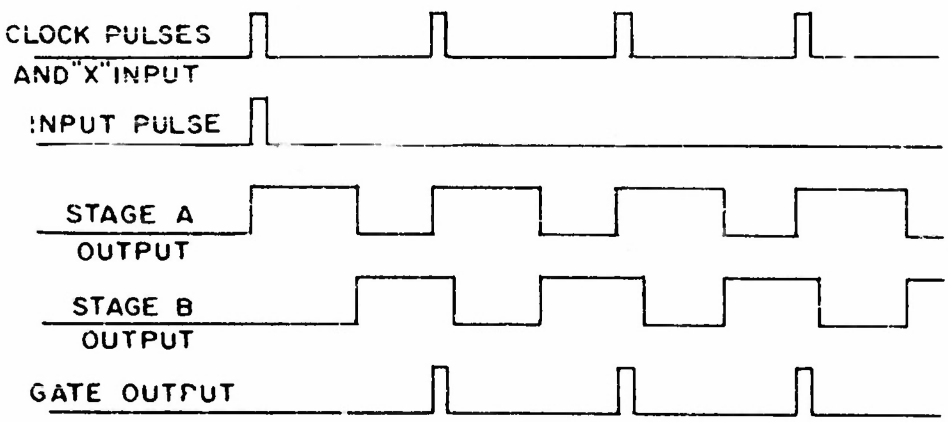

A schematic diagram of the storage cell using two monostable transistor circuits is shown in Fig. 36. Stage A is a monostable circuit using a coil in the base circuit as a means of generating a time delay. The coil and the germanium diode in the collector circuit are used to generate a negative pulse at the end of the delay. The negative pulse base-triggers stage B which in turn generates a delay by means of the capacitor in the emitter circuit. The transistor inhibitor circuit allows clock pulses to be applied to one input of the diode gate circuit provided that there is no inhibitor pulse present. The gate circuit is a conventional diode "and" circuit.

A clock-pulse generator essentially the same as one designed by the Digital Computer Laboratory at M.I.T. was constructed and used until a Burroughs Pulse Generator Type 1002 was purchased.

Further development of a dynamic storage cell using either delay-line cable or two monostable transistor circuits was indefinitely postponed so that emphasis could be placed on the evaluation of the reliability of a bistable transistor circuit by means of marginal checking techniques.

SECRET

* * *

UNCLASSIFIED

D. Bistable Transistor-circuit Research

The work started under the new problem was the reliability evaluation of a transistor flip-flop circuit having two stable, non-saturated states. Marginal-checking techniques[35,36,37], as developed at the Digital Computer Laboratory, M.I.T., were considered to provide the best method for reliability testing.

The method of marginal checking necessitates obtaining considerable amounts of data to be used for plotting various types of curves. The shape and area included within these plots are indications of the reliability of the circuit considering the two parameters used as variables. For a symmetrical plot, the coordinates designating the nominal value of the parameters plotted should fall in the center of the enclosed area for maximum reliability.

A study of marginal-checking methods resulted in a program that should be followed in the evaluation of reliability of the circuit. The program is described briefly below. Plots would be made using many combinations of the following items as parameters: (1) all of the bias voltages applied to the circuit, (2) all of the components used in the circuit, (3) various types of transistors including different transistors of the same type, (4) input pulse-repetition frequency, and (5) amplitude and width of input pulse. Typical of such plots would be curves of collector resistance vs. collector

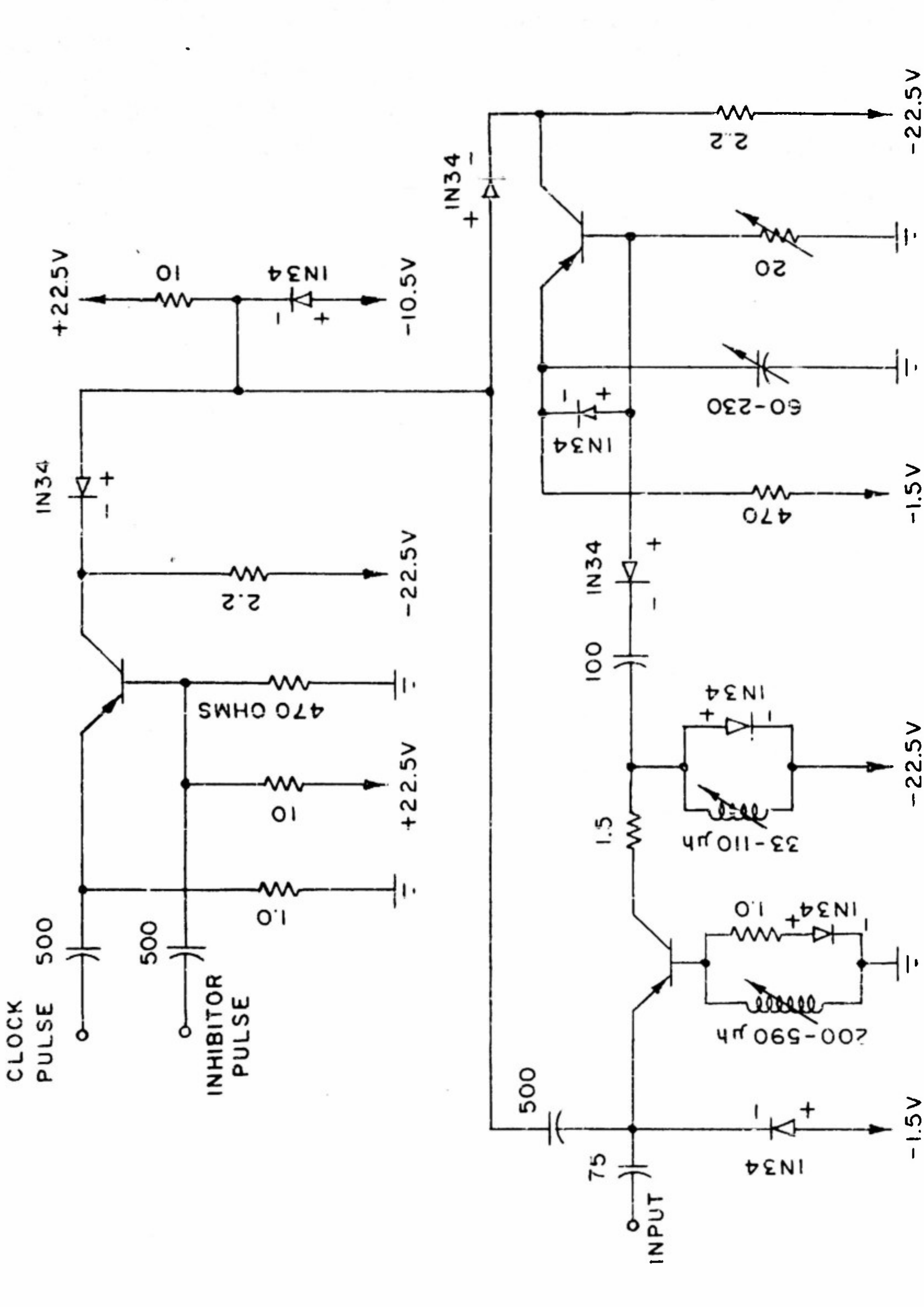

NOTE: ALL RESISTANCE VALUES IN K OHMS AND ALL CAPACITANCE VALUES IN μμf UNLESS OTHERWISE SPECIFIED

FIG. 36. DYNAMIC TRANSISTOR STORAGE CELL USING TWO MONOSTABLE CIRCUITS.

voltage and of collector voltage vs. base resistance. Considering the same two parameters as variables, other plots could be made as follows: (1) all other parameters at nominal values, (2) one or more of the other parameters offset from their nominal value by a specified percentage, and (3) all other parameters offset from their nominal values by amounts considered to create the "worst" possible combination. The accomplishment of the above should provide the necessary information for determining the design center and nominal values of components to be used, as well as an evaluation of reliability of the circuit.

The work was begun by determining the feasibility of obtaining data and by developing the experimental techniques necessary to obtain good data. In order to obtain information of sufficient accuracy to plot the above curves, it was found necessary to use precisely calibrated potentiometers as a means of varying the circuit resistive components such as R_b. A Shallcross Kelvin-Wheatstone Bridge Model 638-R was acquired to make these calibrations. Also accurate high-impedance voltmeters (greater than 20,000 ohms per volt and 1 percent accuracy) were necessary to obtain reliable voltage readings.

Figure 37 shows the schematic diagram of the basic non-saturating transistor circuit. This circuit was used while developing techniques to obtain suitable data for marginal checking tests. It appeared from these tests that data for marginal-checking plots could be readily obtained. Figures 38 and 39 show typical plots of V_{cc} vs. R_b and V_{cc} vs. R_c for the aforementioned circuit. A negative input pulse of 12.5 volts amplitude was used and all other parameters held at their nominalvalues.

The circuit used for the final marginal-checking plots is shown in Fig. 40. Each of the transistor collectors has a diode gate connected to it for pulse steering. The first check performed on this circuit was to determine the repetition frequency to be used for other tests. Spot checks were made using repetition frequencies from single-shot to 1 megacycle. These checks indicated the circuit operation to be independent of the above range of repetition frequencies. For convenience, a frequency of 200 kc was selected as standard for other tests.

In order to perform any tests with single-shot operation, it was necessary to design and construct a single-pulser circuit. The single-shot pulser generates a pulse by gating a Burroughs Pulse Generator Type 1002 so that one pulse is obtained for each operation of a push button. This method was used so that the flip-flop circuit receives a trigger pulse of the same shape and amplitude whether continuous operation from the clock-pulse generator or single-pulse operation is used.

Figure 41 shows the schematic diagram of the single-pulser circuit. The one-shot cathode-coupled multivibrator V1 has a long time delay to cover any switch bounce from the single-pulse switch that might cause multiple pulsing. When the normally conducting side of V1 is cut off, the plate level rises, triggering V2, a one-shot cathode-coupled multivibrator. V2 gates the clock-pulses at the input of the cathode follower V3. The gating pulse of V2 is set to 5 µs width and the clock pulse generator is set for 200 kc. Therefore

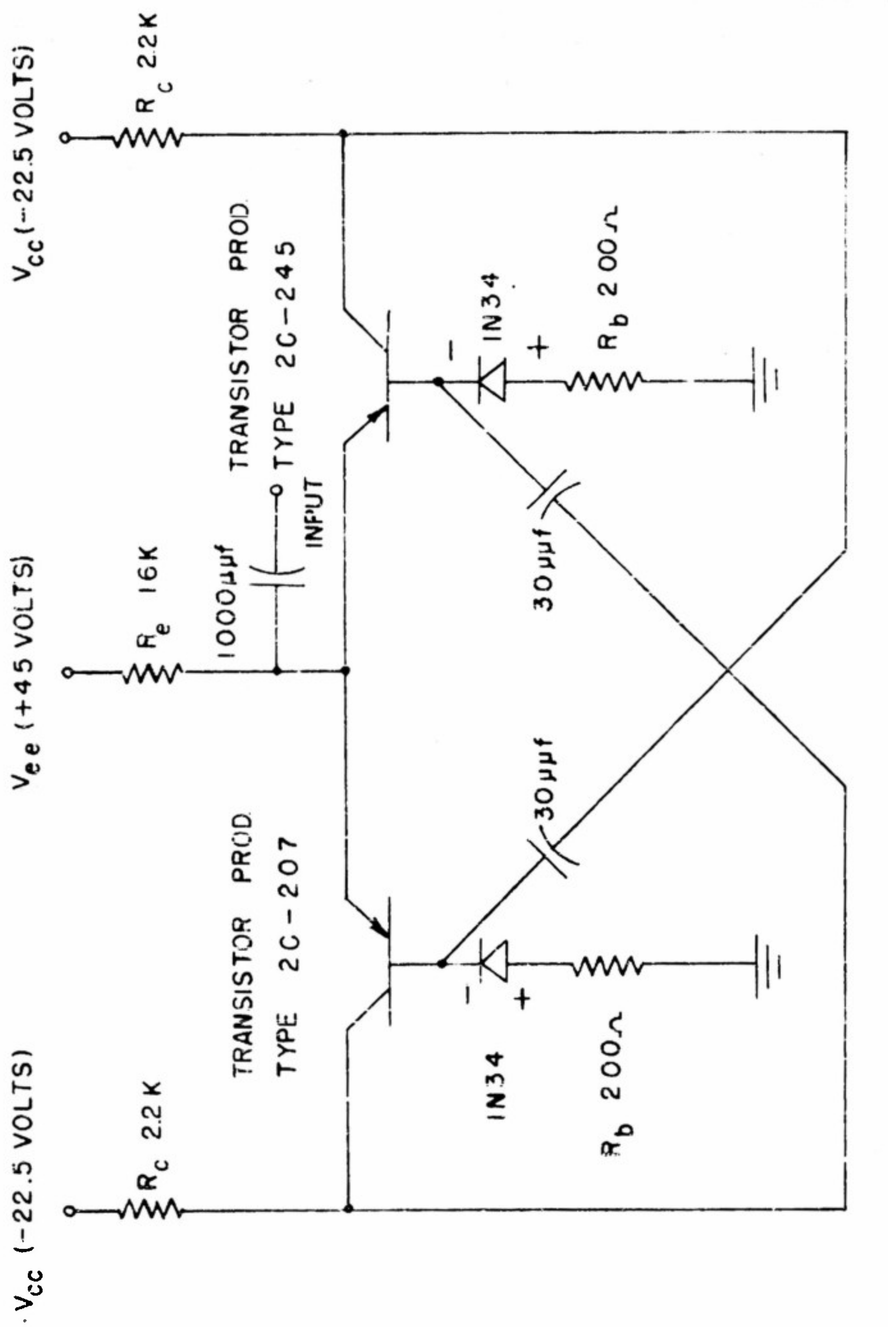

FIG. 37. BISTABLE NON-SATURATING TRANSISTOR CIRCUIT.

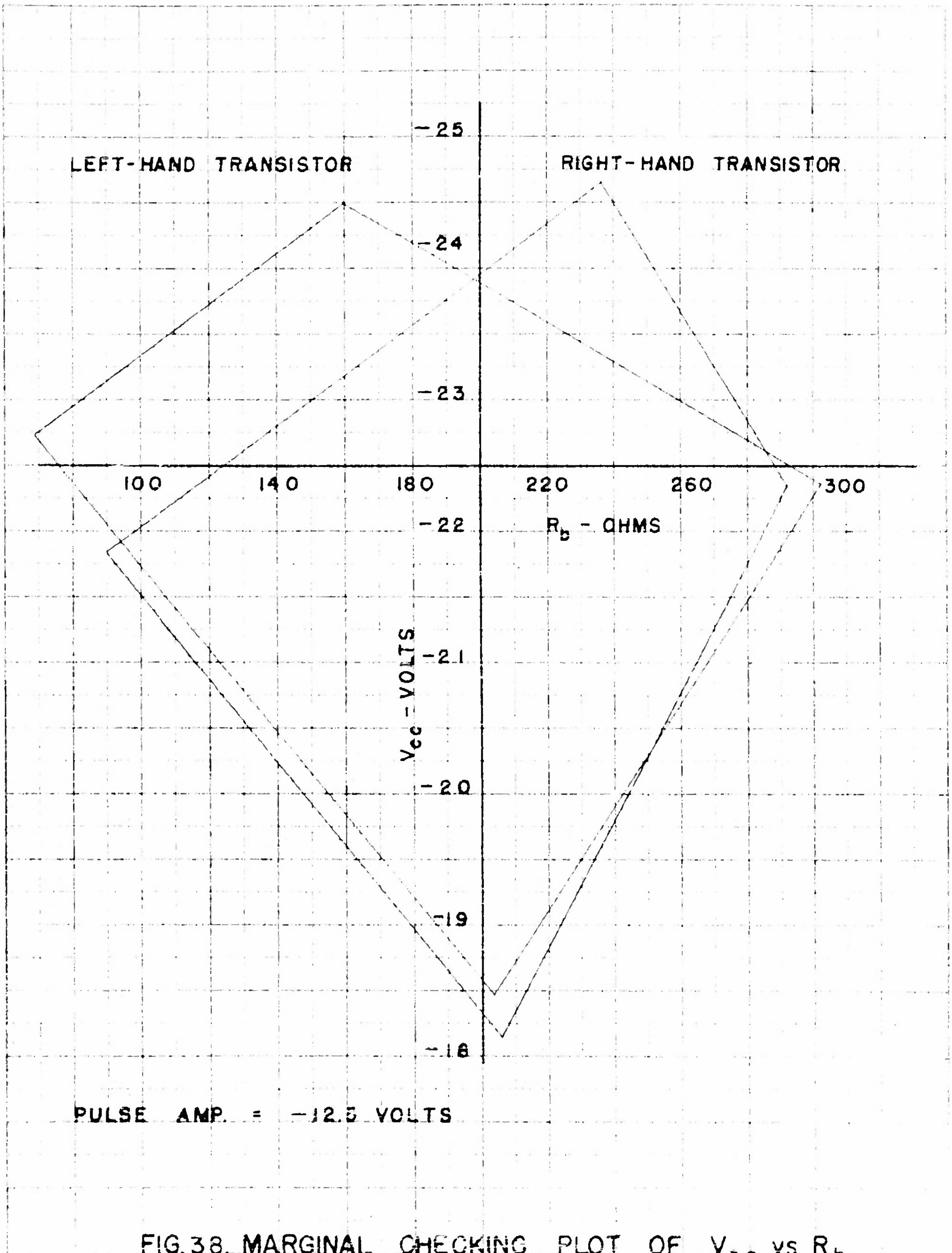

FIG. 38. MARGINAL CHECKING PLOT OF V_{cc} vs. R_b.

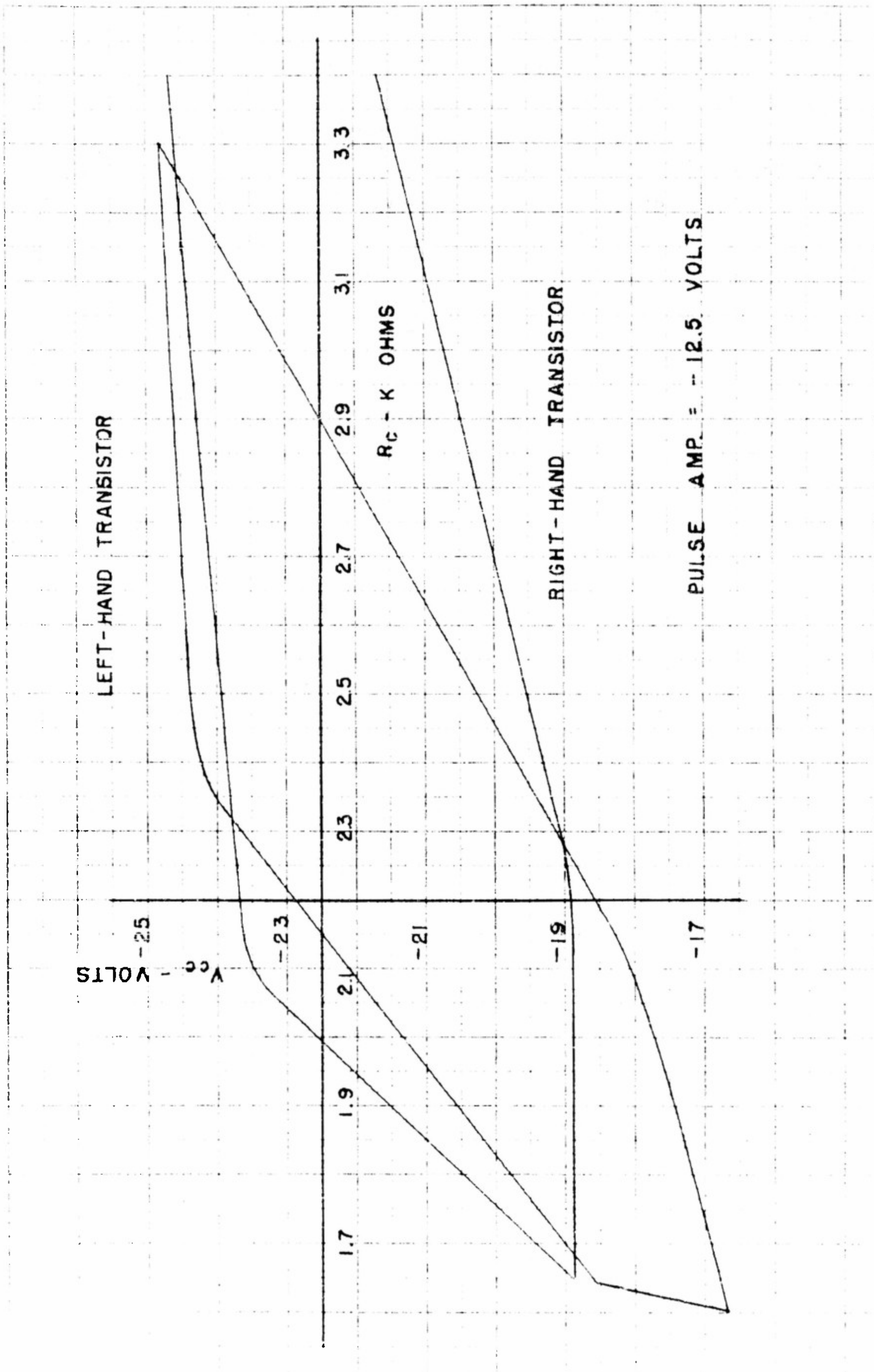

FIG.39. MARGINAL CHECKING PLOT OF V_{CC} v.s. R_C.

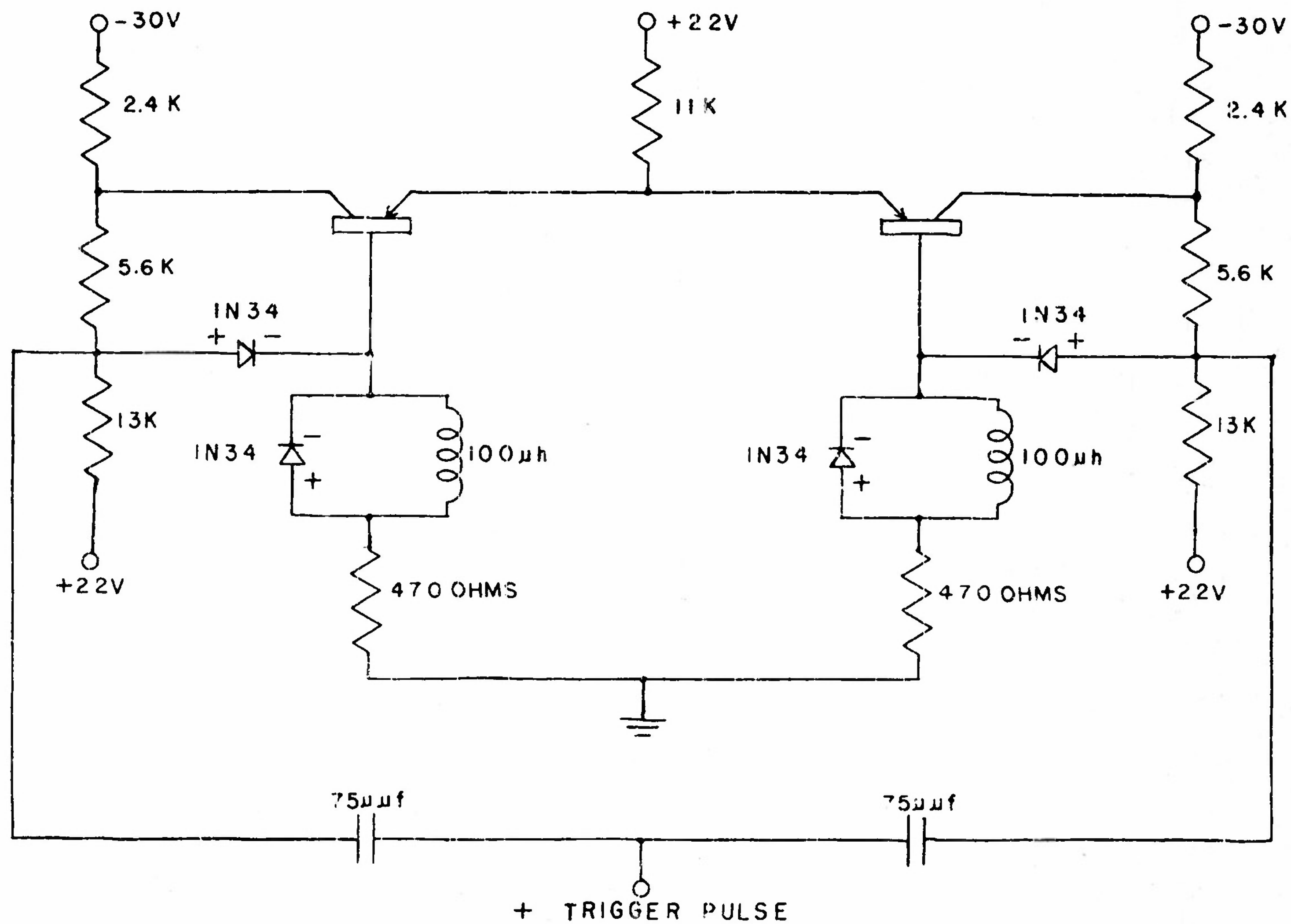

FIG. 40. TRANSISTOR FLIP-FLOP WITH PULSE STEERING CIRCUIT.

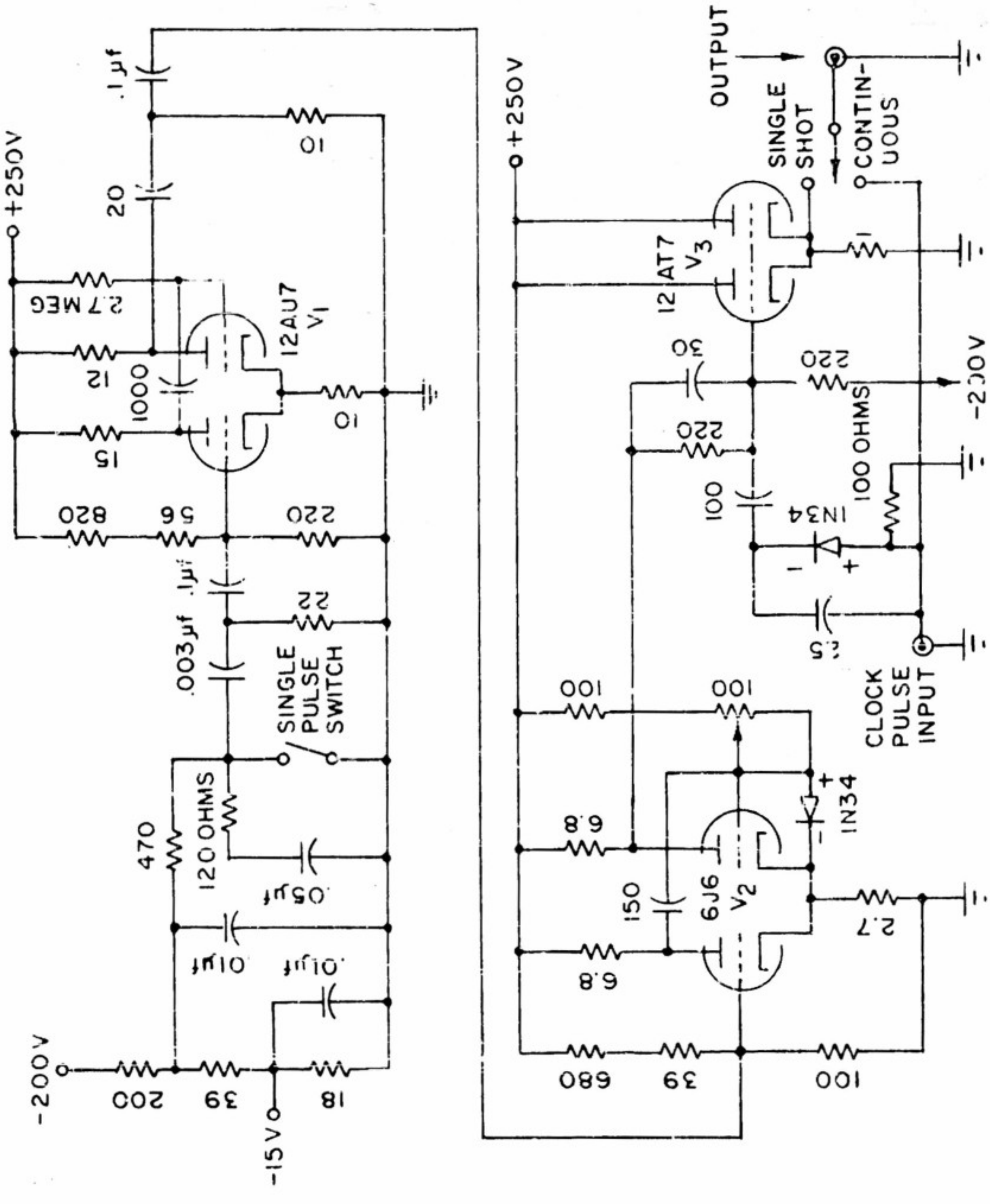

NOTE: ALL RESISTANCE VALUES IN K OHMS AND ALL CAPACITANCE VALUES IN $\mu\mu f$ UNLESS OTHERWISE SPECIFIED

FIG. 41. SINGLE-PULSER CIRCUIT.

only one pulse is obtained from the output of the cathode follower for each gating pulse produced by the single-shot switch. The single-pole double-throw switch at the output of the cathode follower selects either single-pulse operation or continuous operation directly from the pulse generator.

Typical examples of marginal-checking plots are shown in Figs. 43 through 46. In all these tests, Transistor Products Type 2C and X-10 transistors were used. The number indications for each transistor are solely for our own identification system.

Figure 42 shows plots of minimum pulse amplitude required to operate the flip-flop for varying values of collector voltages. All circuit parameters were at nominal values for these tests. Input pulses were 0.1 μs wide and at a 200 kc repetition rate. At low collector voltages, a point is reached where no pulse will trigger the circuit regardless of amplitude. This point occurs when the low collector voltage allows input pulses to pass the supposedly closed gate in the pulse-steering circuit with sufficient amplitude to make the circuit inoperative. The relatively constant values of input pulse amplitude in the intermediate ranges of collector voltage indicate proper operation of the gate circuits and that the minimum input pulse amplitude required is determined by the transistor parameters only. As collector voltages are increased, reverse bias on the diode in the open gate circuit increases so that larger input pulse amplitudes are required to pass through the gate circuit for proper operation. The 20-volt maximum output from the pulse generator and the maximum dissipation ratings of the transistors limit the upper collector voltage to minus 50 volts.

After consideration of the results shown in Fig. 42, a pulse amplitude of 16 volts was selected for the marginal checks of R_b vs. V_{cc} plotted in Fig. 43 to Fig. 46. The coordinate axes for these plots are 470 ohms and minus 30 volts, the nominal values of R_b and V_{cc}, respectively. The graphs indicate the marginal check for the base resistance vs. collector voltage for both transistors in the circuit. As each base resistance is varied, all other circuit components remain at nominal values.

A study of the various typical plots shows that for the same circuit under test, a large variation of plots is obtained when different transistors are used. This shows the effect of the transistor parameters. Only a general description for these plots will be given since sufficient data are not available to explain each plot individually in terms of transistor parameters.

In general, the bottom side of all plots indicate that a minimum amount of added external base resistance is necessary to obtain a negative resistance region in the V_e-I_e characteristic of the transistor that is sufficient to cause proper operation. On the left side of the plots, as the negative collector voltage decreases in magnitude, the reverse bias of the diode in the closed gate decreases allowing portions of the trigger pulses to be applied to the base. The amount of this undesired feed-through together with a particular value of base resistance causes failure of the circuit. Along the top side of the plot, the base resistances are large so that the increased

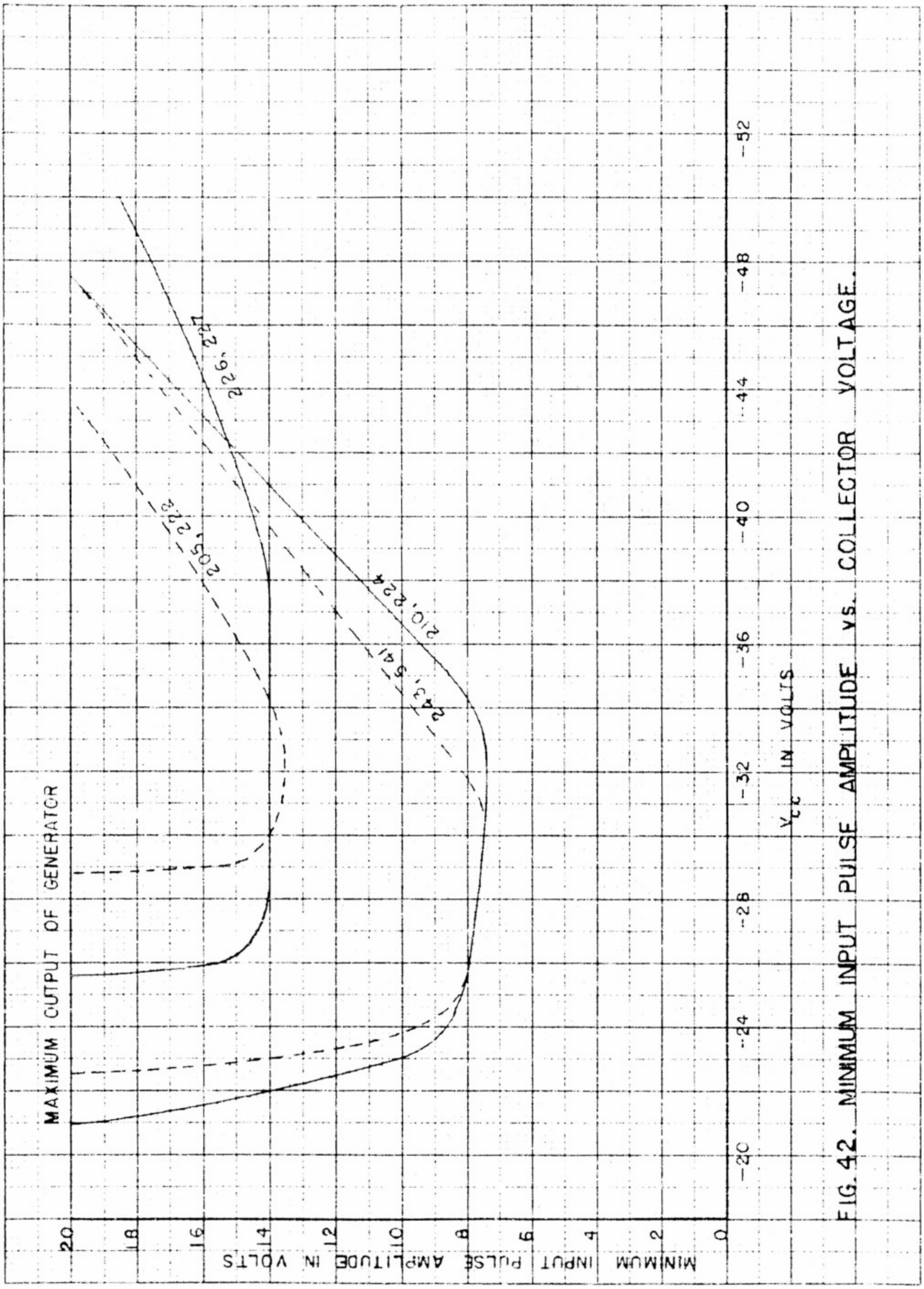

FIG. 42. MINIMUM INPUT PULSE AMPLITUDE vs. COLLECTOR VOLTAGE.

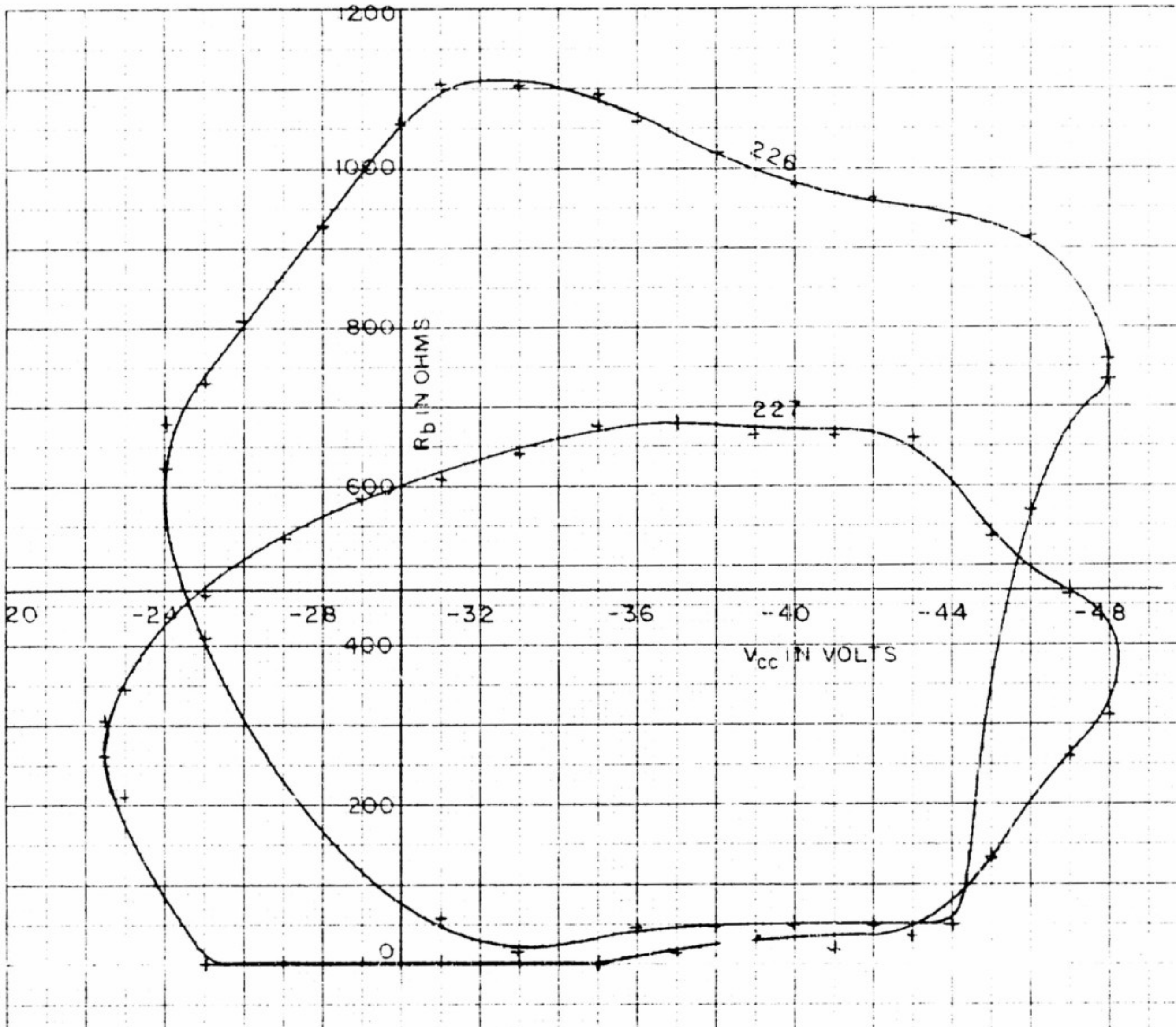

	2C-226	2C-227
r_{11}-OHMS	365	265
r_{12}-OHMS	245	155
r_{21}-K OHMS	33	24
r_{22}-K OHMS	12	8
α	2.3	2.6
f_{co}-mc	>5.0	>5.0

FIG. 43. BASE RESISTANCE VS COLLECTOR VOLTAGE.

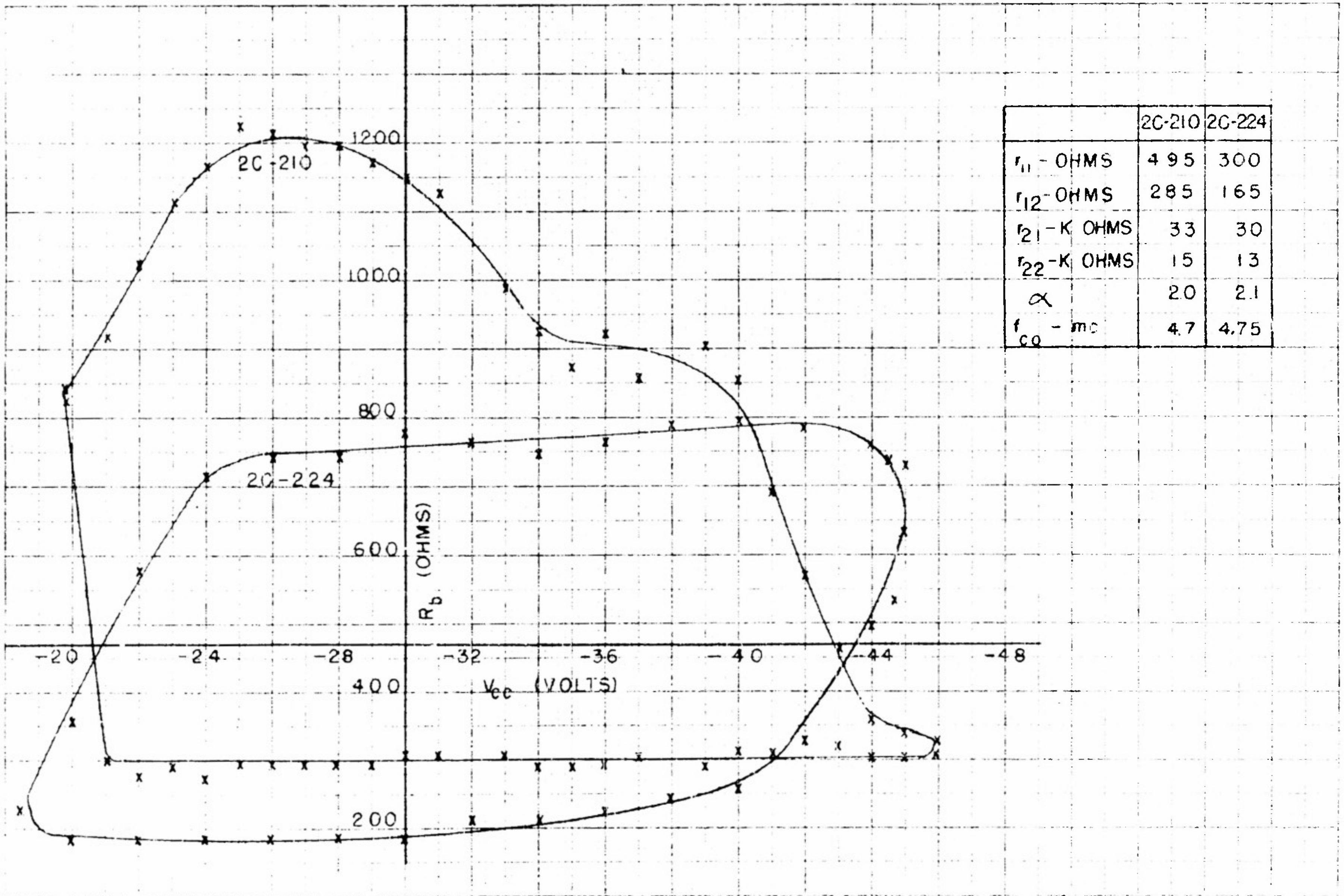

	2C-210	2C-224
r_{11} - OHMS	495	300
r_{12} - OHMS	285	165
r_{21} - K OHMS	33	30
r_{22} - K OHMS	15	13
α	2.0	2.1
f_{co} - mc	4.7	4.75

FIG. 44. BASE RESISTANCE vs. COLLECTOR VOLTAGE.

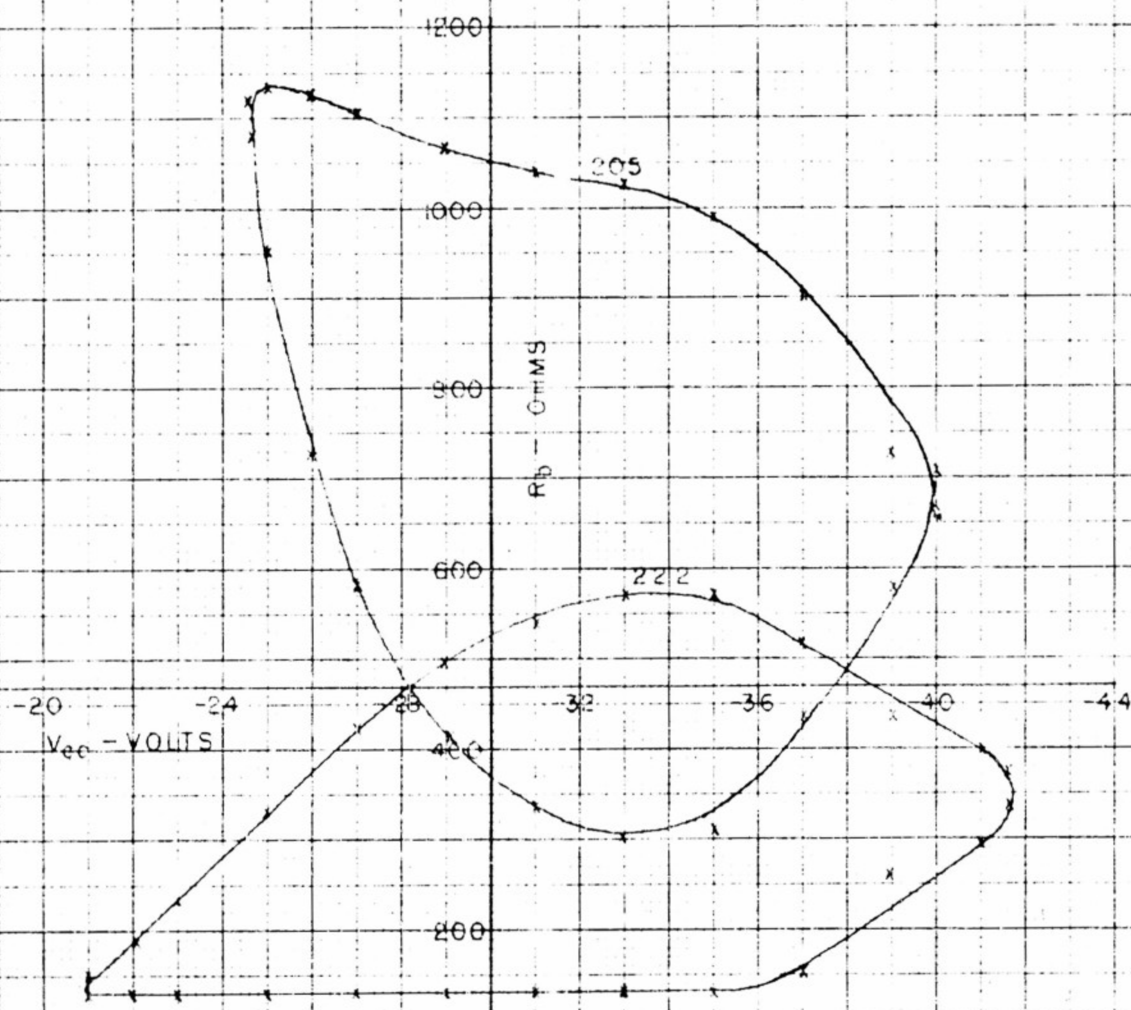

	2C-205	2C-222
r_{11} - OHMS	250	230
r_{12} - OHMS	175	180
r_{21} - K OHMS	39	71
r_{22} - K OHMS	16	24
α	2.1	2.5
f_{co} - mc	4.8	4.7

FIG. 45. BASE RESISTANCE vs. COLLECTOR VOLTAGE.

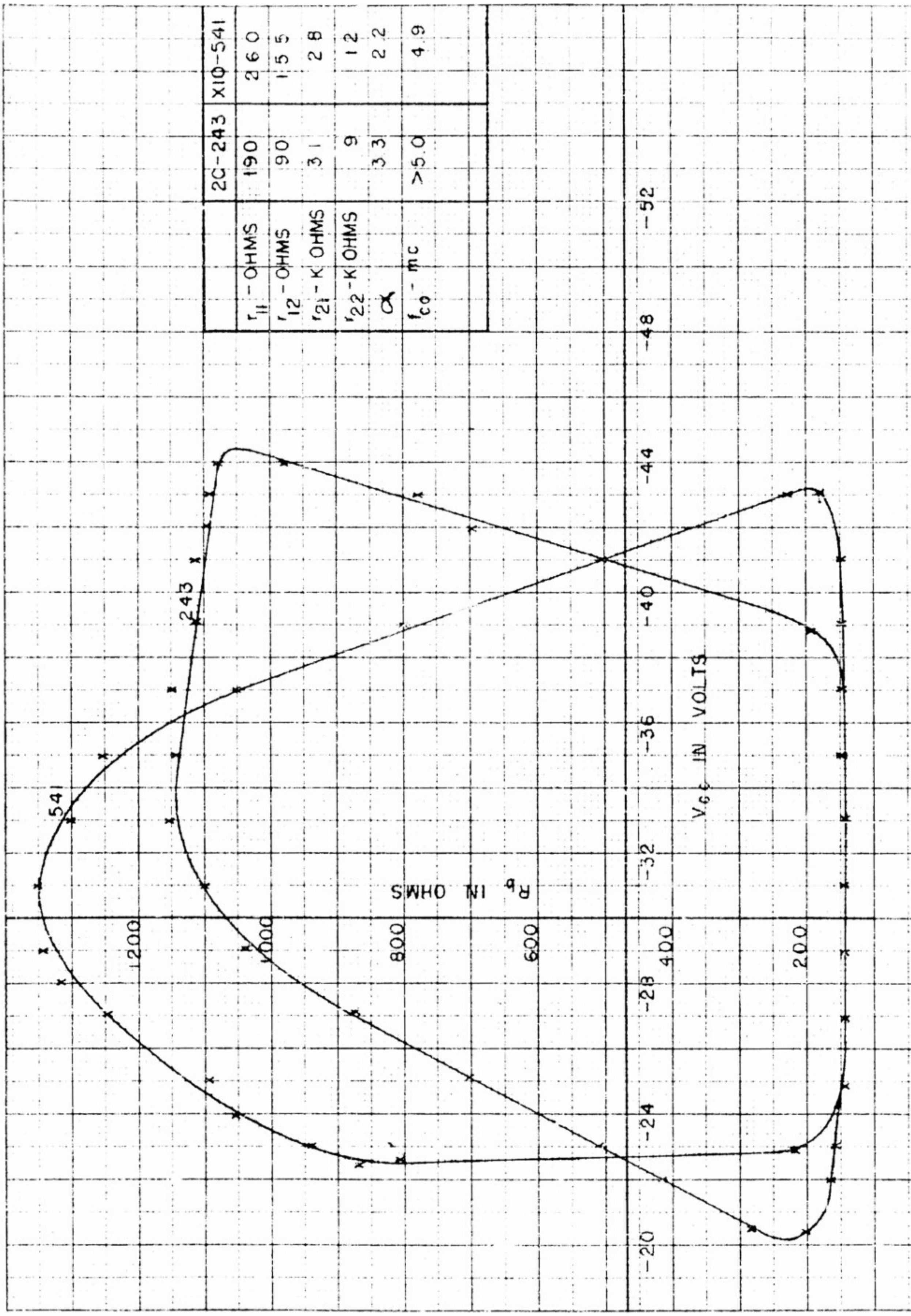

	2C-243	X10-541
r_{11} - OHMS	190	260
r_{12} - OHMS	90	155
r_{21} - K OHMS	31	28
r_{22} - K OHMS	9	12
α	3.3	2.2
f_{co} - mc	>5.0	4.9

FIG. 46. BASE RESISTANCE vs. COLLECTOR VOLTAGE.

slope of the negative resistance region of the V_e-I_e characteristic causes the two stable points of operation to move from the active region to the saturated region. In the saturated region, the 0.1 μs width of the trigger pulses are probably insufficient to overcome hole-storage time. Toward the right side of the plot, as the magnitude of the negative collector voltage increases, the reverse bias of the diode in the open gate increases requiring a greater input pulse amplitude to cause switching action. In this region, consideration should be given to maximum collector dissipation rating.

Marginal checking techniques have proven to be a useful tool in the reliability evaluation of transistor circuits. Using instruments of sufficient accuracy, techniques have been developed for obtaining suitable data. As a result, a smooth curve averaging the plotted points can be drawn allowing design centers and operating margins for the individual plots to be easily recognized.

However, difficulties are encountered when an attempt is made to interpret the shapes of the plots. As shown in Figs. 43 through 46, for plots of R_b vs. V_{cc} and a given circuit, wide variations in the shapes of the marginal-checking curves are obtained when different transistors are used. If a detailed analysis is required, an investigation of each plot in terms of the parameters of the individual transistors must be made. The problem now becomes statistical in nature and a large number of samples must be taken to reliably determine the interchangeability of transistors in a given circuit. For this reason, the analyses to date have been general in nature. Due to the type of circuit studied and the importance of the feedback element R_b, most of the work was concentrated on plots of R_b and minimum input pulse amplitude vs. V_{cc}.

E. Transistor Testing

In order to obtain sufficient data on individual transistors, a testing program was organized. Since the characteristics vary considerably from one unit to the next, it was necessary to have some method of testing to provide the required information for transistor-circuit design.

The testing program includes the measurement of both large and small-signal parameters of the point-contact n-type transistor. The small-signal parameters r_{11}, r_{12}, r_{21}, and r_{22}, are the standard four-terminal equivalent resistances of the transistor and they are measured with the transistor in a grounded-base type of circuit. A fifth small-signal parameter is alpha (α), defined as the ratio of the change in collector current to a change in emitter current made at a constant collector voltage. The equipment used to measure these parameters is the Transtester Model T-61 manufactured by Transistor Products, Inc. This equipment can also be used to measure the corresponding quantities for junction type[38] transistors. Table III gives specific details of transistors tested to date.

The frequency-response characteristics of the point-contact transistors are determined by measuring α as a function of frequency, and defining that

TABLE III

Point-Contact Transistor Parameters, Mean Value With Standard Deviation

Manufacturer and type	No. tested	r_{11} ohms	r_{12} ohms	r_{21} kilohms	r_{22} kilohms	α	Cut-off freq., mc	Rise time, µs	Fall time, µs	Hole storage time, µs
Western Electric Type 1698	911	324±88	164±64	75±28	23±8	2.30±.141	2.21±1.41	.281±.092	.328±.216	3.41±1.22
Western Electric Type 1689	145	345±108	161±63	48±24	22±10	2.19±.40	1.73±1.04			
Western Electric Type 1768	284	244±111	84±27	32±10	11±2	2.78±.47	.511±.259	.71±.27	1.06±.35	4.98±1.88
Western Electric Type 1729	10	227	101	24	10	2.65	3.28	.09	.12	
RCA Type TA165K	91	274±68	120±42	52±21	25±8	2.04±.51	2.69±1.29	.13±.08	.17±.11	.35±.19
Transistor Products Type 2A	6	297	135	53	23	2.30	.711	.70	.94	3.09
Transistor Products Type 2C	51	380±139	235±110	50±27	18±8	2.58±.36	3.52±1.61	.13±.06	.17±.14	
Transistor Products Type 2D	124	396±185	242±96	49±25	19±10	2.28±.72	2.79±.60	.17±.08	.19±.11	
Transistor Products Type X10	207	340±138	205±86	38±17	16±7	2.30±.39	3.35±1.41	.11±.09	.11±.09	
Raytheon Type CK716	41						.872±1.18	.76±.36	1.12±.48	.69±.79
General Electric Type G11	46	553±83	303±91	60±24	25±8	2.39±.33	3.70±1.11	.13±.04	.12±.03	

frequency where α is 3 db below its value at 5 kc as the cut-off frequency. The circuit and associated equipment used for cut-off frequency testing is shown in Fig. 47. This circuit and those used for large-signal testing, to be described next, are essentially duplicates of those developed at the Air Force Cambridge Research Center.

The large-signal test consists of applying a rectangular current pulse to the emitter and measuring the rise and fall time of the collector-circuit response. The ratio of the magnitude of the collector-current pulse to that of the emitter-current pulse defines α for large signals. Some transistors exhibit an unusual delay characteristic which can be measured during the above test.

A parameter which is of considerable importance to circuitry in which transistors are to be pulsed is the hole-storage time. It is a limiting factor on the minimum usable width of control pulse. Hole-storage time has been defined as the time between cutoff of the emitter current and the resulting cutoff of the collector current. If a transistor is placed in a grounded-emitter circuit as shown below, and a square-wave of long period and sufficient magnitude is applied to the base, hole storage time may be measured from the output wave form as shown.

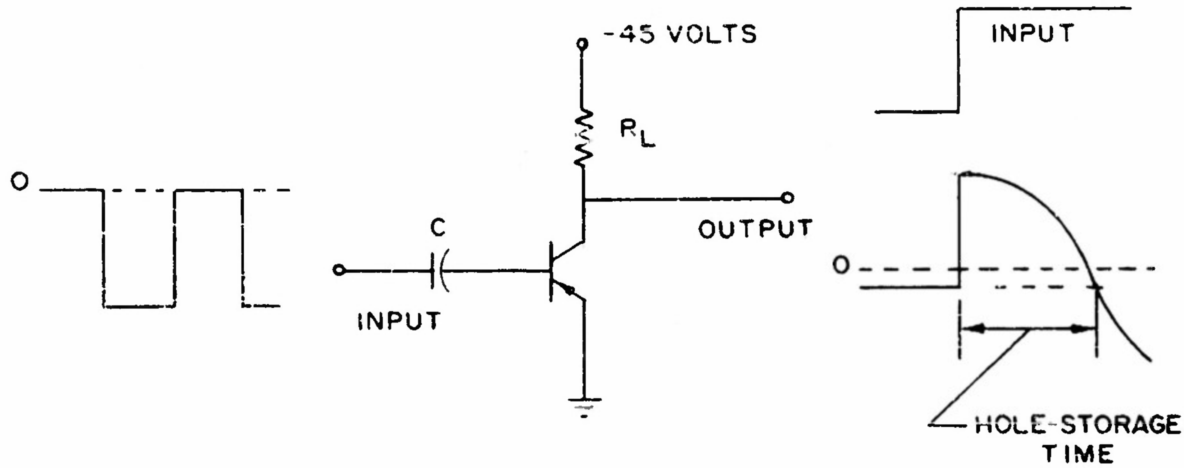

The large-signal and hole-storage-time circuits are combined on the same rack panel with a switching arrangement designed to reduce the number of equipment probe changes. The circuits and associated equipment are shown in Fig. 48. The measurement of hole-storage time was discontinued due to apparent changes produced in the small signal parameters by this test. A representative value of hole-storage time, obtained before measurement of this parameter was discontinued, is included in Table III.

The major portion of the time has been devoted to testing transistors for the Air Force Cambridge Research Center. A considerable variation of the values of the small-signal parameters for a transistor tested at Northeastern

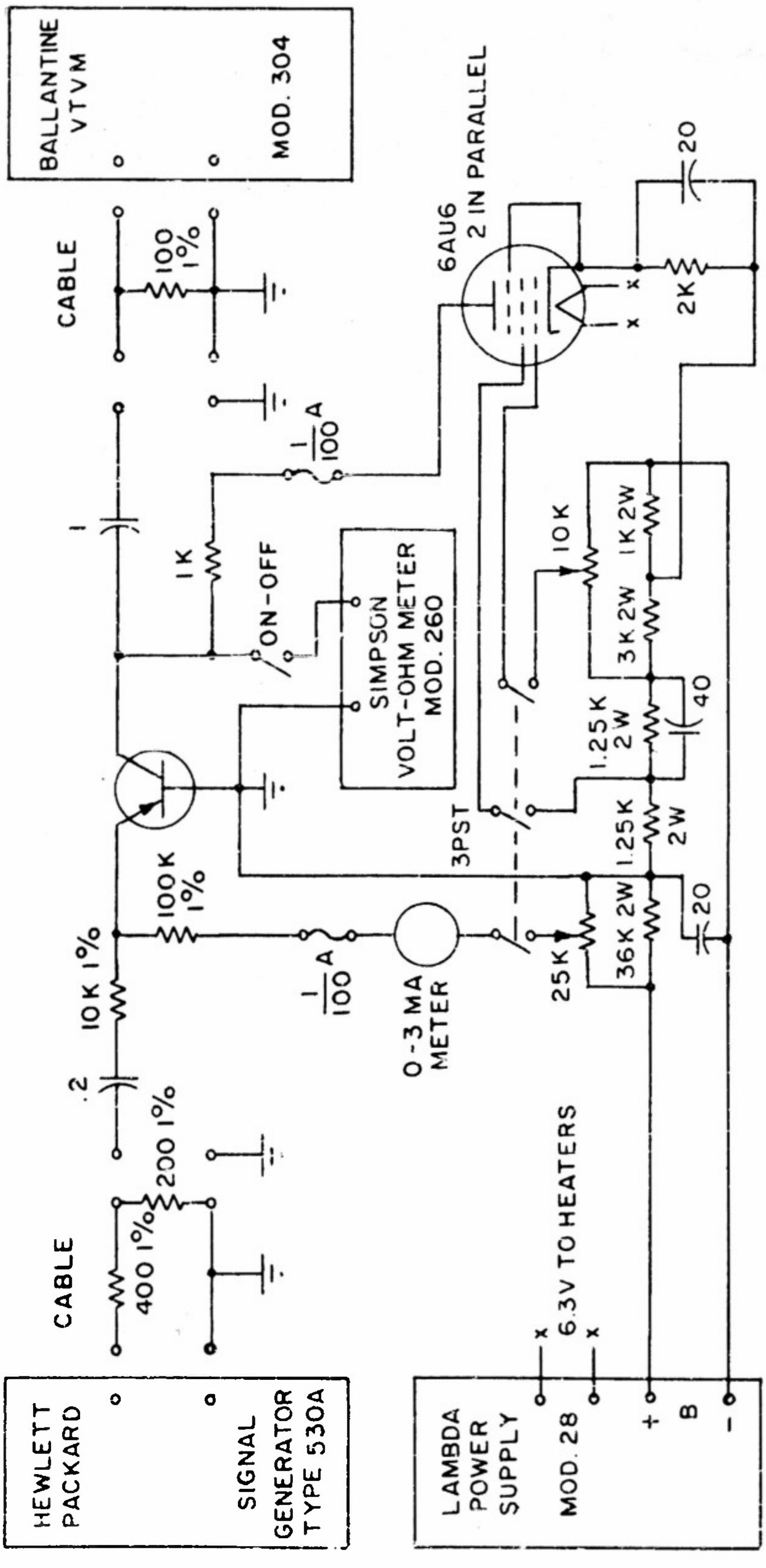

NOTE: ALL RESISTANCE VALUES IN OHMS AND ALL CAPACITANCE VALUES IN $\mu\mu f$ UNLESS OTHERWISE SPECIFIED.

FIG. 47. SCHEMATIC DIAGRAM OF TRANSISTOR CUT-OFF-FREQUENCY MEASURING EQUIPMENT.

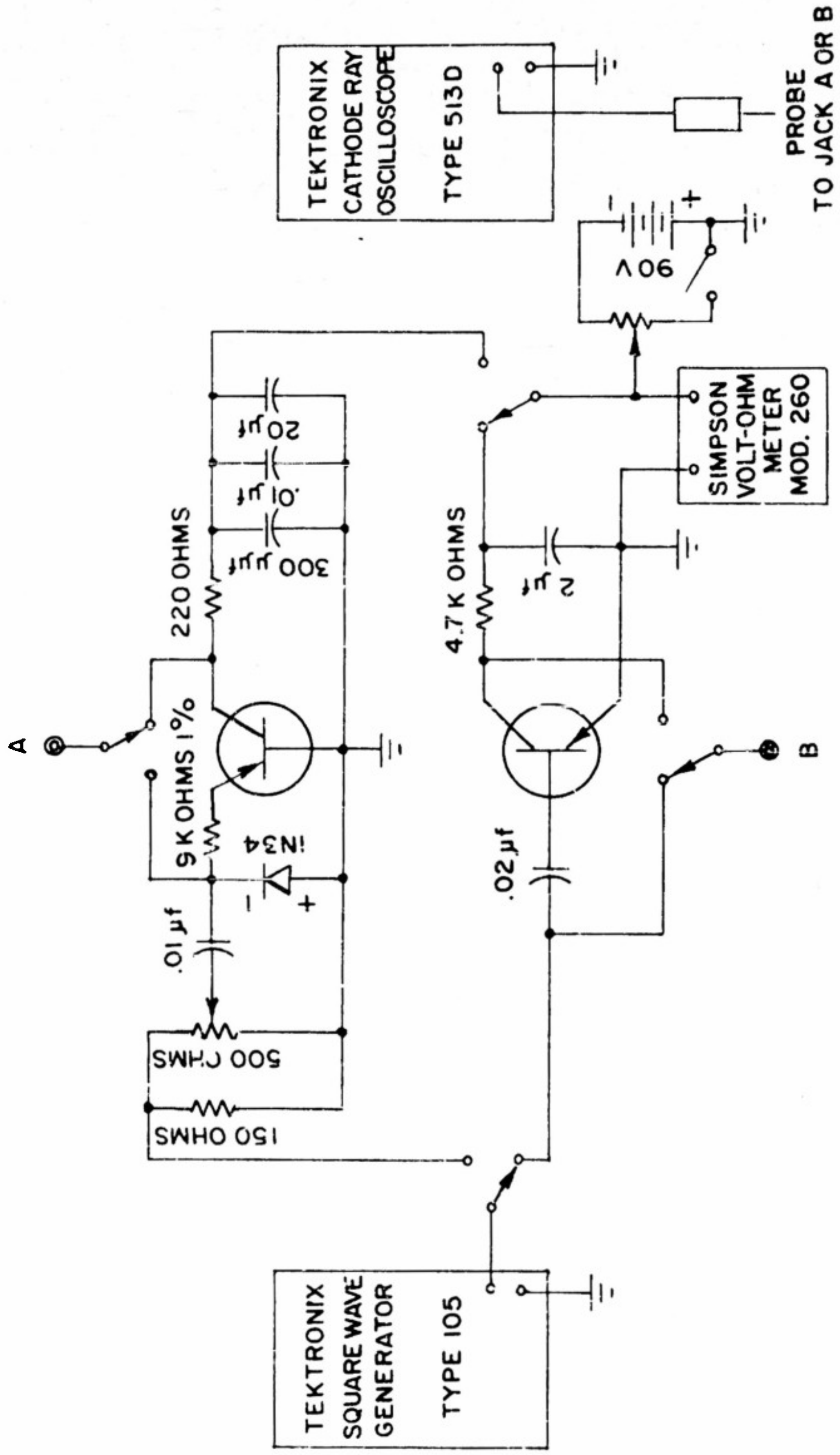

FIG. 48. SCHEMATIC DIAGRAM OF LARGE SIGNAL AND HOLE-STORAGE TIME TRANSISTOR TESTING EQUIPMENT.

from those measured for the same transistor at Air Force Cambridge Research Center, prompted a program for the evaluation of the Transistor Products Transtester.

All transistors were tested for frequency cutoff prior to being tested on the Transtester. The transistors were divided into two groups: Group I had frequency cutoffs of less than 3 mc. and Group II has frequency cutoffs greater than 3 mc. The small-signal parameters of all transistors used in this test were measured at various collector and emitter biases to determine if reliability of the Transtester was a function of the bias value.

For Group I the calculated $\alpha\left(\frac{r_{21}}{r_{22}}\right)$ and measured α were found to be within 10 percent of each other. The average values of all the parameters varied only a small percentage from day to day (less than 10 percent). The transistor manufacturer's recommended test points were found to be optimum bias points for these tests.

For Group II, the measured and calculated values of α were within 10 percent of each other. The average values of the tested parameters varied considerably from day to day for some of these transistors. Variations of 10 to 50 percent were common. The parameters of those transistors having the highest values of frequency cutoff exhibited the largest day-to-day percentage variation.

It is probably safe to conclude that all transistors with a frequency cutoff less than 3 mc will have practically the same measured parameter values from day to day. Slight variations can be attributed to either the physics of the transistor or to changes in the calibration of the Transtester. No definite conclusions can be drawn to cover the results obtained for transistors in Group II. It was impossible to test some of the transistors in Group II because of their tendency to oscillate while in the tester. Although the tendency to oscillate is a function of the emitter and collector biases, as well as the cutoff frequency, it was not possible to predict the test bias settings at which a particular transistor would oscillate from day to day.

A Dunn Engineering Model 3C Transistor Characteristic Plotter was procured to facilitate transistor checking and transistor circuit work. This piece of equipment has been found to be useful in extending the investigation of transistors in Group II as discussed in the preceding paragraph. The visual display of the small-signal characteristics provides a means for observing the areas of erratic operation of these transistors having a high cut-off frequency.

The increasing number of transistors with cut-off frequencies greater than 5 mc has severely limited the value of the original equipment used for this measurement. Equipment was set up to show plots of α vs. frequency on an oscilloscope screen. A block diagram of the set-up is shown in Fig. 49. The Kay Electric Company Marka-Sweep used as a signal source has frequency ranges of 0-5, 0-10, and 0-20 mc. The overall frequency response of the equipment

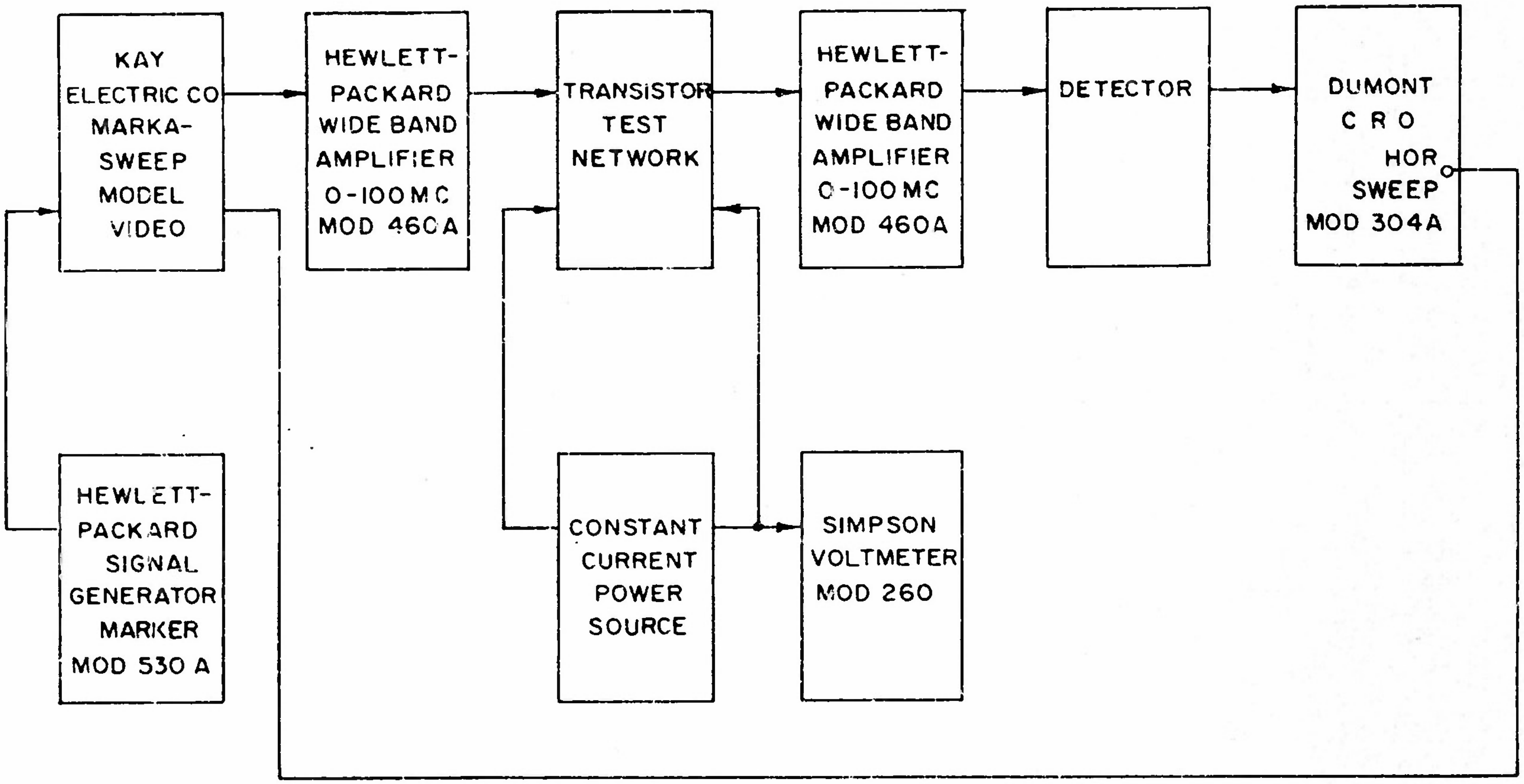

FIG. 49. BLOCK DIAGRAM OF TRANSISTOR ALPHA FREQUENCY CUT-OFF PLOTTER.

is such as to allow measurement of cut-off frequencies up to 20 mc. This equipment not only extends the range of possible cut-off frequency measurements but also provides a rapid means for observing the operation of the transistors at all frequencies from zero to cutoff. Any irregular operation of the transistor, within this frequency range, will be readily observed. A DuMont Polaroid Land Camera Type 297 is available to obtain permanent records of the α vs. frequency plot and the small-signal parameter characteristics as discussed in the preceding paragraph.

CHAPTER VIII

SUMMARY AND CONCLUSIONS

A. Introduction

In summarizing the results of the investigations described in the previous chapters, the IFF system must clearly be considered in two separate parts: ground-to-air and air-to-ground. The latter link has the two distinct advantages, (1) that the correct expected signal is known in advance at the receiver and (2) that size and complexity of equipment are less restricted. For these reasons, it has been possible to describe several effective methods for achieving reliability in the air-to-ground link, while the ground-to-air link must still be considered as a largely unsolved problem.

The matched-filter approach, which takes advantage of the knowledge of the waveform of the individual pulse, is one method which is equally useful in both links. The single-adding-bus type of pulse-train correlator, on the other hand, must be considered as applicable only to the air-to-ground link, since some form of storage and synchronization would be required if the correct challenge were to be known in advance at the airplane. Many forms of redundancy have been proposed, both explicitly and implicitly, to improve the reliability of both links, although in some cases equipment complexity may be an obstacle in applying the procedures to the ground-to-air link. This redundancy can be considered under two headings; namely, redundancy within each pulse train, and redundancy arising from repetition of pulse trains in a multi-channel or multi-round system.

Since it has been impossible to calculate the theoretical effectivensss of some of the proposed methods, and since in other cases the theoretical estimate of the effectiveness is based on assumptions which need to be verified, the equipment described in Chap. IV has been constructed and is now prepared for extensive testing of the matched-filter and pulse-train correlator approaches. This mock-up system can also be adapted to test the effectiveness of some types of redundancy. The various special systems presented in Chap. VI are believed to have considerable merit, but have not been pursued in great detail since they either deviate in some respect from the problem of this contract as stated in Chap. I, or else they give rise to equipment problems beyond the scope of this investigation. They have been included in this report with the expectation that they may be of interest to others working on the IFF problem.

The following paragraphs summarize and evaluate in more detail the progress reported in the earlier chapters. Also included under some of the topics are recommendations for future work. It is to be noted that many other suggestions for further work have been included in the preceding chapters where specific topics were treated individually.

B. Redundancy Approaches

It has been shown in Chap. V and elsewhere that many forms of redundancy

can be utilized to improve IFF reliability. The Shannon channel capacity has been used to calculate the minimum amount of redundancy required within each pulse train, assuming an ideal code. Using codes of practical length, it has been shown that reasonably close approximations to the ideal values can be obtained. If both binary digits (1 and 0) are equally likely to be received incorrectly, the Hamming codes are good approximations to the ideal, which have the additional advantage of providing a simple error-correcting procedure. In particular, for a system using a 4-digit reply, the simplest Hamming single-error-correcting code, which supplies three checking digits, is appropriate.

Two features of the pulse-train correlator may also be interpreted as forms of redundancy within each pulse train. The proposal to fix the values of m and k (whether or not they are chosen equal) introduces redundancy by limiting the number of possible challenges, but permits only detection rather than correction of errors. The pyramid arrangement of spacing between pulses is also a form of redundancy, which serves to reject enemy signals of incorrect spacing as well as portions of friendly signals which are not properly aligned.

Redundancy applied to repeated pulse trains has been shown theoretically to result in very great improvement in reliability, at the price of equipment complexity and a considerable increase in transmission time. The latter, however, is not a critical factor in an IFF system. The two methods of utilizing this redundancy, (1) by making a decision for each pulse train and counting the number of decisions of each type, and (2) by continuous integration of the results of each repetition with no decision made until the series is complete, have both been analyzed for certain assumed conditions.

C. Matched Filtering and Pulse-train Correlation

Matched Filtering

Matched-filtering techniques have been given considerable treatment as a means of improving the detection of pulses and pulse trains in white Gaussian noise. The work of this contract has resulted in the construction of matched filters for rectangular video pulses and pulsed carriers. Preliminary test results have been extremely good, and the procedure planned for rigorously determining the improvement in reliability obtainable with the matched i-f filter has been treated in Chap. IV. Certain refinements in the design, as discussed in Chap. II, will be required in order to make the filter practical for airborne military use.

The development of the above filter hardly terminates the subject of matched filtering and noise jamming. Consideration should be given to the performance of the filter when the signal is other than the correct signal, and when the noise jamming is other than white noise. Furthermore, some consideration should be given to the signal itself lest some other pulsed signal (other than one with a rectangular envelope) should prove to be better in the presence of most types of noise jamming. In the past, investigations of the type suggested above would have involved considerable labor and mathematical manipulation. However, it has been possible to express the relationship between the variables involved in matched filtering in a form which is readily

suitable for the suggested studies.

It is demonstrated in Appendix III that for a given signal $s_i(t)$, and additive noise whose autocorrelation function is $\phi_i(\tau)$, the h(t) which maximizes the signal-to-noise ratio at $t = t_o$ is

$$s_i(t_o - \tau) = \lambda \int_0^\beta h(\xi)\phi_i(\tau - \xi)d\xi$$

$$\text{for} \quad 0 < \tau < \beta$$

$$\text{and} \quad t_o \geq \beta \, .$$

Here λ is a constant, and β is the memory time of the filter, i.e.

$$h(t) = 0 \quad \text{for } t < 0 \text{ and } t > \beta \, .$$

It will be noticed that although the convolution integral on the right is generally defined for $-\infty < \tau < \infty$, it is only necessary that the equality hold for $0 < \tau < \beta$.

To demonstrate the result in the light of known results let $\phi_i(\tau)$ be a delta function, corresponding to white Gaussian noise. Then

$$s_i(t_o - \tau) = \lambda \; h(\tau) \quad \text{for} \quad 0 < \tau < \beta \, .$$

For $t_o = \beta$, this is the relationship discussed in Chap. II.

In general, if $H(\omega)$ need not be physically realizable, nor have finite memory, then the transform of the integral equation is

$$S_i^*(\omega)e^{-j\omega t_o} = H(\omega)N_i(\omega)$$

which is the standard form for a North filter.

The equation derived in Appendix III readily lends itself to a discussion of the inverse problem, i.e. what noise is necessary to ensure that for a given $s_i(t)$ no filter will improve the signal-to-noise ratio. The impulse response of no filter is the impulse which is defined as

$$h(t) = 0 \quad \text{for} \quad t \neq 0$$

$$\text{and} \int_{0-}^{0+} h(t)dt = 1.$$

Substitution in the formula yields the following equation

$$s_i(t_o - \tau) = \lambda \, \phi_i(\tau).$$

The limits on τ can be anything at all from 0^- to 0^+ or from $-\infty$ to $+\infty$. It is necessary, however, that $\phi_i(\tau)$ be a continuous function due to the

stipulation that

$$\int_{-\infty}^{\infty} N_i(\omega)H(\omega)e^{j\omega\tau}d\omega = \int_{-\infty}^{\infty} N_i(\omega)e^{j\omega\tau}d\omega = \phi_i(\tau)$$

be a uniformly convergent integral for $0 < \tau < \beta$. Due to the Gibbs effect of the Fourier transform at a discontinuity, this means that $\phi_i(\tau)$ must have no discontinuities in the interval. Thus, it can be concluded that, if $s_i(t)$ is a pulse, it must be symmetrical about a center line, and must have no discontinuities.

The relationship between $s_i(\tau)$ and $\phi_i(\tau)$ is indicated below for the case where the signal is a triangular pulse.

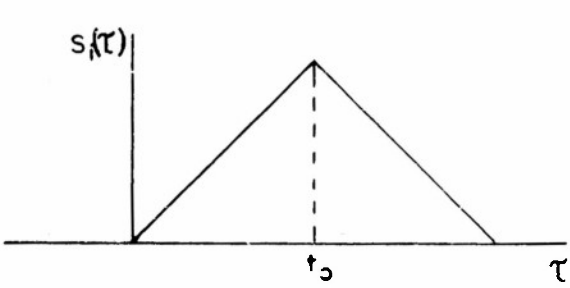

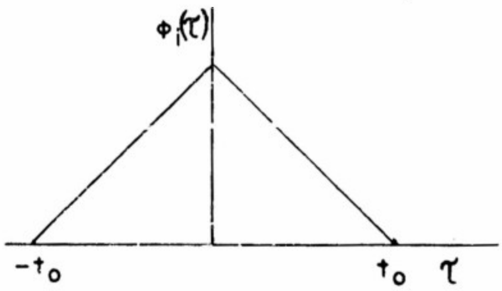

The sketches indicate that, if triangular pulses are used as signals, the enemy merely needs to produce a noise with the pictured correlation function, and thus make matched filtering not only useless, but detrimental.

It would appear from the foregoing that symmetrical signals with no discontinuities can always be jammed so that matched filtering is useless. Signals with discontinuities, on the other hand, can always have their signal-to-noise ratio improved. Consequently it appears that once the best class of signal has been chosen (apparently one with discontinuities), the impulse response which will give improvement (but not maximum) in signal-to-noise ratio for a wide variety of noises can be determined. This can be accomplished by selecting various impulse responses and comparing signals required for different types of noise. How the physical unrealizability of signals with discontinuities affects the above conclusions remains to be investigated.

<u>Pulse-train Correlation.</u>

A new approach to the problem of optimizing the threshold function of the pulse-train correlator may be of value for future improvements of this device. For the purpose of this analysis, consider first the case when the "correct" signal S is absent. The voltage appearing at the output of the adding bus is then

$$V_\Sigma\ (S = 0) = (M - K)J$$

For the special example under concern where the number of places expected to be "occupied" (m) and "unoccupied" (k) by S are both equal to 4, the following matrix of V_Z (S = 0) may be obtained:

K \ M	0	1	2	3	4
0	0	1	2	3	4
1	-1	0	1	2	3
2	-2	-1	0	1	2
3	-3	-2	-1	0	1
4	-4	-3	-2	-1	0

Matrix of

$$\frac{V_Z\ (S = 0)}{J} = M - K$$

The common multiplier J is divided out of the matrix. For convenience of discussion, the corresponding matrix for the probability of occupancy, p_{MK}, of the jamming pulse train under the previous assumption of $P = \frac{1}{2}$ is also reproduced as follows. The numerals along the lines are the marginal probabilities from which the corresponding p_{MK}'s are computed.

K \ M	0	1	2	3	4	
0	.0039	.0156	.0234	.0156	.0039	$\frac{1}{16}$
1	.0156	.0625	.0938	.0625	.0156	$\frac{4}{16}$
2	.0234	.0938	.1408	.0938	.0234	$\frac{6}{16}$
3	.0156	.0625	.0938	.0625	.0156	$\frac{4}{16}$
4	.0039	.0156	.0234	.0156	.0039	$\frac{1}{16}$
	$\frac{1}{16}$	$\frac{4}{16}$	$\frac{6}{16}$	$\frac{4}{16}$	$\frac{1}{16}$	

Matrix of p_{MK} $(P = \frac{1}{2})$

Since the strength of the jamming as appears on the adding bus is proportional to M-K, as shown in the first matrix, it is desirable to construct a graph showing the probability distribution, p_{M-K}, by combining the p_{MK}'s of those squares whose value of M-K are the same. This graph is shown on the next page.

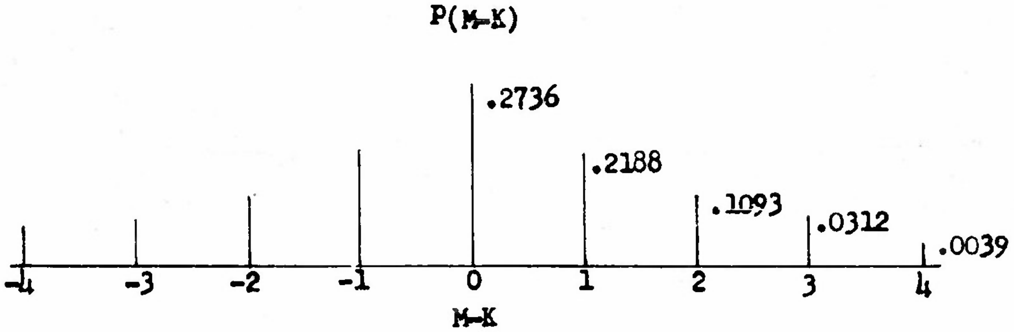

The graph may be used to estimate two types of errors. In statistical terminology, the Type I error β corresponds to the failure to recognize a friend as a friend, the Type II error γ corresponds to the error of mistaken identification of a foe as a friend. The problem at hand is then to find an adequate threshold voltage V_T such that the decisions based upon the criteria that

$$V_\Sigma - V_T > 0 \quad \text{indicates a friend}$$

and

$$V_\Sigma - V_T < 0 \quad \text{indicates a foe}$$

will result in smallest possible values of γ and β .

In the original scheme built in the working model of the pulse-train correlator, the amplitudes of the desired (S) and the jamming (J) pulses are assumed to be approximately determinable, and the threshold voltage is set equal to

$$V_T = AJ-BS$$

where $\quad A = (m-1) + \alpha = 3 + \alpha, \quad \alpha = \text{as small as possible}$

and $\quad B = \text{as large as possible.}$

It was pointed out that the optimum values of α and B will depend upon the consideration of random noise.

The strategy of this setting was that in the absence of S, V_T (= $3 + \alpha$) is large enough to prevent the passing of all possible jamming pulse trains whose M-K < 4. Only in the case M-K = 4 is the jamming inseparable from the signal, and the determination of J and S considered impossible. In other words, the Type II error is quite small (γ = 0.39%), and the Type I error depends upon the strength of the signal-to-jam ratio S/J and the choice of α and B. In the case B = 0, β may be computed as follows: regard the matrix of V_Σ (S = 0) as a three-dimensional pattern and the subtraction of $V_T = (3 + \alpha)J$ corresponding to submerging the whole pattern by this depth. In the absence of S, the only block that emerges from underneath the surface is that of M-K = 4. With added S, V_Σ is increased by 4S, more blocks will emerge, and the sum of the probabilities corresponding to the still submerged blocks is β .

The description up to here is essentially a reinterpretation of the working principle of the correlator. Some discussion of possible improvements is now in order.

Constant Pulse Jamming

In the absence of noise or transmission fluctuation, the logical choice of V_T for minimizing both γ and β is according to the formula:

$$V_T = V_\Sigma \quad (S = 0) \quad = \quad (M - K + \alpha)J$$

This is evident from the three-dimensional picture mentioned above. Here the quiescent surface of $V_\Sigma - V_T$ for the no-signal situation coincides with (or is slightly below) the zero level. Therefore γ is negligible. A slight amount of S will enable V_Σ to emerge above the surface of essentially all blocks and β is practically equal to zero.

If this involves too much complication in circuitry, a first step may be to set V_T according to the last column of the matrix, namely

$$V_T = (M - K + \alpha)J = (4 - K + \alpha)J$$

This simplification would not affect γ, but β would not be as small as could be. Since the KJ term appears both in V_Σ and V_T, this modification means leaving the k taps open in the computation $V_\Sigma - V_T$, although these taps are necessary to estimate the values of J and S.

When the number of digits (M+K) is increased, it may be desirable to protect those regions in the matrix where p_{MK}'s are large. This region corresponds to the central part when $P = \frac{1}{2}$ but may be shifted when P differs from this value. The values of γ and β can be computed and their relative weights considered.

Also to be studied is the use of quantizing devices at the taps of the adding bus, where the threshold for quantization may be adjusted differently for the M and K taps. The former should be dictated by the estimated value of S and the latter by the estimated value of J.

D. Marginal Checking Applied to Equipment Reliability

Marginal checking techniques have been developed that are suitable for use in the reliability evaluation of transistor circuits. These techniques, together with a program such as that outlined in Chap. VII, provide the information needed for determining design centers, nominal values of components, and operating safety margins; and for evaluating the reliability of the circuit.

When reliability evaluation of a transistor circuit is considered, the problem becomes a statistical one requiring a large number of samples. This is due to the large variation of the transistor parameters when transistor interchangeability is considered. The analyses carried out under Chap. VII have been general in nature pending the accumulation of the necessary

quantity of data. Work carried out in this direction can result in reliability evaluation of transistor circuits in terms of transistor parameters as well as in terms of circuit parameters. Some form of a transistor-testing program is a valuable supporting unit to any program for the evaluation of reliability of transistor circuits.

E. Statistical Evaluation of IFF Reliability

The purpose of this section is to suggest a method for evaluating the performance of the overall IFF system and to illustrate its application to the case of a multi-round identification procedure. The general method assumes that some quantity x is being measured at the responsor as a basis for determining whether a friend or enemy is present. This quantity x may be a single variable, either discrete or continuous, or it may be a vector with several such variables as components. In any case, using statistical terminology, the problem is that of testing a hypothesis H_0 that the unidentified airplane is an enemy, against the single alternative H_1 that it is a friend. A probability distribution $f_0(x)$ is assumed for H_0 and $f_1(x)$ for H_1 where both distributions depend on many parameters of the system, some of which may be subject to control. These distributions may be illustrated by the diagram below when x is one-dimensional. A threshold T must be set such that

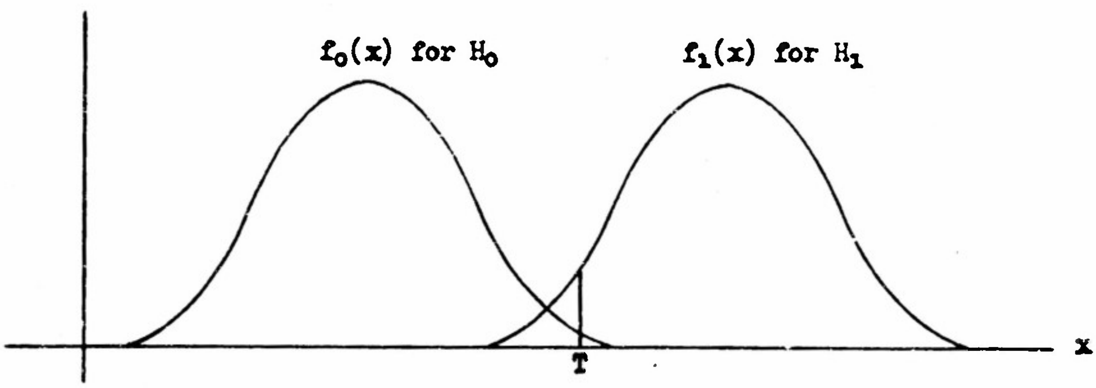

if $x > T$, H_1 is accepted while if $x < T$, H_0 is accepted. If x is multi-dimensional, T applies to some suitable function of the components of x. Let γ represent the probability of accepting H_1 when H_0 is true (that is, the probability of calling an enemy a friend) and β represent the probability of the opposite type of error. Then for the one-dimensional case illustrated, $\gamma = \int_T^{\infty} f_0(x)\,dx$ and $\beta = \int_{-\infty}^{T} f_1(x)dx$.

The value or effectiveness of the system can be measured if we define two quantities w_0 and w_1 as the values (in arbitrary units) of correct identification of an enemy when one is present, and of correct identification of a friend when one is present, respectively. (These are equivalent to the quantities c-d and a-b respectively used in Section C of Chap. I on the Theory of Games.) We also assume *a priori* probabilities p and 1-p that an unidentified airplane is an enemy or a friend respectively. Then the usefulness of the system can be measured by the expected value V of the

identification of one airplane:

$$V = p(1 - \gamma)w_0 + (1 - p)(1 - \beta)w_1$$

In this formula, $(1-\gamma)w_0$ and $(1-\beta)w_1$ are the expected values of the identification when an enemy is present and when a friend is present respectively, and each of these expected values has to be weighted by the a priori probability of that situation existing.

This formula can, of course, be used simply to compute the reliability measure V for comparison of completely specified systems. It can also be used to answer many questions, depending on which quantities are assumed fixed and which ones are assumed variable. Two of the more interesting types of question are the following:

(1) Assuming that all parameters and specifications of the system (including peak transmitter powers, antenna gains, receiver noise characteristics, etc. as well as the characteristics and power of enemy jamming) are known, so that $f_0(x)$ and $f_1(x)$ are completely specified for a given range, what is the value of T which will maximize V, and what is this maximum V?

(2) Assuming that $f_0(x)$ is known but $f_1(x)$ can be controlled by such means as increasing transmitter power, and assuming that a specified value of $V = V_0$ (say 95% of its value when $\gamma = \beta = 0$ which is $V = pw_0 + (1 - p)w_1$) is required, what is the value of T which will minimize the generalized signal-to-noise parameter ρ required to attain V_0? This question may be put differently by assuming that the friendly signal power is fixed, and that γ is variable at the control of the enemy. Then the question is, what is the maximum jamming power which can be tolerated if we are still to attain V_0?

Both of these questions assume that both γ and β may vary, as in the "Ideal Observer" approach used by Siegert. In the Neyman-Pearson method used for a similar problem by Middleton[30], the method is to fix γ when testing H_0. In either approach the fundamental Neyman-Pearson lemma says that the threshold, or in the case of a multi-dimensional x, the boundary between acceptance and rejection regions should be characterized by a constant value of the maximum likelihood ratio $\frac{f_0(x)}{f_1(x)}$.

An illustration of the use of this statistical approach to reliability is for the case of a multi-round IFF system, where x is now the discrete variable i defined as the number of correct replies in a total of n rounds. In this case, both $f_0(i)$ and $f_1(i)$ are binomial distributions based on the probabilities for correct replies in a single round. Then the threshold T is the minimum number of correct replies required for identification as a friend. Either question (1) or question (2) can be considered in this case. Also, a further approach which can be used in this case is the sequential approach, where the number n is not fixed in advance, but the identification of a friend is considered complete when the k-th correct reply is received.

It should be emphasized that the proposed statistical analysis will be useful only in evaluating a system whose characteristics can be accurately

enough specified to determine the required probability distributions and their dependence on the levels of signal power and jamming power. Since in most cases these probabilities are difficult to calculate theoretically, the use of models (such as the mock-up system of Chap. IV) is necessary.

APPENDIX I

The Problem of Number Conversion

It is desired to represent an arbitrary k-digit binary number by an n-digit binary number such that the latter number is constrained to have m and only m units. In this connection one will also specify that this process should be unique.

There are

$$^{n}C_{m} = \frac{n!}{m!(n-m)!} \tag{I-1}$$

n-digit binary numbers containing exactly m ones or units, and exactly (n - m) zeros. Then, if an arbitrary k-digit binary number is to be represented uniquely by the n-digit number

$$2^{k} \leq {^{n}C_{m}} = \frac{n!}{m!(n-m)!} \tag{I-2}$$

If one uses Stirling's formula

$$n! \approx \sqrt{2\pi n}\left(\frac{n}{e}\right)^{n}, \tag{I-3}$$

and defines $\delta = 2\left(\frac{m}{n}\right) - 1$, then it is (I-4)

approximately true that

$$2^{k} = \frac{n!}{m!(n-m)!} \tag{I-5}$$

if

$$n \approx \frac{k + 1.66 \log_{10} n(1-\delta^{2}) + .326}{1 + 3.33\left[\log_{10}\frac{1}{1-\delta} - \frac{1+\delta}{2}\log_{10}\frac{1+\delta}{1-\delta}\right]}. \tag{I-6}$$

If $|\delta| < \frac{1}{2}$ this reduces to

$$n \approx \frac{k + 1.66 \log_{10} n(1-\delta^{2}) + .326}{1 - .722\left[\delta^{2} + \frac{\delta^{4}}{6}\right]} \tag{I-7}$$

It is proved elsewhere in this report that the greatest advantage in correlation accrues when $m = \frac{n}{2}$, or $\delta = 0$; that is, the numbers should contain half ones, half zeros.

Substituting in eq. (I-7) yields

$$n = k + .326 + 1.66 \log_{10} n.$$

If k and n are constrained to be even numbers, then they can differ by no less than two. For n = 10, note that

$$n - k = 1.986 \approx 2$$

$$k = 8$$

Thus one can tabulate that for a given k digits, the number, n, of digits with $\frac{n}{2}$ units, $\frac{n}{2}$ ones, is:

k	n
2	4
4	6
6	8
8*	10*

For $$10 < n < 40$$

$$2 < n-k < 3$$

and so if k and n are even, one needs only four extra digits, hence

k	n	
8	12	
10	14	
12	16	
16	20	
24	28	etc.

While it is possible to convert twenty-four digits to 27 (14 + 13) or 28 (14 + 14), the circuitry required for this would be large. As a beginning the easier conversions were first attempted. The method here is to take four digits (say) at a time from a larger number, and to convert each set of four to a set of six, three digits of the latter being ones.

(a) 2-4. Conversion from two to four is trivial. For any number a unit can be converted into the sequence 01, and a zero to 10. One may also add the complement of any digit on the end, and achieve similar results.

(b) 4-6. Two ways of accomplishing this have been discovered.

(1) If the six-digit binary numbers are written as decimals they are:

* Actually the approximation by Stirling's formula is inaccurate here since $2^8 = 256$ and ${}^{10}C_5 = 252$. Thus, when k = 8, the correct value of n is 11.

Binary No.	Decimal Equiv.	Complement	Decimal Equiv.
000111	7	111000	56
001011	11	110100	52
001101	13	110010	50
001110	14	110001	47
010011	19	101100	44
010101	21	101010	42
010110	22	101001	41
011001	25	100110	38
011010	26	100101	37
011100	28	100011	35

They are written in this fashion for a reason. One decides that if the fourth digit of the input is a one, he will take the complement of whatever number is chosen by the first three digits. This halves the problem. One needs now an automatic method for choosing eight numbers, at most one from each of the above ten lines, using the first three digits of the input number.

In instrumenting this method, one starts with a counter which contains the number seven. If the first digit is a one, one adds four to this number. In all cases an input zero will change nothing.

If the second digit is a one, one doubles the amount in the counter. If the third digit is a one, one adds an additional 14 to the counter. This yields the eight numbers 7, 11, 14, 22, 21, 25, 28, 36. The last number 36 is not in the above group, but 37 is. Hence, for this number, one will adjust the circuit so that if 22 is in the counter, and the third input pulse a one, one adds 15 instead of 14. If the last or fourth input digit is a one, one complements the contents of the counter.

Figure 50 is a circuit which will accomplish this. The results are tabulated below.

Input	Output
0000	000111
0001	111000
0010	010101
0011	101010
0100	001110
0101	110001
0110	011100
0111	100011
1000	001011
1001	110100
1010	011001
1011	100110
1100	010110
1101	101001
1110	100101
1111	011010

(2) In the second method of attack, one assumes first that the counter contains 7, i.e. 000111.

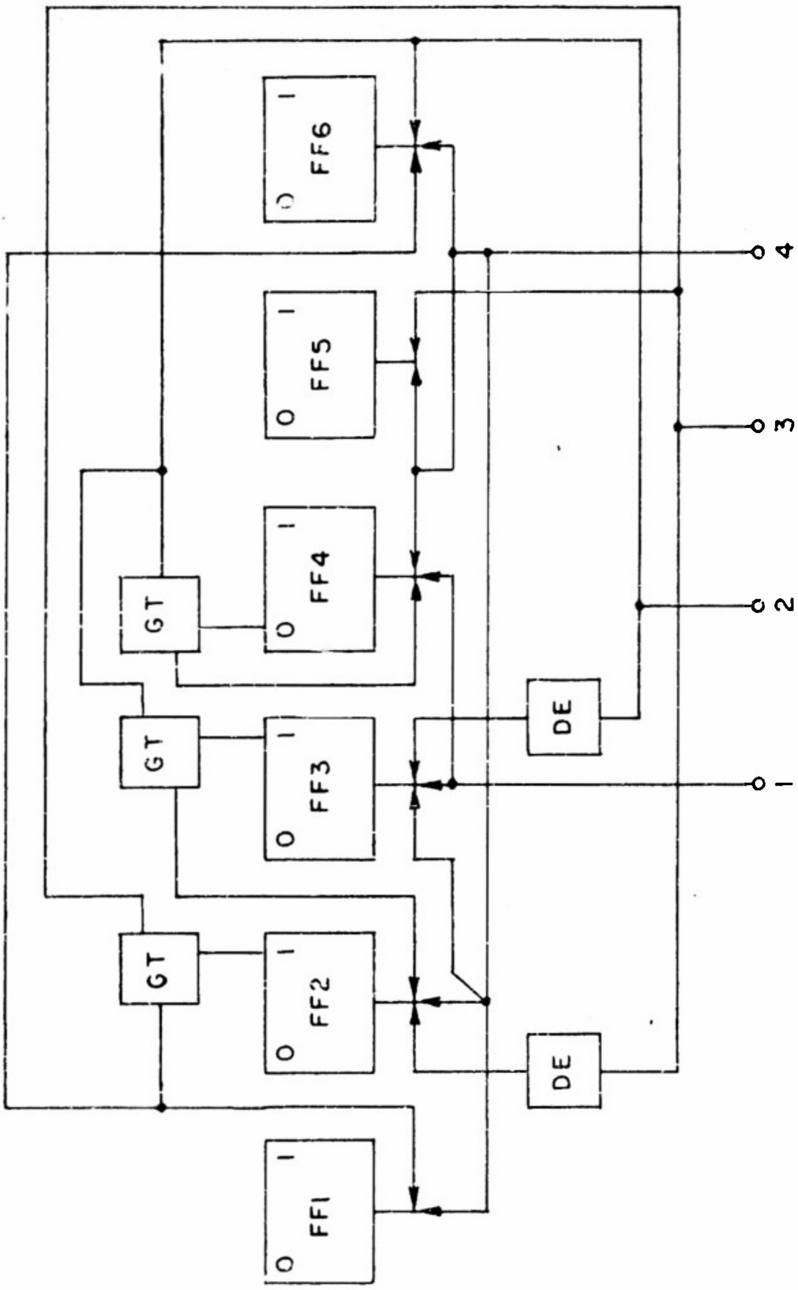

LEGEND: FF (FLIPFLOP)-BISTABLE STORAGE, GT-GATE TUBE, DE-DELAY ELEMENT,
← RECTIFIER

FIG. 50. A FOUR TO SIX DIGIT CONVERSION UNIT.

If the first digit of the input is a one change digits 3 and 4, this gives 001011.

If the second digit of the input is a one change digits 2 and 5.

If the third input digit is a one change digits 5 and 6 (i.e. replace each by its complement) and if the second digit is zero and the fourth a one change one and three also. If the second digit is a zero, and the third a one, change two and four as well as the aforementioned 5 and 6.

If the fourth input digit is a one, complement the number in the counter. This yields the circuit of Fig. 51.

Tabulated below are the numbers thus obtained.

Input	Output
0000	000111
0001	111000
0010	101100
0011	010011
0100	010101
0101	101010
0110	010110
0111	101001
1000	001011
1001	110100
1010	011100
1011	100011
1100	011001
1101	100110
1110	011010
1111	100101

(c) <u>6-8</u>. The task of choosing 64 out of the 70 possible combinations is somewhat greater. It is almost impossible to do this effectively unless the input number is stored.

The list of the decimal equivalents and their complements is given below.

No.	Complement	No.	Complement	No.	Complement	No.	Complement
15	240	51	204	78	177	102	153
23	232	53	202	83	172	105	150
27	228	54	201	85	170	106	149
29	226	57	198	86	169	108	147
30	225	58	197	89	166	113	142
39	216	60	195	90	165	114	141
43	212	71	184	92	163	116	139
45	210	75	180	99	156	120	135
46	209	77	178	101	154		

This can be done with a shift register, as follows:

Start with 15 in the counter.
Change 4 and 5 if first input digit is a one.
Double the amount in the counter.

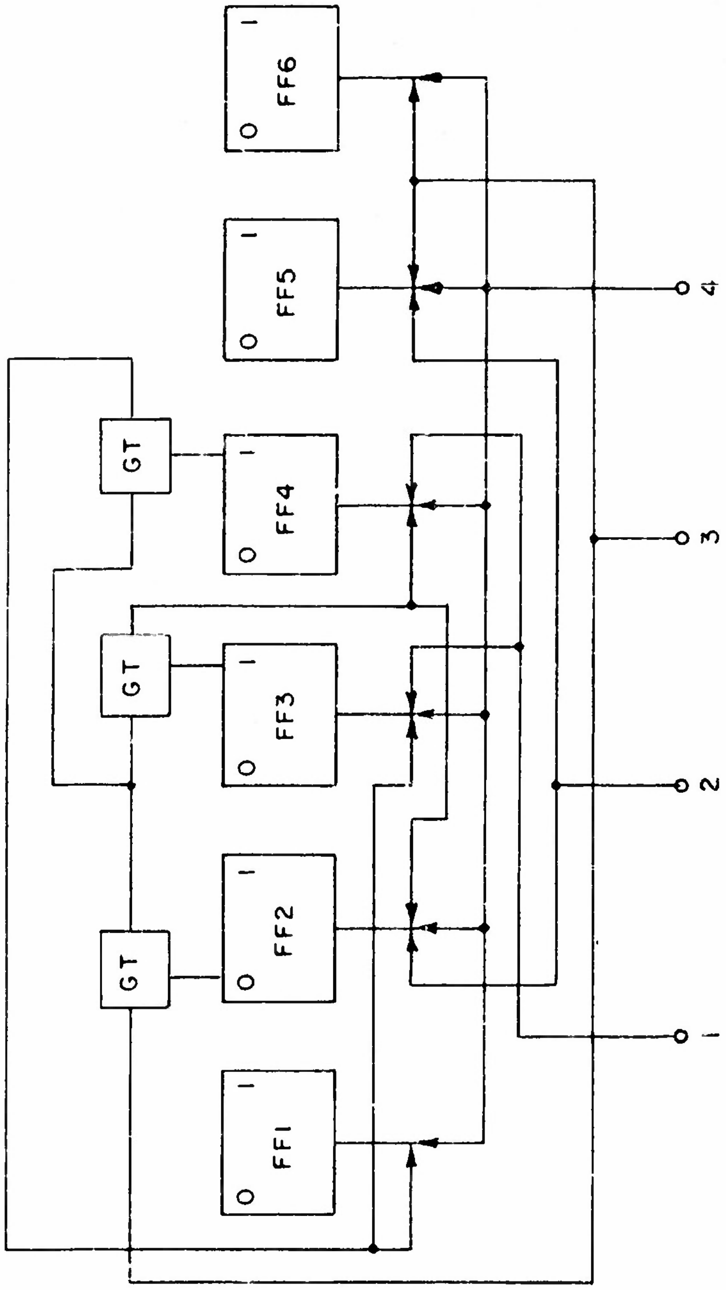

FIG. 51 AN ALTERNATE FOUR TO SIX DIGIT CONVERSION UNIT

Double the amount in the counter and subtract 3.

Double the amount in the counter if either the second or third digit of the input was a one. If neither was a one change 15 to 51, or 23 to 75.

If the second and the fourth digits of the input are zeros, double the counter reading and subtract one. If the second input digit was a one, and the third and fourth zeros, double the counter reading and subtract two. If the fourth digit was a one, double the counter reading.

These rules give the sequence:

Start	1st Digit	2nd Digit	3rd Digit	4th Digit	5th Digit
15	23	30	27	60	29
		46	43	92	45
			57	54	53
			89	86	85
				114	113
				178	177
				51	58
				75	90
					120
					184
					108
					172
					-228-
					-356-
					102
					150

All these numbers are acceptable except 356, which is too large, and 228, which is the complement of 27. Since the sixth digit is to complement the number, this would amount to a double duplication. The 356 is easy to handle. If a carry is installed such that an overflow changes the last digit of the output, then one gets 101 instead of 356. Still, 228 needs to be changed, and this can be done by complementing digits one and four after the shift, giving 116.

A circuit for accomplishing this is shown in Fig. 52. Note that no provision is made for reading out the result after the sixth pulse, or for clearing the register and replacing 15. In addition, the input number is a time sequence of pulses, which needs to be separated. A circuit which will accomplish this for the 4-6 case is discussed below. Note that the shift register used, that which is after point A in the figure, is not by any means the simplest obtainable.

Summary. If 24 digits are to be converted to a number, half of whose digits were ones, the simplest procedure would be to add on the complement of the number at the end. This requires challenges of 48 digits.

If six 4-6 counters are used, this gives a total of 36 digits, a saving of 25 percent. If four 6-8 counters are used, it would yield 32 digit challenges, and a slightly more complicated network.

Evidently no simple scheme appears in the offing. With sufficient effort a 24-28 could be constructed, but it would probably be quite complicated.

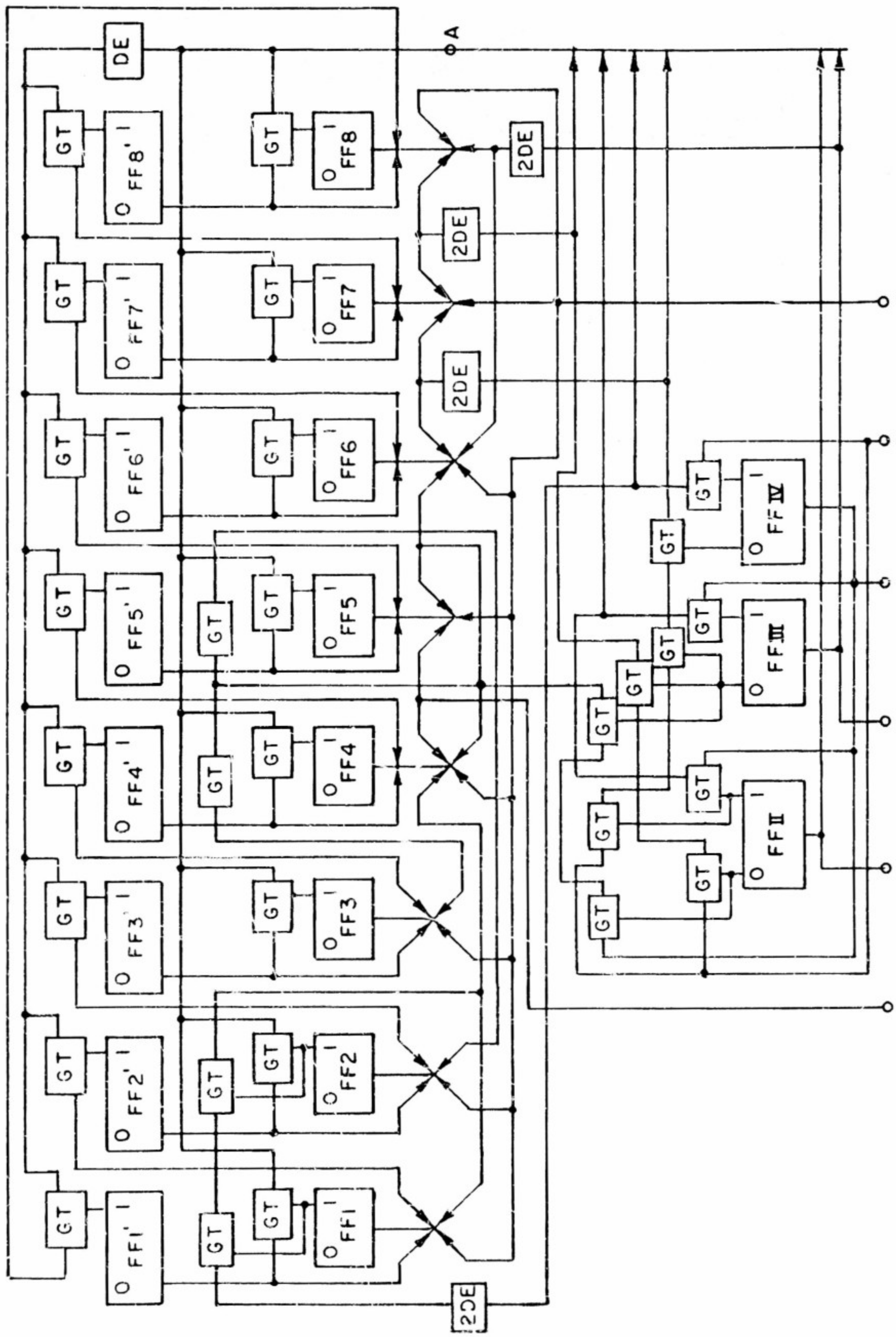

FIG. 52. A SIX TO EIGHT DIGIT CONVERSION UNIT.

APPENDIX II

Procedure for Analysis of Airborne Repeated-challenge System Including Effect of Noise During the Space Interval

The purpose of this section is to describe the modifications of the procedures given in Chap. V that must be made in order to take into account the effect of noise during the space interval. The probability P_N of obtaining a count due to noise is given by

$$P_N = \int_V^{\infty} p_o^{(o)}(V_\Sigma)dV_\Sigma \qquad \text{(II-1)}$$

where $p_o^{(o)}(V_\Sigma)$ can be obtained by evaluating $p_o(V_\Sigma)$ for $\rho = 0$, or directly from eq. (5-1) of Chap. V. The false-alarm probability now takes the form

$$P_F^! = P_F + P_N \qquad \text{(II-2)}$$

where P_F is given by eq. (5-22) and P_N by eq. (5-33). The new value of threshold voltage is the value of V which makes the sum of $P_F^!$ and P_M a minimum. (P_M is again the value determined by eq. 5-21)

The probability P_s given by eq. (5-27) and the false-alarm probabilities given by eqs. (5-23 to 5-26) will need to be redetermined for the new value V. Letting these new values be $P_s^!$, $P_{F_1}^!$, $P_{F_2}^!$, $P_{F_3}^!$, and $P_{F_4}^!$, the new value of $\theta(k)$ is given by

$$\theta'(k) = \sum_{i=k}^{m} \theta_i'(k) \qquad \text{(II-3)}$$

where

$$\theta_i'(k) = \theta_{i1} + \theta_{i2}$$

$$\theta_{i1} = Q_{i0}\, Q_{i1}^4\, Q_{i2}^6\, Q_{i3}^4\, Q_{i4}$$

$$\theta_{i2} = S_{i0}\, S_{i1}^4\, S_{i2}^6\, S_{i3}^4\, S_{i4}$$

in which $Q_{i0} = \sum_{x=0}^{k-1} [C_x^{i-1} (P_s^!)^{s+1}(1 - P_s^!)^{i-1-x}\, C_{k-1-x}^{i-1}\, P_N^{k-1-x}\,(1 - P_N)^{i-k+x}]$

and $Q_{in} = \sum_{x=0}^{k-1} [C_x^i (P_{F_n}^!)^x (1 - P_{F_n}^!)^{i-x} \sum_{j=0}^{k-1-x} C_j^{i-1}\, P_N^j\, (1 - P_N)^{i-1-j}]$

$n = 1, 2, 3, 4.$

The new value of $\mu(k)$ is given by $\mu'(k) = R_o R_1^4 R_2^6 R_3^4 R_4$ (II-4)

where
$$R_o = \sum_{i=0}^{k-1} [C_i^m (P_s')^i (1 - P_s)^{m-i} \sum_{j=0}^{k-1-i} C_j^m P_N^j (1 - P_N)^{m-j}]$$

and
$$R_n = \sum_{i=0}^{k-1} [C_i^m (P_{F_n}')^i (1 - P_{F_n}')^{m-i} \sum_{j=0}^{k-1-i} C_j^m P_N^j (1 - P_N)^{m-j}]$$

$n = 1, 2, 3, 4.$

The remainder of the procedure for determining K is the same as that used in the previous analysis where the noise was neglected.

APPENDIX III

Derivation of Matched-filtering Relations

Suppose that one is given a certain signal $s_i(t)$ immersed in a noise whose frequency spectrum is $N_i(\omega)$. It is desired to design that filter (which is both realizable and has finite memory) which will yield the greatest improvement in signal-to-noise ratio.

Let

$$\phi_i(\tau) = \frac{1}{2\pi} \int_{-\infty}^{\infty} N_i(\omega) e^{j\omega\tau} d\omega \qquad \text{(III-1)}$$

be the autocorrelation function of the noise, and $\phi_i(0)$ be the rms noise power. If $H(\omega)$ is the Fourier transform of the desired $h(t)$ (the impulse response of the matched filter) then,

$$\phi_o(\tau) = \frac{1}{2\pi} \int_{-\infty}^{\infty} N_i(\omega) H(\omega) H^*(\omega) e^{j\omega\tau} d\omega \qquad \text{(III-2)}$$

can be shown to be the correlation function of the output noise, and $\phi_o(0)$ the output noise power.

If $s_o(t)$ is the signal output of the filter due to $s_i(t)$ as input, then

$$s_o(t) = \int_{-\infty}^{\infty} h(\tau) s_i(t - \tau) d\tau \qquad \text{(III-3)}$$

It is now desired to maximize the output signal power-to-noise power ratio at some instant of time, say when $t = t_o$. Thus one wishes to maximize

$$\rho_o = \frac{s_o^2(t_o)}{\phi_o(0)} \quad \text{by suitable choice of } h(t).$$

Using the notation of the Calculus of Variations this implies that

$$\delta\rho_o = \frac{\phi_o(0) 2 s_o(t_o) \delta s_o(t_o) - s_o^2(t_o) \delta\phi_o(0)}{\phi_o^2(0)} = 0$$

or

$$\frac{2 s_o(t_o)}{\phi_o(0)} \left[\delta s_o(t_o) - \frac{s_o(t_o)}{2\phi_o(0)} \delta\phi_o(0) \right] = 0$$

Assuming that $h(t)$ is the extremal, $\dfrac{s_o(t_o)}{\phi_o(0)}$ is a constant, call it λ,

and noting that $\Phi_o(0) < \infty$ and $s_o(t_o) > 0$

$$\delta s_o(t_o) - \frac{\lambda}{2}\,\delta\,\Phi_o(0) = 0. \qquad \text{(III-4)}$$

From (III-3)

$$\delta s_o(t_o) = \int_{-\infty}^{\infty} s_i(t_o - \tau)\,\delta\,h(\tau)d\tau \qquad \text{(III-5)}$$

Setting $\tau = 0$ in eq. (III-2), and taking the variation of both sides:

$$\delta\,\phi_o(0) = \frac{1}{2\pi}\int_{-\infty}^{\infty} N_i(\omega)\,\delta\,[H(\omega)H^*(\omega)]\,d\omega \qquad \text{(III-6)}$$

One now applies the conditions of realisability and finite memory on h(t), viz.

$$h(t) = 0 \quad \text{for} \quad t < 0 \quad \text{and} \quad t > \beta$$

$$\text{and} \quad \delta\,h(t) = 0 \quad \text{for} \quad t < 0 \quad \text{and} \quad t > \beta$$

hence eq. (III-5) may be written

$$\delta s_o(t_o) = \int_{0}^{\beta} s_i(t_o - \tau)\,\delta\,h(\tau)d\tau \qquad \text{(III-7)}$$

Since

$$H(\omega) = \int_{-\infty}^{\infty} h(\tau)e^{-j\omega\tau}d\tau = \int_{0}^{\beta} h(\tau)e^{-j\omega\tau}d\tau$$

$$\delta\,H(\omega) = \int_{0}^{\beta} e^{-j\omega\tau}\,\delta\,h(\tau)d\tau$$

and

$$\delta\,H^*(\omega) = \int_{0}^{\beta} e^{j\omega\tau}\,\delta\,h(\tau)d\tau \qquad \text{(III-8)}$$

Hence

$$\delta\,[H(\omega)H^*(\omega)] = H(\omega)\,\delta\,H^*(\omega) + H^*(\omega)\,\delta\,H(\omega)$$

$$= H(\omega)\int_{0}^{\beta} e^{+j\omega\tau}\,\delta\,h(\tau)d\tau \qquad \text{(III-9)}$$

$$+ H^*(\omega)\int_{0}^{\beta} e^{-j\omega\tau}\,\delta\,h(\tau)d\tau.$$

Substituting (III-9) in (III-6)

$$\delta\phi_o(0) = \frac{1}{2\pi}\int_{-\infty}^{\infty} N_1(\omega)H(\omega)\left[\int_0^{\beta} e^{j\omega\tau}\,\delta h(\tau)d\tau\right]d\omega$$

$$+ \frac{1}{2\pi}\int_{-\infty}^{\infty} N_1(\omega)H^*(\omega)\left[\int_0^{\beta} e^{-j\omega\tau}\,\delta h(\tau)d\tau\right]d\omega.$$

The order of integration in both integrals may be reversed if $\int_{-\infty}^{\infty} N_1(\omega)H(\omega)e^{j\omega\tau}d\omega$ converges uniformly for all $0 \leq \tau \leq \beta$

$$\delta\phi_o(0) = \int_0^{\beta}\delta h(\tau)\left[\frac{1}{2\pi}\int_{-\infty}^{\infty} N_1(\omega)H(\omega)e^{j\omega\tau}d\omega\right]d\tau$$

$$+ \int_0^{\beta}\delta h(\tau)\left[\frac{1}{2\pi}\int_{-\infty}^{\infty} N_1(\omega)H^*(\omega)e^{-j\omega\tau}d\omega\right]d\tau \qquad \text{(III-10)}$$

But $N_1(\omega)$ is an even function of ω, and $H^*(\omega) = H(-\omega)$, so

$$\frac{1}{2\pi}\int_{-\infty}^{\infty} N_1(\omega)H^*(\omega)e^{-j\omega\tau}d\omega = \frac{1}{2\pi}\int_{-\infty}^{\infty} N_1(-\omega)H(-\omega)e^{j(-\omega)\tau}d\omega$$

Replacing $-\omega$ by ω on the right hand side

$$\frac{1}{2\pi}\int_{-\infty}^{\infty} N_1(\omega)H^*(\omega)e^{-j\omega\tau}d\omega = \frac{1}{2\pi}\int_{-\infty}^{\infty} N_1(\omega)H(\omega)e^{j\omega\tau}d\omega.$$

Using this result in (III-10)

$$\delta\phi_o(0) = 2\int_0^{\beta}\left[\frac{1}{2\pi}\int_{-\infty}^{\infty} N_1(\omega)H(\omega)e^{j\omega\tau}d\omega\right]\delta h(\tau)d\tau \qquad \text{(III-11)}$$

But the quantity in brackets in eq. (III-11), by the convolution theorem, is

$$\frac{1}{2\pi}\int_{-\infty}^{\infty} N_1(\omega)H(\omega)e^{j\omega\tau}d\omega = \int_0^{\beta} h(\xi)\phi_1(\tau-\xi)d\xi \qquad \text{(III-12)}$$

so

$$\delta\Phi_o(0) = 2\int_0^\beta\left[\int_0^\beta h(\xi)\,\phi_1(\tau-\xi)\,d\xi\right]\delta h(\tau)\,d\tau \qquad \text{(III-13)}$$

Substituting eqs. (III-13) and (III-7) in eq. (III-4):

$$\delta s_o(t_o) - \frac{\lambda}{2}\,\delta\Phi_o(0) = \int_0^\beta\left[s_1(t_o-\tau) - \lambda\left\{\int_0^\beta h(\xi)\,\phi_1(\tau-\xi)\,d\xi\right\}\right]\delta h(\tau)\,d\tau = 0.$$

Since this equation must hold independent of $\delta h(\tau)$ then

$$s_1(t_o-\tau) = \lambda\int_0^\beta h(\xi)\,\phi_1(\tau-\xi)\,d\xi$$

$$\text{for} \quad 0 \leq \tau \leq \beta\,. \qquad \text{(III-14)}$$

If $s_1(t)$ is to vanish for t negative, then

$$t_o \geq \beta. \qquad \text{(III-15)}$$

APPENDIX IV

Selected Bibliography

1. Cleeton, C. E., "Garbling of Range Coding", NRL Letter Report S-3450-29A/50 (6 Sept. 1950) (SECRET)

2. "Proposal for a New IFF System", USNEL Report 3 DPS Index No. 207-1.1, Buships Problem D19.38 (18 April 1947) (SECRET)

3. Cleeton, C. E., "Coding and Security of Electronic Recognition and Identification Systems", NRL Report R-2972 (12 Sept. 1946) (SECRET)

4. Cleeton, C. E., "Proposed System of Electronic Recognition", NRL Report R-3131 (June 1947) (SECRET)

5. Cleeton, C. E., "Proposed High Security IFF System", NRL Report S-3450-36/51OC (15 Aug. 1951) (SECRET)

6. Final report on "Test of MX IFF with Pule Train Coding", Navy Air Navigation Electronics Project, Electronics Test Division, NATC Patuxent River, Md. (21 Dec. 1950) (SECRET)

7. von Neumann, J. and Morgenstern, O., Theory of Games and Economic Behavior, Princeton University Press (1947)

8. McKinsey, J. C. C., Introduction to the Theory of Games, McGraw-Hill Book Co., Inc. (1952)

9. "Application of the Theory of Games to IFF Problems", Report RM-396, Rand Corporation (1950) (SECRET)

10. "Theory and Applications of Games of Strategy", U. S. Air Force Project Rand, Report R-216 (1 Dec. 1951) (SECRET)

11. North, D. O., "Analysis of the Factors which Determine Signal/Noise Discrimination in Radar", Report PTR-6C, RCA Laboratories (June 1943)

12. Van Vleck, J. H. and Middleton, D., "A Theoretical Comparison of the Visual, Aural, and Meter Reception of Pulsed Signals in the Presence of Noise", Jour. Appl. Phys., Vol. 17 (Nov. 1946) p. 940

13. Dwork, B. M., "Detection of a Pulse Superimposed on Fluctuation Noise", Proc. I.R.E., Vol. 38 (July 1950) p. 771

14. Woodward, P. M., "Information Theory and the Design of Radar Receivers", Proc. I.R.E., Vol. 39 (Dec. 1951) p. 1521

15. Final report on "Experimental ASW Anti-Clutter Amplifier", Research Division, Philco Corporation, Philadelphia, Pa., Bureau of Aeronautics, U. S. Navy Contract No. NO(a)-10661 (CONFIDENTIAL)

16. "Secure Communications using Correlation Techniques", Research Laboratory of Electronics, M.I.T., Cambridge, Mass., Quarterly Progress Report dated January 30, 1952 (SECRET)

17. Zadeh, L. A. and Ragazzini, J. R., "Optimum Filters for the Detection of Signals in Noise", Proc. I.R.E., Vol. 40 (Oct. 1952) p. 1223

18. Harris, H. E., "Simplified Q Multiplier", Electronics, Vol. 24, No. 5 (May 1951) p. 130

19. Fano, R. M., "Signal-to-noise Ratio in Correlation Detectors", Research Laboratory of Electronics, M.I.T., Cambridge, Mass., Tech. Report 186, (Feb. 1951)

20. Davenport, W. B., Jr., "Correlation Erros Due to Finite Observation Intervals", Research Laboratory of Electronics, M.I.T., Cambridge, Mass., Tech. Report 191 (March 1951)

21. "Secure Communications using Correlation Techniques", Research Laboratory of Electronics, M.I.T., Cambridge, Mass., Quarterly Progress Reports dated April 30, July 30, and October 30, 1951 (SECRET)

22. "Coding and Decoding of Pulse Trains", USNEL Report 23, Buships Problem D19.4 (18 Nov. 1947) (CONFIDENTIAL)

23. Shannon, C. E. and Weaver, W., The Mathematical Theory of Communications, University of Illinois Press (1949)

24. Fano, R. M., "Information Theory", Notes for Course 6.574 at M.I.T., (1952)

25. Lawson, J. L. and Uhlenbeck, G. E., Threshold Signals, Vol. 24, Radiation Laboratory Series, M.I.T., (1950)

26. Hamming, R. W., "Error Detecting and Error Correcting Codes", Bell Telephone System Monograph 17S7 (1950). Originally Bell System Technical Journal, Vol. 29 (April 1950) pp. 147-160

27. Fano, R. M., "The Transmission of Information - II", Research Laboratory of Electronics, M.I.T., Tech. Report 149 (6 Feb. 1950)

28. Harrington, J. V., "An Analysis of the Detection of Repeated Signals in Noise by Binary Integration", Lincoln Laboratory, M.I.T., Tech. Report No. 13 (14 Aug. 1952)

29. Rice, S. O., "Mathematical Analysis of Random Noise", Bell Telephone System Monograph B-1589. Originally Bell System Technical Journal, Vol. 23 (July 1944) pp. 282-332 and Vol. 24 (Jan. 1945) pp. 46-156

30. Middleton, D., "Statistical Criteria for the Detection of Pulsed Carriers in Noise", AFCRC Report E5091 (Nov. 1952)

31. Dancoff, S., "On Signals Imbedded in Noise", Co
tory, University of Illinois, Contract DA-11-02
(May 1952)

32. Wandell, W., M/Sgt., "Multiple Corridor Identifi
Permanently in the West", Communications and El
(June 1952) pp. 19-22 (SECRET)

33. Lee, Y. W., "Application of Statistical Methods
lems", Research Laboratory of Electronics, M.I.
(1 Sept. 1950) pp. 25-28

34. Carlson, A. W., "High Speed Transistor Flip-Flop
(June 1953)

35. Forrester, J. W., "Designs and Tests of Electro
ting Safety Margins", Digital Computer Laborato
Note E-536 (27 Jan. 1953)

36. Daggett, W. L., and Rich, E. S., "Diagnostic Pr
Checking in the Whirlwind I Computer", Digital
M.I.T., Engineering Note E-536 (26 March 1953)

37. Boyd, H., "Final Specifications of the High-Sp
Computer Laboratory, M.I.T., Engineering Note

38. Knight, G. Jr., Johnson, R. A., and Holt, R. B
Small Signal Parameters of Transistors", Repor
Specialties Corporation and Transistor Product

39. Franklin, P., Treatise on Advanced Calculus, J